NIST NCSTAR 1-5D

Federal Building and Fire Safety Investigation of the World Trade Center Disaster

Reaction of Ceiling Tile Systems to Shocks

Richard G. Gann
Michael A. Riley
Joshua M. Repp
Andrew S. Whittaker
Andrei M. Reinhorn
Paul A. Hough

NIST National Institute of Standards and Technology • Technology Administration • U.S. Department of Commerce

NIST NCSTAR 1-5D

Federal Building and Fire Safety Investigation of the World Trade Center Disaster

Reaction of Ceiling Tile Systems to Shocks

Richard G. Gann
Michael A. Riley
Building and Fire Research Laboratory
National Institute of Standards and Technology

Joshua M. Repp
Andrew S. Whittaker
Andrei M. Reinhorn
State University of New York at Buffalo

Paul A. Hough
Armstrong World Industries

September 2005

U.S. Department of Commerce
Carlos M. Gutierrez, Secretary

Technology Administration
Michelle O'Neill, Acting Under Secretary for Technology

National Institute of Standards and Technology
William Jeffrey, Director

Disclaimer No. 1

Certain commercial entities, equipment, products, or materials are identified in this document in order to describe a procedure or concept adequately or to trace the history of the procedures and practices used. Such identification is not intended to imply recommendation, endorsement, or implication that the entities, products, materials, or equipment are necessarily the best available for the purpose. Nor does such identification imply a finding of fault or negligence by the National Institute of Standards and Technology.

Disclaimer No. 2

The policy of NIST is to use the International System of Units (metric units) in all publications. In this document, however, units are presented in metric units or the inch-pound system, whichever is prevalent in the discipline.

Disclaimer No. 3

Pursuant to section 7 of the National Construction Safety Team Act, the NIST Director has determined that certain evidence received by NIST in the course of this Investigation is "voluntarily provided safety-related information" that is "not directly related to the building failure being investigated" and that "disclosure of that information would inhibit the voluntary provision of that type of information" (15 USC 7306c).

In addition, a substantial portion of the evidence collected by NIST in the course of the Investigation has been provided to NIST under nondisclosure agreements.

Disclaimer No. 4

NIST takes no position as to whether the design or construction of a WTC building was compliant with any code since, due to the destruction of the WTC buildings, NIST could not verify the actual (or as-built) construction, the properties and condition of the materials used, or changes to the original construction made over the life of the buildings. In addition, NIST could not verify the interpretations of codes used by applicable authorities in determining compliance when implementing building codes. Where an Investigation report states whether a system was designed or installed as required by a code *provision*, NIST has documentary or anecdotal evidence indicating whether the requirement was met, or NIST has independently conducted tests or analyses indicating whether the requirement was met.

Use in Legal Proceedings

No part of any report resulting from a NIST investigation into a structural failure or from an investigation under the National Construction Safety Team Act may be used in any suit or action for damages arising out of any matter mentioned in such report (15 USC 281a; as amended by P.L. 107-231).

National Institute of Standards and Technology National Construction Safety Team Act Report 1-5D
Natl. Inst. Stand. Technol. Natl. Constr. Sfty. Tm. Act Rpt. 1-5D, 146 pages (September 2005)
CODEN: NSPUE2

U.S. GOVERNMENT PRINTING OFFICE
WASHINGTON: 2005

For sale by the Superintendent of Documents, U.S. Government Printing Office
Internet: bookstore.gpo.gov — Phone: (202) 512-1800 — Fax: (202) 512-2250
Mail: Stop SSOP, Washington, DC 20402-0001

ABSTRACT

The degree of damage to the ceiling tile systems of the World Trade Center towers following the aircraft impacts on September 11, 2001, could have affected the rate at which the ensuing fires heated the steel-trussed concrete slab floor systems above. Accordingly, a series of shaking table tests was conducted to estimate the magnitude of distress to the ceiling tile systems that would result in substantial displacement of ceiling tiles. Ceiling tile systems indicative of those used in the core and tenant spaces were subjected to both single and complex impulses of varying magnitude. The systems resisted significant damage up to about 1g applied to the test platform, corresponding to about 2.5g to 3g at the ceiling frame. The data suggest that major system failure would occur at impulse values near 4g to 5g at the ceiling frame.

Keywords: Ceiling, ceiling tiles, shake, World Trade Center.

This page intentionally left blank.

TABLE OF CONTENTS

LIST OF FIGURES

This page intentionally left blank.

LIST OF TABLES

This page intentionally left blank.

LIST OF ACRONYMS AND ABBREVIATIONS

Acronyms

AWI	Armstrong World Industries
DBE	design basis earthquake
DTAP	dissemination and technical assistance program
FEMA	Federal Emergency Management Agency
LVDT	linear variable displacement transducer
MCE	maximum considered earthquake
NEHRP	National Earthquake Hazards Reduction Program
NIST	National Institute of Standards and Technology
R&D	research and development
RRS	required response spectrum
SEESL	Structural Engineering Earthquake Simulation Laboratory
UB	University at Buffalo of the State University of New York
WTC	World Trade Center
WTC 1	World Trade Center 1 (North Tower)
WTC 2	World Trade Center 2 (South Tower)
WTC 7	World Trade Center 7

Abbreviations

μm	micrometer
°C	degrees Celsius
ft	foot
ft^2	square foot
g	acceleration (gravity) (9.81 m/s^2, 32.2 ft/s^2)
Hz	Hertz
kg	kilogram
kip	a force equal to 1,000 pounds
kN	kiloNewton
in.	inch
lb	pound

m	meter
min	minute
mm	millimeter
mph	miles per hour
s	second

METRIC CONVERSION TABLE

To convert from	to	Multiply by
AREA AND SECOND MOMENT OF AREA		
square foot (ft^2)	square meter (m^2)	9.290 304 E-02
square inch ($in.^2$)	square meter (m^2)	6.4516 E-04
square inch ($in.^2$)	square centimeter (cm^2)	6.4516 E+00
square yard (yd^2)	square meter (m^2)	8.361 274 E-01
FORCE		
kilogram-force (kgf)	newton (N)	9.806 65 E+00
kilopond (kilogram-force) (kp)	newton (N)	9.806 65 E+00
kip (1 kip=1,000 lbf)	newton (N)	4.448 222 E+03
kip (1 kip=1,000 lbf)	kilonewton (kN)	4.448 222 E+00
pound-force (lbf)	newton (N)	4.448 222 E+00
FORCE DIVIDED BY LENGTH		
pound-force per foot (lbf/ft)	newton per meter (N/m)	1.459 390 E+01
pound-force per inch (lbf/in.)	newton per meter (N/m)	1.751 268 E+02
LENGTH		
foot (ft)	meter (m)	3.048 E-01
inch (in)	meter (m)	2.54 E-02
inch (in.)	centimeter (cm)	2.54 E+00
micron (m)	meter (m)	1.0 E-06
yard (yd)	meter (m)	9.144 E-01
MASS and MOMENT OF INERTIA		
kilogram-force second squared per meter ($kgf \cdot s^2/m$)	kilogram (kg)	9.806 65 E+00
pound foot squared ($lb \cdot ft^2$)	kilogram meter squared ($kg \cdot m^2$)	4.214 011 E-02
pound inch squared ($lb \cdot in.^2$)	kilogram meter squared ($kg \cdot m^2$)	2.926 397 E-04
ton, metric (t)	kilogram (kg)	1.0 E+03
ton, short (2,000 lb)	kilogram (kg)	9.071 847 E+02

To convert from	to	Multiply by
MASS DIVIDED BY AREA		
pound per square foot (lb/ft^2)	kilogram per square meter (kg/m^2)	4.882 428 E+00
pound per square inch (*not* pound force) (lb/in.^{2})	kilogram per square meter (kg/m^2)	7.030 696 E+02
MASS DIVIDED BY LENGTH		
pound per foot (lb/ft)	kilogram per meter (kg/m)	1.488 164 E+00
pound per inch (lb/in.)	kilogram per meter (kg/m)	1.785 797 E+01
pound per yard (lb/yd)	kilogram per meter (kg/m)	4.960 546 E-01
PRESSURE or STRESS (FORCE DIVIDED BY AREA)		
kilogram-force per square centimeter (kgf/cm^2)	pascal (Pa)	9.806 65 E+04
kilogram-force per square meter (kgf/m^2)	pascal (Pa)	9.806 65 E+00
kilogram-force per square millimeter (kgf/mm^2)	pascal (Pa)	9.806 65 E+06
kip per square inch (ksi) (kip/in.^{2})	pascal (Pa)	6.894 757 E+06
kip per square inch (ksi) (kip/in.^{2})	kilopascal (kPa)	6.894 757 E+03
pound-force per square foot (lbf/ft^2)	pascal (Pa)	4.788 026 E+01
pound-force per square inch (psi) (lbf/in.^{2})	pascal (Pa)	6.894 757 E+03
pound-force per square inch (psi) (lbf/in.^{2})	kilopascal (kPa)	6.894 757 E+00
psi (pound-force per square inch) (lbf/in.^{2})	pascal (Pa)	6.894 757 E+03
psi (pound-force per square inch) (lbf/in.^{2})	kilopascal (kPa)	6.894 757 E+00

PREFACE

Genesis of This Investigation

Immediately following the terrorist attack on the World Trade Center (WTC) on September 11, 2001, the Federal Emergency Management Agency (FEMA) and the American Society of Civil Engineers began planning a building performance study of the disaster. The week of October 7, as soon as the rescue and search efforts ceased, the Building Performance Study Team went to the site and began its assessment. This was to be a brief effort, as the study team consisted of experts who largely volunteered their time away from their other professional commitments. The Building Performance Study Team issued its report in May 2002, fulfilling its goal "to determine probable failure mechanisms and to identify areas of future investigation that could lead to practical measures for improving the damage resistance of buildings against such unforeseen events."

On August 21, 2002, with funding from the U.S. Congress through FEMA, the National Institute of Standards and Technology (NIST) announced its building and fire safety investigation of the WTC disaster. On October 1, 2002, the National Construction Safety Team Act (Public Law 107-231), was signed into law. The NIST WTC Investigation was conducted under the authority of the National Construction Safety Team Act.

The goals of the investigation of the WTC disaster were:

- To investigate the building construction, the materials used, and the technical conditions that contributed to the outcome of the WTC disaster.
- To serve as the basis for:
  - Improvements in the way buildings are designed, constructed, maintained, and used;
  - Improved tools and guidance for industry and safety officials;
  - Recommended revisions to current codes, standards, and practices; and
  - Improved public safety.

The specific objectives were:

1. Determine why and how WTC 1 and WTC 2 collapsed following the initial impacts of the aircraft and why and how WTC 7 collapsed;
2. Determine why the injuries and fatalities were so high or low depending on location, including all technical aspects of fire protection, occupant behavior, evacuation, and emergency response;
3. Determine what procedures and practices were used in the design, construction, operation, and maintenance of WTC 1, 2, and 7; and
4. Identify, as specifically as possible, areas in current building and fire codes, standards, and practices that warrant revision.

NIST is a nonregulatory agency of the U.S. Department of Commerce's Technology Administration. The purpose of NIST investigations is to improve the safety and structural integrity of buildings in the United States, and the focus is on fact finding. NIST investigative teams are authorized to assess building performance and emergency response and evacuation procedures in the wake of any building failure that has resulted in substantial loss of life or that posed significant potential of substantial loss of life. NIST does not have the statutory authority to make findings of fault nor negligence by individuals or organizations. Further, no part of any report resulting from a NIST investigation into a building failure or from an investigation under the National Construction Safety Team Act may be used in any suit or action for damages arising out of any matter mentioned in such report (15 USC 281a, as amended by Public Law 107-231).

Organization of the Investigation

The National Construction Safety Team for this Investigation, appointed by the then NIST Director, Dr. Arden L. Bement, Jr., was led by Dr. S. Shyam Sunder. Dr. William L. Grosshandler served as Associate Lead Investigator, Mr. Stephen A. Cauffman served as Program Manager for Administration, and Mr. Harold E. Nelson served on the team as a private sector expert. The Investigation included eight interdependent projects whose leaders comprised the remainder of the team. A detailed description of each of these eight projects is available at http://wtc.nist.gov. The purpose of each project is summarized in Table P–1, and the key interdependencies among the projects are illustrated in Fig. P–1.

Table P–1. Federal building and fire safety investigation of the WTC disaster.

Technical Area and Project Leader	Project Purpose
Analysis of Building and Fire Codes and Practices; Project Leaders: Dr. H. S. Lew and Mr. Richard W. Bukowski	Document and analyze the code provisions, procedures, and practices used in the design, construction, operation, and maintenance of the structural, passive fire protection, and emergency access and evacuation systems of WTC 1, 2, and 7.
Baseline Structural Performance and Aircraft Impact Damage Analysis; Project Leader: Dr. Fahim H. Sadek	Analyze the baseline performance of WTC 1 and WTC 2 under design, service, and abnormal loads, and aircraft impact damage on the structural, fire protection, and egress systems.
Mechanical and Metallurgical Analysis of Structural Steel; Project Leader: Dr. Frank W. Gayle	Determine and analyze the mechanical and metallurgical properties and quality of steel, weldments, and connections from steel recovered from WTC 1, 2, and 7.
Investigation of Active Fire Protection Systems; Project Leader: Dr. David D. Evans; Dr. William Grosshandler	Investigate the performance of the active fire protection systems in WTC 1, 2, and 7 and their role in fire control, emergency response, and fate of occupants and responders.
Reconstruction of Thermal and Tenability Environment; Project Leader: Dr. Richard G. Gann	Reconstruct the time-evolving temperature, thermal environment, and smoke movement in WTC 1, 2, and 7 for use in evaluating the structural performance of the buildings and behavior and fate of occupants and responders.
Structural Fire Response and Collapse Analysis; Project Leaders: Dr. John L. Gross and Dr. Therese P. McAllister	Analyze the response of the WTC towers to fires with and without aircraft damage, the response of WTC 7 in fires, the performance of composite steel-trussed floor systems, and determine the most probable structural collapse sequence for WTC 1, 2, and 7.
Occupant Behavior, Egress, and Emergency Communications; Project Leader: Mr. Jason D. Averill	Analyze the behavior and fate of occupants and responders, both those who survived and those who did not, and the performance of the evacuation system.
Emergency Response Technologies and Guidelines; Project Leader: Mr. J. Randall Lawson	Document the activities of the emergency responders from the time of the terrorist attacks on WTC 1 and WTC 2 until the collapse of WTC 7, including practices followed and technologies used.

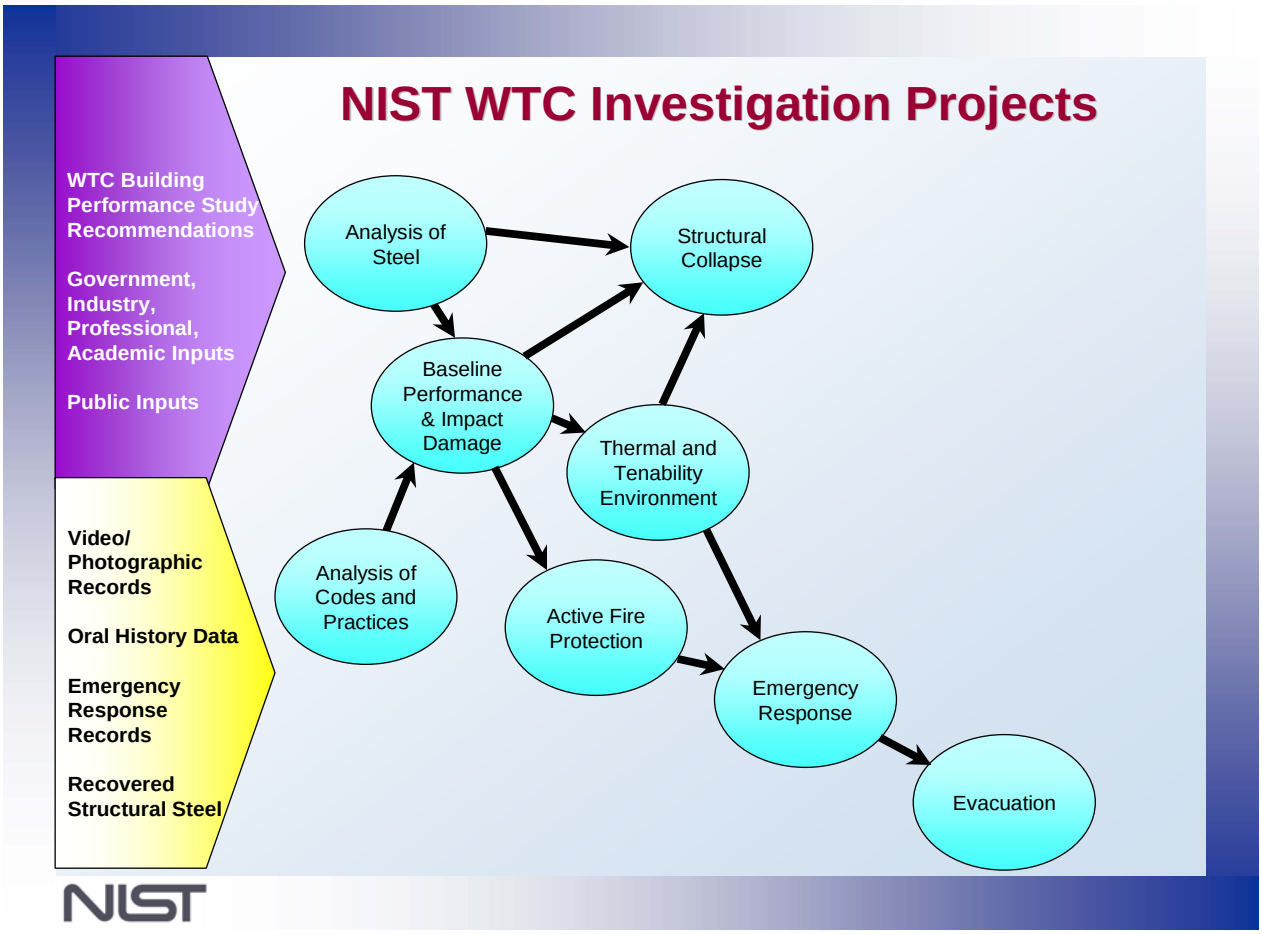

Figure P–1. The eight projects in the federal building and fire safety investigation of the WTC disaster.

National Construction Safety Team Advisory Committee

The NIST Director also established an advisory committee as mandated under the National Construction Safety Team Act. The initial members of the committee were appointed following a public solicitation. These were:

- Paul Fitzgerald, Executive Vice President (retired) FM Global, National Construction Safety Team Advisory Committee Chair
- John Barsom, President, Barsom Consulting, Ltd.
- John Bryan, Professor Emeritus, University of Maryland
- David Collins, President, The Preview Group, Inc.
- Glenn Corbett, Professor, John Jay College of Criminal Justice
- Philip DiNenno, President, Hughes Associates, Inc.

- Robert Hanson, Professor Emeritus, University of Michigan
- Charles Thornton, Co-Chairman and Managing Principal, The Thornton-Tomasetti Group, Inc.
- Kathleen Tierney, Director, Natural Hazards Research and Applications Information Center, University of Colorado at Boulder
- Forman Williams, Director, Center for Energy Research, University of California at San Diego

This National Construction Safety Team Advisory Committee provided technical advice during the Investigation and commentary on drafts of the Investigation reports prior to their public release. NIST has benefited from the work of many people in the preparation of these reports, including the National Construction Safety Team Advisory Committee. The content of the reports and recommendations, however, are solely the responsibility of NIST.

Public Outreach

During the course of this Investigation, NIST held public briefings and meetings (listed in Table P–2) to solicit input from the public, present preliminary findings, and obtain comments on the direction and progress of the Investigation from the public and the Advisory Committee.

NIST maintained a publicly accessible Web site during this Investigation at http://wtc.nist.gov. The site contained extensive information on the background and progress of the Investigation.

NIST's WTC Public-Private Response Plan

The collapse of the WTC buildings has led to broad reexamination of how tall buildings are designed, constructed, maintained, and used, especially with regard to major events such as fires, natural disasters, and terrorist attacks. Reflecting the enhanced interest in effecting necessary change, NIST, with support from Congress and the Administration, has put in place a program, the goal of which is to develop and implement the standards, technology, and practices needed for cost-effective improvements to the safety and security of buildings and building occupants, including evacuation, emergency response procedures, and threat mitigation.

The strategy to meet this goal is a three-part NIST-led public-private response program that includes:

- A federal building and fire safety investigation to study the most probable factors that contributed to post-aircraft impact collapse of the WTC towers and the 47-story WTC 7 building, and the associated evacuation and emergency response experience.
- A research and development (R&D) program to (a) facilitate the implementation of recommendations resulting from the WTC Investigation, and (b) provide the technical basis for cost-effective improvements to national building and fire codes, standards, and practices that enhance the safety of buildings, their occupants, and emergency responders.

Table P–2. Public meetings and briefings of the WTC Investigation.

Date	Location	Principal Agenda
June 24, 2002	New York City, NY	Public meeting: Public comments on the *Draft Plan* for the pending WTC Investigation.
August 21, 2002	Gaithersburg, MD	Media briefing announcing the formal start of the Investigation.
December 9, 2002	Washington, DC	Media briefing on release of the *Public Update* and NIST request for photographs and videos.
April 8, 2003	New York City, NY	Joint public forum with Columbia University on first-person interviews.
April 29–30, 2003	Gaithersburg, MD	NCST Advisory Committee meeting on plan for and progress on WTC Investigation with a public comment session.
May 7, 2003	New York City, NY	Media briefing on release of *May 2003 Progress Report.*
August 26–27, 2003	Gaithersburg, MD	NCST Advisory Committee meeting on status of the WTC investigation with a public comment session.
September 17, 2003	New York City, NY	Media and public briefing on initiation of first-person data collection projects.
December 2–3, 2003	Gaithersburg, MD	NCST Advisory Committee meeting on status and initial results and release of the *Public Update* with a public comment session.
February 12, 2004	New York City, NY	Public meeting on progress and preliminary findings with public comments on issues to be considered in formulating final recommendations.
June 18, 2004	New York City, NY	Media/public briefing on release of *June 2004 Progress Report.*
June 22–23, 2004	Gaithersburg, MD	NCST Advisory Committee meeting on the status of and preliminary findings from the WTC Investigation with a public comment session.
August 24, 2004	Northbrook, IL	Public viewing of standard fire resistance test of WTC floor system at Underwriters Laboratories, Inc.
October 19–20, 2004	Gaithersburg, MD	NCST Advisory Committee meeting on status and near complete set of preliminary findings with a public comment session.
November 22, 2004	Gaithersburg, MD	NCST Advisory Committee discussion on draft annual report to Congress, a public comment session, and a closed session to discuss pre-draft recommendations for WTC Investigation.
April 5, 2005	New York City, NY	Media and public briefing on release of the probable collapse sequence for the WTC towers and draft reports for the projects on codes and practices, evacuation, and emergency response.
June 23, 2005	New York City, NY	Media and public briefing on release of all draft reports for the WTC towers and draft recommendations for public comment.
September 12–13, 2005	Gaithersburg, MD	NCST Advisory Committee meeting on disposition of public comments and update to draft reports for the WTC towers.
September 13–15, 2005	Gaithersburg, MD	WTC Technical Conference for stakeholders and technical community for dissemination of findings and recommendations and opportunity for public to make technical comments.

- A dissemination and technical assistance program (DTAP) to (a) engage leaders of the construction and building community in ensuring timely adoption and widespread use of proposed changes to practices, standards, and codes resulting from the WTC Investigation and the R&D program, and (b) provide practical guidance and tools to better prepare facility owners, contractors, architects, engineers, emergency responders, and regulatory authorities to respond to future disasters.

The desired outcomes are to make buildings, occupants, and first responders safer in future disaster events.

National Construction Safety Team Reports on the WTC Investigation

A final report on the collapse of the WTC towers is being issued as NIST NCSTAR 1. A companion report on the collapse of WTC 7 is being issued as NIST NCSTAR 1A. The present report is one of a set that provides more detailed documentation of the Investigation findings and the means by which these technical results were achieved. As such, it is part of the archival record of this Investigation. The titles of the full set of Investigation publications are:

NIST (National Institute of Standards and Technology). 2005. *Federal Building and Fire Safety Investigation of the World Trade Center Disaster: Final Report on the Collapse of the World Trade Center Towers.* NIST NCSTAR 1. Gaithersburg, MD, September.

NIST (National Institute of Standards and Technology). 2006. *Federal Building and Fire Safety Investigation of the World Trade Center Disaster: Final Report on the Collapse of World Trade Center 7.* NIST NCSTAR 1A. Gaithersburg, MD.

Lew, H. S., R. W. Bukowski, and N. J. Carino. 2005. *Federal Building and Fire Safety Investigation of the World Trade Center Disaster: Design, Construction, and Maintenance of Structural and Life Safety Systems.* NIST NCSTAR 1-1. National Institute of Standards and Technology. Gaithersburg, MD, September.

Fanella, D. A., A. T. Derecho, and S. K. Ghosh. 2005. *Federal Building and Fire Safety Investigation of the World Trade Center Disaster: Design and Construction of Structural Systems.* NIST NCSTAR 1-1A. National Institute of Standards and Technology. Gaithersburg, MD, September.

Ghosh, S. K., and X. Liang. 2005. *Federal Building and Fire Safety Investigation of the World Trade Center Disaster: Comparison of Building Code Structural Requirements.* NIST NCSTAR 1-1B. National Institute of Standards and Technology. Gaithersburg, MD, September.

Fanella, D. A., A. T. Derecho, and S. K. Ghosh. 2005. *Federal Building and Fire Safety Investigation of the World Trade Center Disaster: Maintenance and Modifications to Structural Systems.* NIST NCSTAR 1-1C. National Institute of Standards and Technology. Gaithersburg, MD, September.

Grill, R. A., and D. A. Johnson. 2005. *Federal Building and Fire Safety Investigation of the World Trade Center Disaster: Fire Protection and Life Safety Provisions Applied to the Design and Construction of World Trade Center 1, 2, and 7 and Post-Construction Provisions Applied after Occupancy.* NIST NCSTAR 1-1D. National Institute of Standards and Technology. Gaithersburg, MD, September.

Razza, J. C., and R. A. Grill. 2005. *Federal Building and Fire Safety Investigation of the World Trade Center Disaster: Comparison of Codes, Standards, and Practices in Use at the Time of the Design and Construction of World Trade Center 1, 2, and 7.* NIST NCSTAR 1-1E. National Institute of Standards and Technology. Gaithersburg, MD, September.

Grill, R. A., D. A. Johnson, and D. A. Fanella. 2005. *Federal Building and Fire Safety Investigation of the World Trade Center Disaster: Comparison of the 1968 and Current (2003) New*

York City Building Code Provisions. NIST NCSTAR 1-1F. National Institute of Standards and Technology. Gaithersburg, MD, September.

Grill, R. A., and D. A. Johnson. 2005. *Federal Building and Fire Safety Investigation of the World Trade Center Disaster: Amendments to the Fire Protection and Life Safety Provisions of the New York City Building Code by Local Laws Adopted While World Trade Center 1, 2, and 7 Were in Use*. NIST NCSTAR 1-1G. National Institute of Standards and Technology. Gaithersburg, MD, September.

Grill, R. A., and D. A. Johnson. 2005. *Federal Building and Fire Safety Investigation of the World Trade Center Disaster: Post-Construction Modifications to Fire Protection and Life Safety Systems of World Trade Center 1 and 2*. NIST NCSTAR 1-1H. National Institute of Standards and Technology. Gaithersburg, MD, September.

Grill, R. A., D. A. Johnson, and D. A. Fanella. 2005. *Federal Building and Fire Safety Investigation of the World Trade Center Disaster: Post-Construction Modifications to Fire Protection, Life Safety, and Structural Systems of World Trade Center 7*. NIST NCSTAR 1-1I. National Institute of Standards and Technology. Gaithersburg, MD, September.

Grill, R. A., and D. A. Johnson. 2005. *Federal Building and Fire Safety Investigation of the World Trade Center Disaster: Design, Installation, and Operation of Fuel System for Emergency Power in World Trade Center 7*. NIST NCSTAR 1-1J. National Institute of Standards and Technology. Gaithersburg, MD, September.

Sadek, F. 2005. *Federal Building and Fire Safety Investigation of the World Trade Center Disaster: Baseline Structural Performance and Aircraft Impact Damage Analysis of the World Trade Center Towers.* NIST NCSTAR 1-2. National Institute of Standards and Technology. Gaithersburg, MD, September.

Faschan, W. J., and R. B. Garlock. 2005. *Federal Building and Fire Safety Investigation of the World Trade Center Disaster: Reference Structural Models and Baseline Performance Analysis of the World Trade Center Towers.* NIST NCSTAR 1-2A. National Institute of Standards and Technology. Gaithersburg, MD, September.

Kirkpatrick, S. W., R. T. Bocchieri, F. Sadek, R. A. MacNeill, S. Holmes, B. D. Peterson, R. W. Cilke, C. Navarro. 2005. *Federal Building and Fire Safety Investigation of the World Trade Center Disaster: Analysis of Aircraft Impacts into the World Trade Center Towers*, NIST NCSTAR 1-2B. National Institute of Standards and Technology. Gaithersburg, MD, September.

Gayle, F. W., R. J. Fields, W. E. Luecke, S. W. Banovic, T. Foecke, C. N. McCowan, T. A. Siewert, and J. D. McColskey. 2005. *Federal Building and Fire Safety Investigation of the World Trade Center Disaster: Mechanical and Metallurgical Analysis of Structural Steel.* NIST NCSTAR 1-3. National Institute of Standards and Technology. Gaithersburg, MD, September.

Luecke, W. E., T. A. Siewert, and F. W. Gayle. 2005. *Federal Building and Fire Safety Investigation of the World Trade Center Disaster: Contemporaneous Structural Steel Specifications.* NIST Special Publication 1-3A. National Institute of Standards and Technology. Gaithersburg, MD, September.

Banovic, S. W. 2005. *Federal Building and Fire Safety Investigation of the World Trade Center Disaster: Steel Inventory and Identification.* NIST NCSTAR 1-3B. National Institute of Standards and Technology. Gaithersburg, MD, September.

Banovic, S. W., and T. Foecke. 2005. *Federal Building and Fire Safety Investigation of the World Trade Center Disaster: Damage and Failure Modes of Structural Steel Components.* NIST NCSTAR 1-3C. National Institute of Standards and Technology. Gaithersburg, MD, September.

Luecke, W. E., J. D. McColskey, C. N. McCowan, S. W. Banovic, R. J. Fields, T. Foecke, T. A. Siewert, and F. W. Gayle. 2005. *Federal Building and Fire Safety Investigation of the World Trade Center Disaster: Mechanical Properties of Structural Steels.* NIST NCSTAR 1-3D. National Institute of Standards and Technology. Gaithersburg, MD, September.

Banovic, S. W., C. N. McCowan, and W. E. Luecke. 2005. *Federal Building and Fire Safety Investigation of the World Trade Center Disaster: Physical Properties of Structural Steels.* NIST NCSTAR 1-3E. National Institute of Standards and Technology. Gaithersburg, MD, September.

Evans, D. D., R. D. Peacock, E. D. Kuligowski, W. S. Dols, and W. L. Grosshandler. 2005. *Federal Building and Fire Safety Investigation of the World Trade Center Disaster: Active Fire Protection Systems.* NIST NCSTAR 1-4. National Institute of Standards and Technology. Gaithersburg, MD, September.

Kuligowski, E. D., D. D. Evans, and R. D. Peacock. 2005. *Federal Building and Fire Safety Investigation of the World Trade Center Disaster: Post-Construction Fires Prior to September 11, 2001.* NIST NCSTAR 1-4A. National Institute of Standards and Technology. Gaithersburg, MD, September.

Hopkins, M., J. Schoenrock, and E. Budnick. 2005. *Federal Building and Fire Safety Investigation of the World Trade Center Disaster: Fire Suppression Systems.* NIST NCSTAR 1-4B. National Institute of Standards and Technology. Gaithersburg, MD, September.

Keough, R. J., and R. A. Grill. 2005. *Federal Building and Fire Safety Investigation of the World Trade Center Disaster: Fire Alarm Systems.* NIST NCSTAR 1-4C. National Institute of Standards and Technology. Gaithersburg, MD, September.

Ferreira, M. J., and S. M. Strege. 2005. *Federal Building and Fire Safety Investigation of the World Trade Center Disaster: Smoke Management Systems.* NIST NCSTAR 1-4D. National Institute of Standards and Technology. Gaithersburg, MD, September.

Gann, R. G., A. Hamins, K. B. McGrattan, G. W. Mulholland, H. E. Nelson, T. J. Ohlemiller, W. M. Pitts, and K. R. Prasad. 2005. *Federal Building and Fire Safety Investigation of the World Trade Center Disaster: Reconstruction of the Fires in the World Trade Center Towers.* NIST NCSTAR 1-5. National Institute of Standards and Technology. Gaithersburg, MD, September.

Pitts, W. M., K. M. Butler, and V. Junker. 2005. *Federal Building and Fire Safety Investigation of the World Trade Center Disaster: Visual Evidence, Damage Estimates, and Timeline Analysis.* NIST NCSTAR 1-5A. National Institute of Standards and Technology. Gaithersburg, MD, September.

Hamins, A., A. Maranghides, K. B. McGrattan, E. Johnsson, T. J. Ohlemiller, M. Donnelly, J. Yang, G. Mulholland, K. R. Prasad, S. Kukuck, R. Anleitner and T. McAllister. 2005. *Federal Building and Fire Safety Investigation of the World Trade Center Disaster: Experiments and Modeling of Structural Steel Elements Exposed to Fire.* NIST NCSTAR 1-5B. National Institute of Standards and Technology. Gaithersburg, MD, September.

Ohlemiller, T. J., G. W. Mulholland, A. Maranghides, J. J. Filliben, and R. G. Gann. 2005. *Federal Building and Fire Safety Investigation of the World Trade Center Disaster: Fire Tests of Single Office Workstations.* NIST NCSTAR 1-5C. National Institute of Standards and Technology. Gaithersburg, MD, September.

Gann, R. G., M. A. Riley, J. M. Repp, A. S. Whittaker, A. M. Reinhorn, and P. A. Hough. 2005. *Federal Building and Fire Safety Investigation of the World Trade Center Disaster: Reaction of Ceiling Tile Systems to Shocks.* NIST NCSTAR 1-5D. National Institute of Standards and Technology. Gaithersburg, MD, September.

Hamins, A., A. Maranghides, K. B. McGrattan, T. J. Ohlemiller, and R. Anleitner. 2005. *Federal Building and Fire Safety Investigation of the World Trade Center Disaster: Experiments and Modeling of Multiple Workstations Burning in a Compartment.* NIST NCSTAR 1-5E. National Institute of Standards and Technology. Gaithersburg, MD, September.

McGrattan, K. B., C. Bouldin, and G. Forney. 2005. *Federal Building and Fire Safety Investigation of the World Trade Center Disaster: Computer Simulation of the Fires in the World Trade Center Towers.* NIST NCSTAR 1-5F. National Institute of Standards and Technology. Gaithersburg, MD, September.

Prasad, K. R., and H. R. Baum. 2005. *Federal Building and Fire Safety Investigation of the World Trade Center Disaster: Fire Structure Interface and Thermal Response of the World Trade Center Towers.* NIST NCSTAR 1-5G. National Institute of Standards and Technology. Gaithersburg, MD, September.

Gross, J. L., and T. McAllister. 2005. *Federal Building and Fire Safety Investigation of the World Trade Center Disaster: Structural Fire Response and Probable Collapse Sequence of the World Trade Center Towers.* NIST NCSTAR 1-6. National Institute of Standards and Technology. Gaithersburg, MD, September.

Carino, N. J., M. A. Starnes, J. L. Gross, J. C. Yang, S. Kukuck, K. R. Prasad, and R. W. Bukowski. 2005. *Federal Building and Fire Safety Investigation of the World Trade Center Disaster: Passive Fire Protection.* NIST NCSTAR 1-6A. National Institute of Standards and Technology. Gaithersburg, MD, September.

Gross, J., F. Hervey, M. Izydorek, J. Mammoser, and J. Treadway. 2005. *Federal Building and Fire Safety Investigation of the World Trade Center Disaster: Fire Resistance Tests of Floor Truss Systems.* NIST NCSTAR 1-6B. National Institute of Standards and Technology. Gaithersburg, MD, September.

Zarghamee, M. S., S. Bolourchi, D. W. Eggers, Ö. O. Erbay, F. W. Kan, Y. Kitane, A. A. Liepins, M. Mudlock, W. I. Naguib, R. P. Ojdrovic, A. T. Sarawit, P. R Barrett, J. L. Gross, and

T. P. McAllister. 2005. *Federal Building and Fire Safety Investigation of the World Trade Center Disaster: Component, Connection, and Subsystem Structural Analysis.* NIST NCSTAR 1-6C. National Institute of Standards and Technology. Gaithersburg, MD, September.

Zarghamee, M. S., Y. Kitane, Ö. O. Erbay, T. P. McAllister, and J. L. Gross. 2005. *Federal Building and Fire Safety Investigation of the World Trade Center Disaster: Global Structural Analysis of the Response of the World Trade Center Towers to Impact Damage and Fire.* NIST NCSTAR 1-6D. National Institute of Standards and Technology. Gaithersburg, MD, September.

McAllister, T., R. W. Bukowski, R. G. Gann, J. L. Gross, K. B. McGrattan, H. E. Nelson, L. Phan, W. M. Pitts, K. R. Prasad, F. Sadek. 2006. *Federal Building and Fire Safety Investigation of the World Trade Center Disaster: Structural Fire Response and Probable Collapse Sequence of World Trade Center 7.* (Provisional). NIST NCSTAR 1-6E. National Institute of Standards and Technology. Gaithersburg, MD.

Gilsanz, R., V. Arbitrio, C. Anders, D. Chlebus, K. Ezzeldin, W. Guo, P. Moloney, A. Montalva, J. Oh, K. Rubenacker. 2006. *Federal Building and Fire Safety Investigation of the World Trade Center Disaster: Structural Analysis of the Response of World Trade Center 7 to Debris Damage and Fire*. (Provisional). NIST NCSTAR 1-6F. National Institute of Standards and Technology. Gaithersburg, MD.

Kim, W. 2006. *Federal Building and Fire Safety Investigation of the World Trade Center Disaster: Analysis of September 11, 2001, Seismogram Data*. (Provisional). NIST NCSTAR 1-6G. National Institute of Standards and Technology. Gaithersburg, MD.

Nelson, K. 2006. *Federal Building and Fire Safety Investigation of the World Trade Center Disaster: The Con Ed Substation in World Trade Center 7.* (Provisional). NIST NCSTAR 1-6H. National Institute of Standards and Technology. Gaithersburg, MD.

Averill, J. D., D. S. Mileti, R. D. Peacock, E. D. Kuligowski, N. Groner, G. Proulx, P. A. Reneke, and H. E. Nelson. 2005. *Federal Building and Fire Safety Investigation of the World Trade Center Disaster: Occupant Behavior, Egress, and Emergency Communication.* NIST NCSTAR 1-7. National Institute of Standards and Technology. Gaithersburg, MD, September.

Fahy, R., and G. Proulx. 2005. *Federal Building and Fire Safety Investigation of the World Trade Center Disaster: Analysis of Published Accounts of the World Trade Center Evacuation.* NIST NCSTAR 1-7A. National Institute of Standards and Technology. Gaithersburg, MD, September.

Zmud, J. 2005. *Federal Building and Fire Safety Investigation of the World Trade Center Disaster: Technical Documentation for Survey Administration.* NIST NCSTAR 1-7B. National Institute of Standards and Technology. Gaithersburg, MD, September.

Lawson, J. R., and R. L. Vettori. 2005. *Federal Building and Fire Safety Investigation of the World Trade Center Disaster: The Emergency Response Operations.* NIST NCSTAR 1-8. National Institute of Standards and Technology. Gaithersburg, MD, September.

ACKNOWLEDGMENTS

The Structural Engineering and Earthquake Simulation Laboratory (SEESL) staff of the State University of New York at Buffalo performed the ceiling tile system tests. Mark Pitman, Technical Services Manager, and Scot Weinreber, Laboratory Assistant, played pivotal roles in the development and execution of these tests, and their support is gratefully acknowledged.

Armstrong World Industries (AWI) supplied the ceiling tile systems to SEESL. Thomas Fritz of AWI provided significant contributions to the project, including information on the ceiling tile systems installed in the World Trade Center buildings. Steven Newcomer and Barry Buhay of the Armstrong Building Products Installation School did the lion's share of the work in installing and repairing the systems during the tests.

This page left intentionally blank.

EXECUTIVE SUMMARY

E.1 CONTEXT OF THIS REPORT

The collapses of the World Trade Center (WTC) towers in New York City on September 11, 2001, were a result of damage inflicted by the aircraft and the ensuing fires within the two buildings. As seen through the windows of the towers, the fires appeared and disappeared in various segments of the affected floors. At some point in each building, the fires burned hot enough and long enough to weaken the already damaged structure to the point where it no longer could support itself.

The floor systems, each consisting of a concrete slab supported by a network of open web steel trusses, would have been exposed to the flames from combustibles burning on the floor below but for the presence of the drop ceiling system. While this ceiling system was not fire-rated, estimates indicated that they might have stayed in place for approximately 10 min to 15 min in the standard ASTM E 119 furnace environment, perhaps somewhat less in the presence of a rapidly growing fire. Observations of the fires on September 11, 2001, and computer simulations of those fires indicate that the fires did not burn more than approximately 20 min in any location. Thus, an intact ceiling tile system could have provided an important delay to the heating of the floor trusses.

Occupants of the towers reported that the impact of the airplanes resulted in some dislodging of ceiling tiles and damage to the suspension system, but descriptions of the magnitude and spatial extent of the damage were neither quantitative nor comprehensive. Thus, additional information was needed in order to estimate where the ceiling system was intact and where the heat from the fires might have impinged unabated on the floor joist assemblies.

Accordingly, a series of tests was conducted to estimate the magnitude of distress to the ceiling tile systems that would result in substantial displacement of ceiling tiles. In addition, this study was less concerned with the accelerations on the impact floors, since flying debris would likely have damaged or destroyed most of the ceiling tiles there. Instead, the concern was for the floors just above or below the impact zone, which were not directly damaged by the airplane, but had significant fires after the impact.

Under a contract from National Institute of Standards and Technology (NIST), these tests were performed using the earthquake simulator ("shaking table") at the University at Buffalo of the State University of New York (UB) from August 27 through 29, 2003. NIST and University staff provided multiple paradigms to bracket the impulses from the airplane impacts. University staff conducted the tests. Armstrong World Industries, the supplier of the original ceiling tile systems for the WTC towers, supplied the ceiling systems and assisted with the test program. The suspension system and tiles were close replicates of those originally in the towers and expected to still have been in most locations on September 11, 2001.

E.2 DESCRIPTION OF EXPERIMENTS

The UB shaking table is 12 ft (3.66 m) square and has five controlled degrees of freedom (excluding the transverse translational movement). A 20 ft (6.1 m) square testing platform was located on top of the

simulator. The maximum payload was 85 kip (378 kN), the working frequency range was 0 to 50 Hz, and the maximum displacement was ± 6 in. (0.15 m). The ceiling tile systems were mounted on a steel frame fixed to the shaking table. Accelerometers and displacement transducers monitored the response of the simulator platform, the test frame, and the ceiling support grid for each ceiling system.

Two types of ceiling tile systems were tested:

- A near replicate of that in the core areas of the towers used 12 in. (0.30 m) square tiles on a concealed suspension system.
- The original systems for the tenant spaces used 20 in. (0.51 m) square lay-in tiles on an exposed tee bar grid system. These were manufactured only for the WTC towers and were no longer available. These tests were of a nearly identical system using 24 in. (0.61 m) tiles that might have been present in many tenant spaces on September 11, 2001.

The tile suspension systems have some directionality, i.e., they are not the same along the two orthogonal horizontal directions; and the shaking table translates in only one horizontal direction. Thus, two suspension systems of each type were tested, aligned parallel and perpendicular, respectively, to the shaking table motion. Each ceiling system included two light fixtures.

Estimation of the forces and accelerations that occurred in the WTC towers was difficult due to the large number of unknown or poorly known parameters affecting the response, and because at the time there was little information available on the forces generated during such an impact. The project team thus conducted tests under a variety of excitations, hypothesizing that from the test results a pattern would emerge that would enable reasonable extrapolation to the behavior of the actual ceiling tile systems on September 11, 2001.

Each of the four ceiling tile systems was subjected to a series of single impulses that represented the simplest formulation of the aircraft impact. These ranged from 0.15g to the intensity limit of the shaking table, 1.25g. Each shake intensity was performed for a single horizontal impulse, an equal vertical impulse, and then the biaxial combination of the two. The acceleration signals for tests with small peak target accelerations were ramped displacement histories; the signals for tests exceeding a peak target acceleration of 0.085g were sinusoidal-type acceleration histories, with the frequency determined from the results of a test with white noise applied to the test fixture and ceiling tile system. The ceiling tile systems were also subjected to a standard earthquake simulation that is a sequence of complex impulses. This was deemed germane since some tower occupants reported experiencing multiple shocks. The earthquake tests began with a white noise excitation and continued with intensities of 0.25g, 0.50g, 0.75g, 1.00g, 1.25g, 1.50g, 1.75g, and 2.50g. If any distortion or damage to the system was experienced during a given test, the system was repaired before proceeding to the next test.

The outcome of each test was verbally characterized by the extent of displacement of ceiling tiles and the degree of damage to the suspension system. For summary purposes, the outcome was also described in terms of two limit states:

1. Loss of one or more tiles from the ceiling system.

2. Sufficient damage to one or more components of the suspension system such that repair or replacement of part or all of the suspension system would be required.

E.3 TEST RESULTS

The performance of the different types of ceiling systems is summarized in Table E–1, where the performance for the two limit states is given in terms of target peak acceleration of the simulator.

All four combinations of impulse and ceiling system resisted significant damage up to about 1g applied to the test platform. Since the motion of the test frame and suspension systems was considerably larger than the motion at the base of the test frame, this corresponded to about 2.5g to 3g at the ceiling frame. Tile motion intensified with increasing impulse strength, and significant damage occurred (or began to occur) for relatively modest further increments in impulse strength. Analysis of this ascending effect for all systems under all the impulses suggested that gross distortion of the framing and near-complete dropping of tiles would occur at values near 4g to 5g at the ceiling frame.

Comparison of this magnitude with the results of the impact calculations must take into account that these tests are not exact replications of the initiating events on September 11, 2001, that the installed ceiling tile systems had been in service for up to 30 years, that the tower frames were different from the test frame, and that the dimensions of the ceiling systems in the towers were the same size or smaller.

Table E–1. Performance of ceiling systems.

System Description	Impulse	Qualification Level (g)	
		Limit State 1[a]	Limit State 2[b]
East-west direction; 12 in. (305 mm) square tiles	H	>1.25	>1.25
	V	>1.25	>1.25
	H&V	>1.00	> 1.00
	EQ	–	–
East-west direction; 24 in. (610 mm) square tiles	H	>1.25	>1.00
	V	>1.25	>1.25
	H&V	>1.25	1.00
	EQ	1.75	1.75
North-south direction; 12 in. (305 mm) square tiles	H	>1.25	>1.00
	V	>1.25	1.00
	H&V	>1.25	0.75
	EQ	1.75	1.50
North-south direction; 24 in. (610 mm) square tiles	H	>1.25	>1.25
	V	>1.25	>1.25
	H&V	1.25	1.25
	EQ	1.25	12.0

a. Limit state 1 is the loss of one or more tiles.
b. Limit state 2 is sufficient damage to one or more components of the suspension system such that repair or replacement of part or all of the suspension system would be required.

Key: EQ, earthquake; H, horizontal; V, vertical.

This page intentionally left blank.

Chapter 1
INTRODUCTION

1.1 CONTEXT OF THIS REPORT

The collapses of the World Trade Center (WTC) towers 1 and 2 in New York City on September 11, 2001, were a result of damage inflicted by the aircraft and the ensuing fires within the two buildings. Fires in both buildings were observed from the times of impact of the aircraft until the collapses occurred. These fires were not stationary. As seen through the windows of the towers, they appeared and disappeared in various segments of the affected floors. At some point in each building, the fires burned hot enough and long enough to weaken the already damaged structure to the point where it no longer could support itself.

The floors in and near the aircraft impact zones in the WTC towers were large, open spaces, affording unobstructed views of much of New York City from nearly all locations. There were relatively few fire barriers. Between each tenant space and the building core there were demising walls that ran from the top of the floor slab to the bottom of the ceiling slab. A few of the floors in and near the aircraft impact zones had two tenants, and these spaces were also separated by demising walls. There were a small number of walls interior to some of the tenant spaces, generally limited to a few perimeter offices or conference rooms. These walls ran from the top of the floor slab to just above the suspension system of the drop ceiling. The ceiling tile suspension system was hung from the bottom of the floor joists, resulting in an apparent room height of 8.6 ft (2.6 m) and an above-ceiling height of approximately 3.4 ft (1.0 m). (There were two systems in the original construction, differing mainly in the size of the tiles.) In principle, then, each tenant space appeared to a fire as two wide and long "boxes." The lower box contained the combustibles; the upper box contained the floor joists that provided support for the concrete floor slab above.

An intact ceiling tile system could then have played a significant role in the event of a fire. The hot gases from a fire would have risen and formed a hot layer across the top of a room. The temperatures in this layer would have exceeded 1,000 °C, well above the threshold temperatures at which the strength of unprotected structural steels diminishes. However, as long as the ceiling tile system remained intact, this layer would have formed *below* the floor joists, and the temperature in the upper "box" would have remained relatively cool for some time interval. This delay time is most often characterized by a fire resistance rating, obtained from a standard furnace test such as ASTM E 119 (ASTM 2000).

The two particular ceiling tile systems originally installed in the WTC towers were not required to be fire rated, although the tiles themselves were rated for flame spread. Nonetheless, two independent estimates[1,2] indicated that they might have stayed in place for approximately 10 min to 15 min in the standard ASTM E 119 furnace environment, perhaps somewhat less in the presence of a rapidly growing

[1] Fritz, T.A., and P.A. Hough. 2002. Armstrong World Industries, Lancaster, PA, personal communication to R.G. Gann, National Institute of Standards and Technology, Gaithersburg, MD, December.

[2] Shipp, P. 2002. U.S. Gypsum, Northbrook, IL, personal communication to R.G. Gann, National Institute of Standards and Technology, Gaithersburg, MD, December.

fire. Observations of the fires on September 11 and computer simulations of those fires indicated that the fires did not burn more than approximately 20 min in any location. The comparability of these times suggested that information regarding the integrity of the ceiling tile systems would be pivotal in assessing the role of the floor truss assemblies in the eventual collapse of the towers.

It is clear from the accounts of building occupants that the impact of the airplanes resulted in some dislodging of ceiling tiles and damage to the suspension system (NIST NCSTAR 1-7[3]). Descriptions of the magnitude of the damage at the observers' locations and the spatial extent of the damage were neither quantitative nor comprehensive. Thus, additional information was needed in order to estimate where the ceiling system was intact and where the heat from the fires might have impinged unabated on the floor joist assemblies.

Accordingly, a series of tests was conducted to estimate the magnitude of distress to the ceiling tile systems that would result in substantial displacement of ceiling tiles. These tests were performed using the earthquake simulator ("shaking table") at the University at Buffalo of the State University of New York. NIST and University staff provided multiple paradigms to bracket the impulses from the airplane impacts. University staff conducted the tests. Armstrong World Industries, the supplier of the original ceiling tile systems for the twin towers, provided information regarding the system materials and construction and assisted with the test program. The suspension system and tiles were close replicates of those originally in the towers and expected to still have been in most locations on September 11.

The NIST Investigation also included dynamic modeling of the impact of the aircraft with the two WTC towers (NIST NCSTAR 1-2). The output of the simulations included the magnitudes and time histories of the impulses from these impacts, as felt at various locations in the buildings. The combination of those findings with these from the present report enabled estimation of the extent of displacement of the ceiling tiles throughout the zones where the fires were most intense. Conversely, the degree of agreement of this estimation of the locations where occupants observed extensive ceiling damage provided a further check on the accuracy of the impact modeling. This analysis is included in the report on the reconstruction of the fires in the WTC towers (NIST NCSTAR 1-5).

1.2 REFERENCE

ASTM International. 2000. Standard Test Methods for Fire Tests of Building Construction and Materials, vol. 4.07. ASTM E 119-00a, Annual Book of ASTM Standards, West Conshohocken, PA.

[3] This reference is to one of the companion documents from this Investigation. A list of these documents appears in the Preface to this report.

Chapter 2
DESCRIPTION OF EXPERIMENTS

2.1 GENERAL DESCRIPTION

The test series was conducted at the Structural Engineering Earthquake Simulation Laboratory (SEESL) of the University at Buffalo of the State University of New York (UB), August 27 through 29, 2003. Numerous studies related to suspended ceiling systems have been completed in recent years by the SEESL team and Armstrong World Industries, Inc. (Repp et al. 2003; Badillo 2003; Badillo et al. 2002, 2003a, 2003b; Kusumastuti et al. 2002). All of these studies and research programs have addressed the behavior of ceiling systems under earthquake excitation. This test series is related to the previous studies, but focuses on impact-type excitation on the response of selected ceiling systems.

The ceiling tile systems were mounted on a frame fixed to the shaking table. There were two ceiling tile systems—one indicative of the core space in the towers, the other indicative of the tenant spaces. (Both are described in detail in Section 2.3.) The suspension systems have some directionality, i.e., they are not the same along the two orthogonal horizontal directions; and the shaking table translates in only one horizontal direction. Thus, two suspension systems of each system type were tested, aligned parallel and perpendicular, respectively, to the shaking table motion. The table was shaken at an increasing range of intensities. Each shake intensity was performed for a single horizontal impulse, an equal vertical impulse, and then the sum of the two. The impulse shapes were based on best estimates of the airplane strikes. A few tests were conducted using a more complex impulse sequence, indicative of an earthquake. This was deemed germane since some tower occupants reported experiencing multiple shocks. If any distortion or damage to the system was experienced during a given test, the system was repaired before proceeding to the next test.

2.2 TEST FIXTURE

2.2.1 Simulator Table

The 12 ft (3.66 m) square simulator, or shaking table, had five controlled degrees of freedom (excluding the transverse translational movement), a maximum payload of 110 kip (489 kN), and a working frequency range of 0 Hz to 50 Hz. A composite reinforced concrete testing platform of plan dimensions 20 ft (6.1 m) by 10 ft (3.05 m) extended the useful testing area of the simulator, but limited the payload to 85 kip (378 kN). The testing platform included holes on a 1 ft square grid for attaching test specimens. The table was capable of testing a variety of specimens up to a height of 22 ft (6.7 m). The longitudinal (horizontal), vertical, and roll degrees of freedom were programmable with feedback control to control displacement, velocity, and acceleration simultaneously. The performance envelope of the table was ± 6 in. (0.15 m) displacement, ± 30 in./s (0.76 m/s) velocity, and 1.15g acceleration at a payload of 44 kip (197 kN) in the horizontal direction, and ± 3 in. (76 mm) displacement, ± 20 in./s (0.51 m/s) velocity, and 2.30g acceleration in the vertical direction. For a payload of 110 kip (489 kN), the maximum platform accelerations were 0.55g in the horizontal direction and 1.1g in the vertical direction.

The frequency limit of the simulator system was determined by the natural frequency of the table and the supporting actuator oil columns, both of which had a natural frequency of approximately 60 Hz. This facilitated operation of the simulator over a wide band of frequencies with small error. Input or command signals to the table could be of the following types: harmonic motions (sinusoidal, square, triangular), random motions, earthquake histories, and blast histories. Additional software was available for the collection and processing of data. Frequency and time-domain analysis of data were routinely performed. Data could also be rapidly transferred via the Internet to other computers within the University computing systems or to outside systems.

2.2.2 Test Frame

A 16 ft (4.88 m) by 16 ft (4.88 m) square frame of ASTM Grade 50 steel was constructed to test all four ceiling systems. Figures 2–1 through 2–10 present detailed information about the frame. Figure 2–1 is a plan view of the base of the frame. The frame was attached to the simulator platform using 1 in. (25 mm) diameter bolts in the beams that were oriented in the east-west direction. The frame was designed and detailed so that it could be disassembled easily.

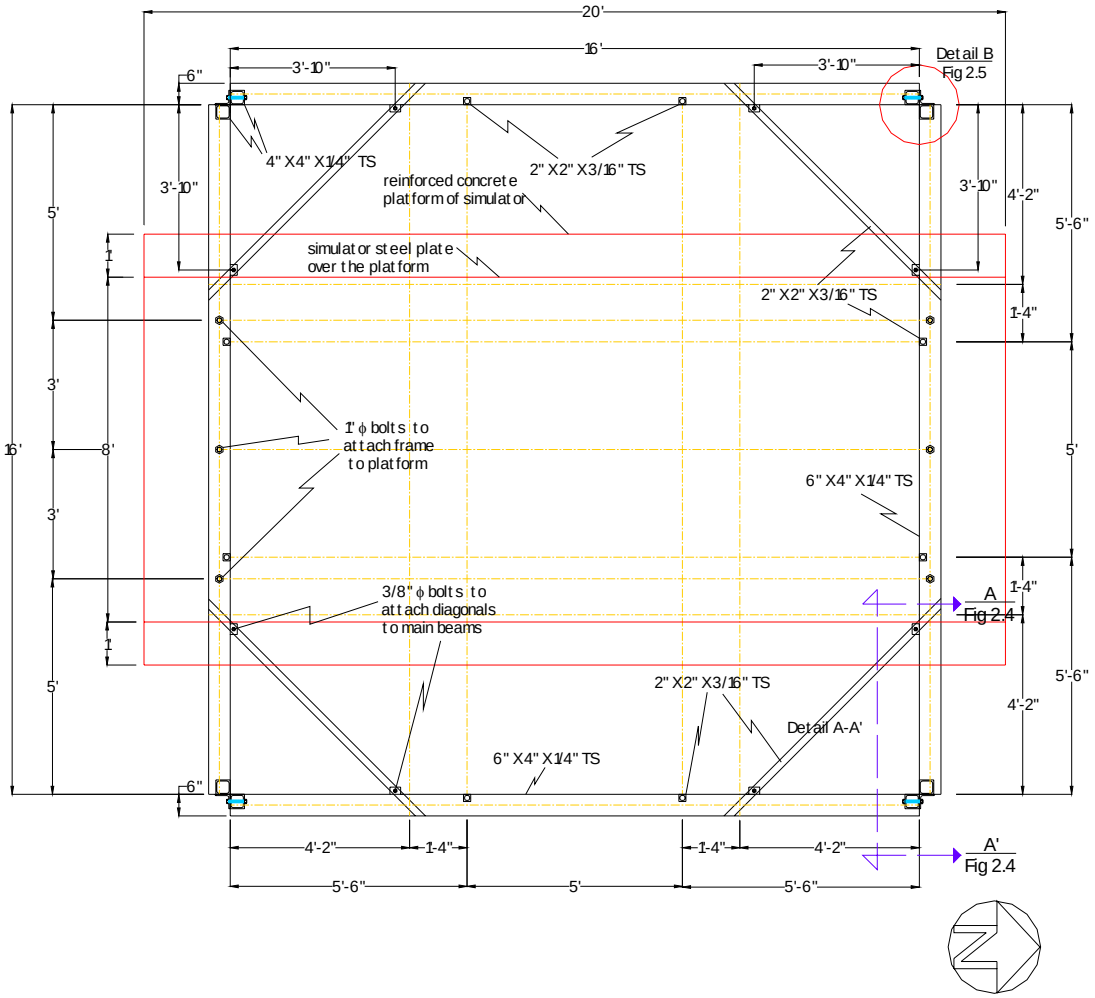

Figure 2–1. Plan view of the base of the frame.

Figure 2–2 shows the details of the top of the frame. To facilitate rapid disassembling of the test frame, the top of the frame was connected to the perimeter beams with 3/8 in. (10 mm) diameter bolts; the top of the frame was divided into two equal parts along the east-west axis. Both halves of the roof were connected with 3/8 in. (10 mm) diameter bolts as shown in the following figures.

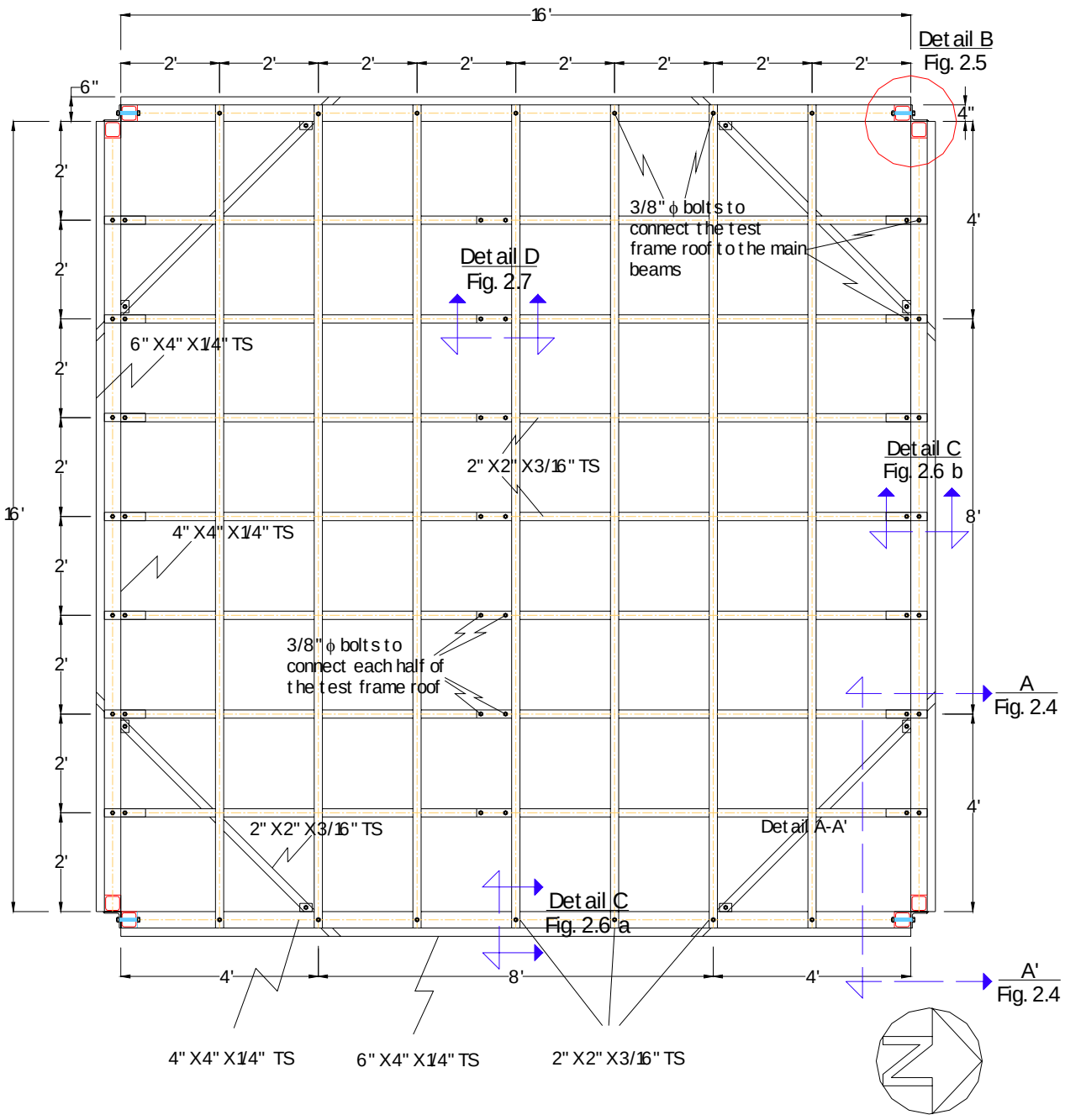

Figure 2–2. Plan view of the top of the frame.

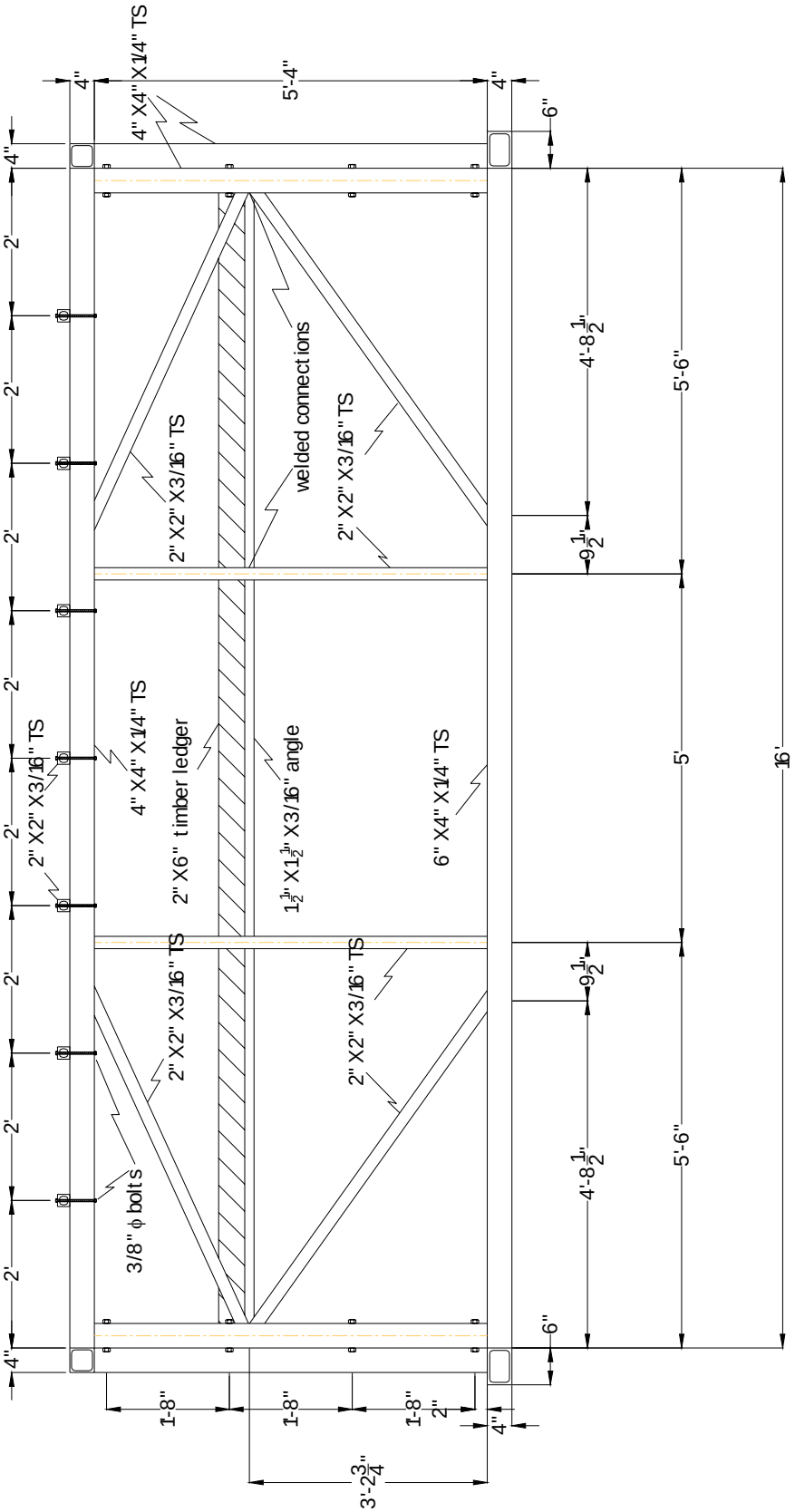

Figure 2–3. Elevation of the east side of the frame.

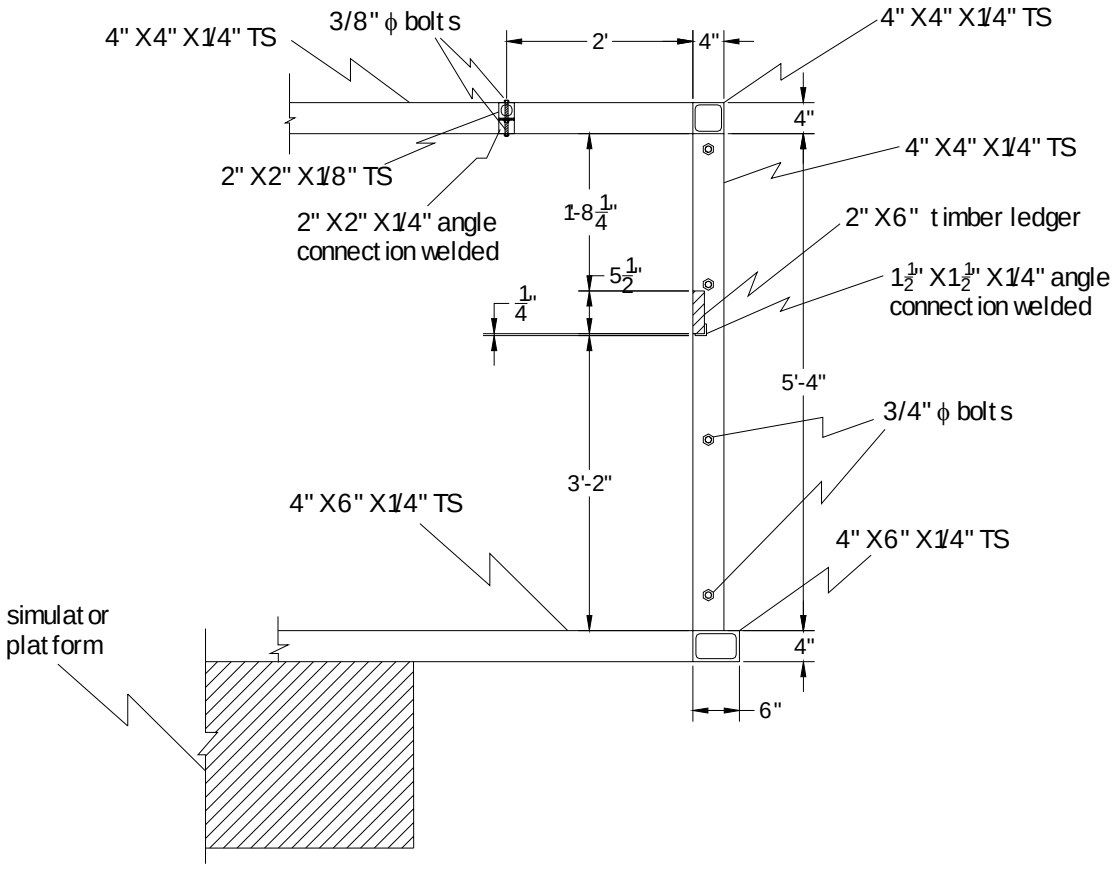

Figure 2–4. Detail A-A' frontal view of frame.

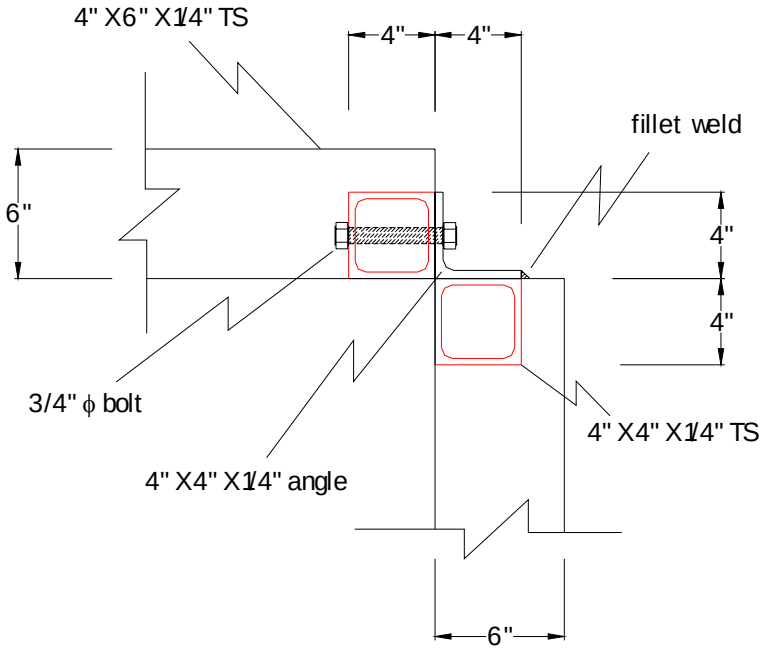

Figure 2–5. Detail B connection of corner of the frame.

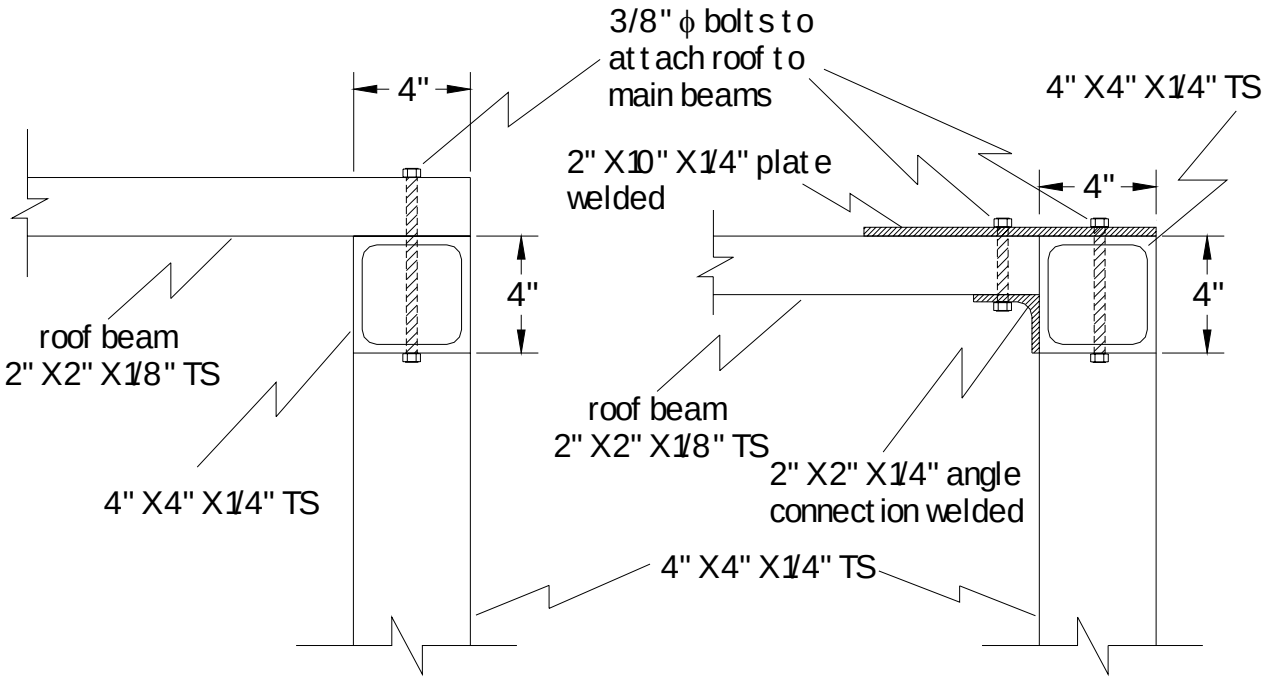

Figure 2–6. Detail C, connection of the roof with main beams.

a (left): connection in the east-west direction, b (right): connection in the north-south direction.

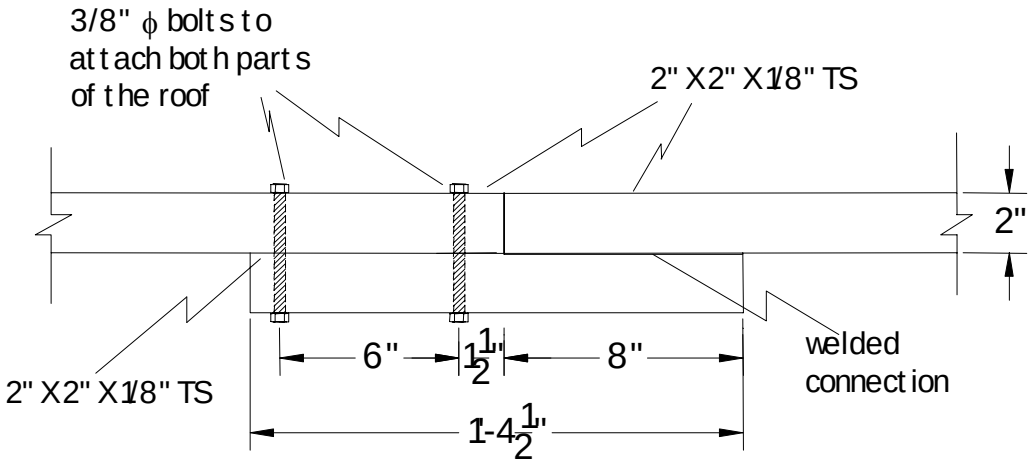

Figure 2–7. Detail D, connection of the two parts of the roof along the east-west direction.

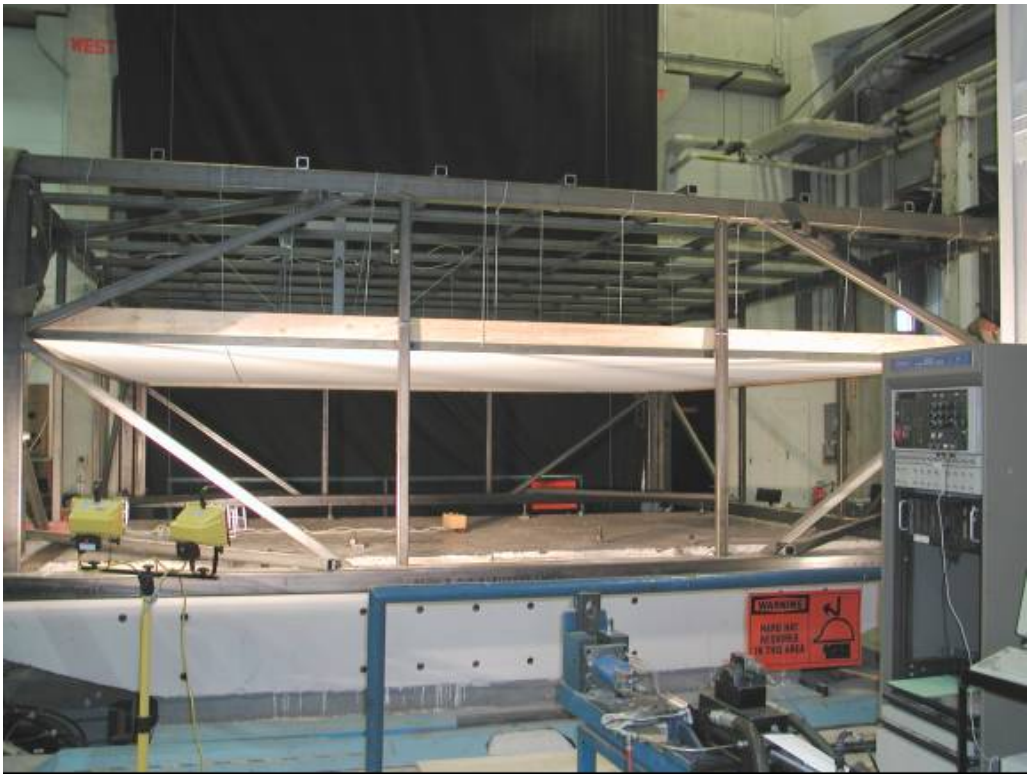

Source: NIST.

Figure 2–8. Test frame mounted on the shaking table at the University at Buffalo.

Source: NIST.

Figure 2–9. Connection of the roof to the main beams on the north side of the frame.

Source: NIST.

Figure 2–10. Connection of the roof to the main beams on the west side of the frame.

Table 2–1 lists the dynamic properties of the frame alone (no ceiling system installed and no suspension grid). The modal frequencies were determined using data from the accelerometers mounted in the frame.

Table 2–1. Dynamic properties of the frame alone.

Direction	Frequency (Hz)	Period (s)	Damping
Horizontal	12.6	0.08	4.4 %
Vertical	9.6	0.10	0.4 %

2.2.3 Instrumentation

Accelerometers and displacement transducers were used to monitor the response of the simulator platform, the test frame, and the ceiling support grid for each ceiling system. Accelerometers were located in different locations of the simulator platform (Fig. 2–11a), on top of the test frame (Figs. 2–11b and 2–12a) and on the ceiling support grid (Figs. 2–11c and 2–12b). Table 2–2 presents detailed information on the characteristics and locations of the accelerometers.

The horizontal displacement was measured with linear variable displacement transducers (LVDT). The actuators that drive the simulator platform are each equipped with two transducers (one LVDT and one accelerometer) installed in the actuator. The transducers used to measure the horizontal displacement of the frame were located on the south side of the frame. Three LVDTs were located on the top of the frame, one on each of the corners of the south side of the frame and the other in the center of that side of the frame. A fourth LVDT was located in the middle of the bottom of the south side of the test frame.

Table 2–2 lists the transducers used to monitor the displacement of the test frame. Figures 2–13 and 2–14 show the location of each transducer.

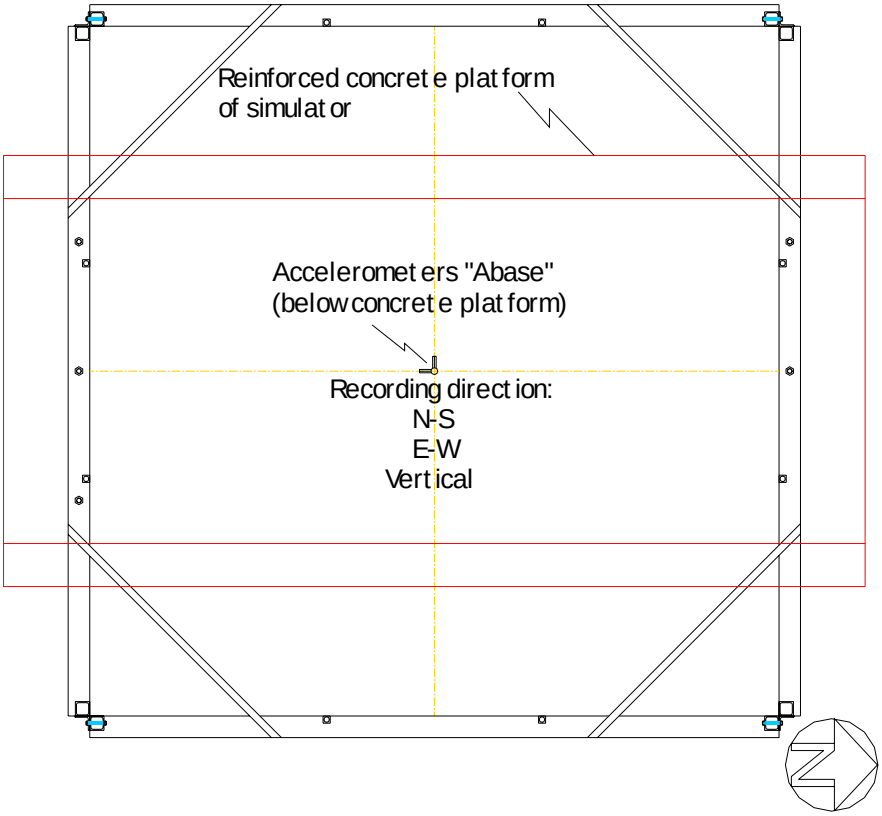

Figure 2–11a. Locations of the accelerometers on the simulator platform.

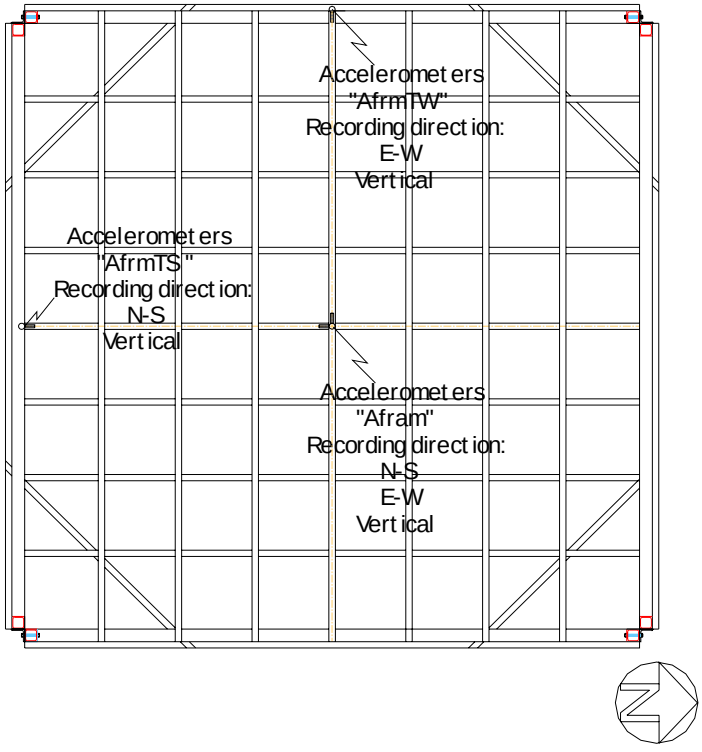

Figure 2–11b. Locations of the accelerometers on top of the testing frame.

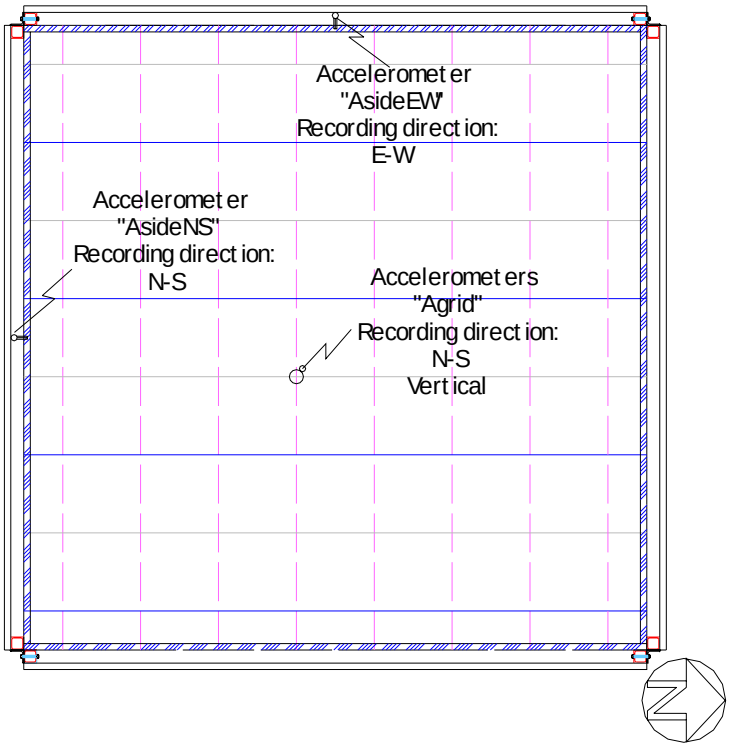

Figure 2–11c. Locations of the accelerometers on the ceiling support grid.

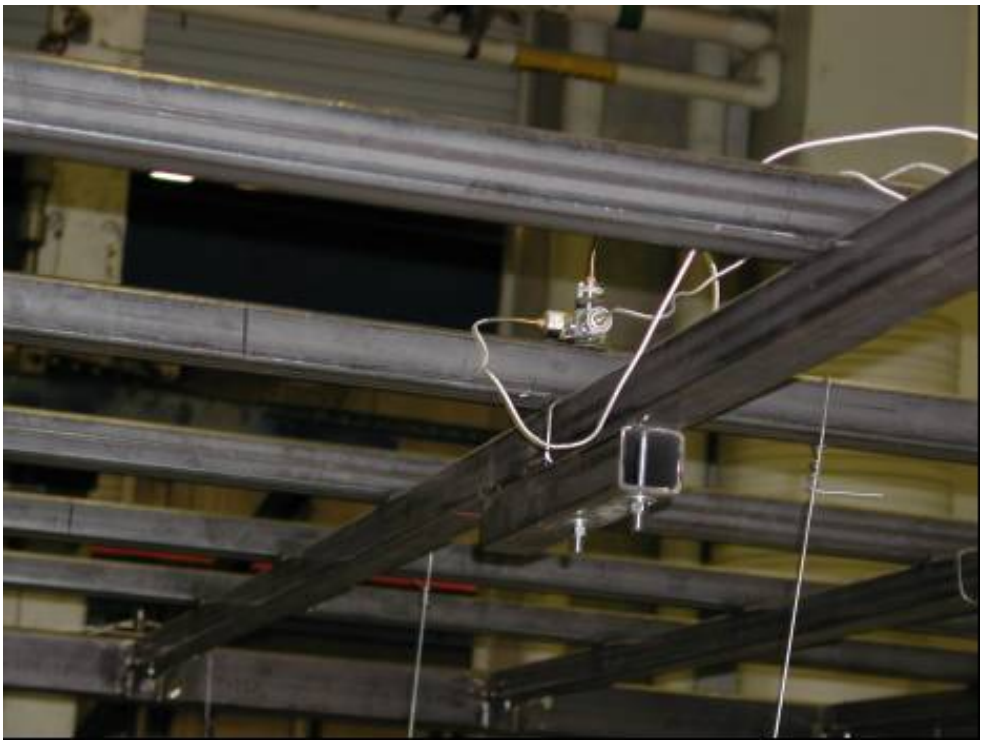

Source: NIST.

Figure 2–12a. Accelerometers monitoring the response of the test assembly in the center at the top of the test frame.

Source: NIST.

Figure 2–12b. Accelerometers monitoring the response of the test assembly on the ceiling support grid.

Table 2–2. Transducers used for the testing program.

ID	Type of Measurement	Direction of Recording	Brand	Range	Sensitivity	Location on the Test Frame
D_west	Displacement	Horizontal N-S	MTS Temposonic	± 8.2 in. (208 mm)	$2.5 \cdot 10^{-4}$ in. (6.4 μm)	West side of top of frame
D_cntr	Displacement	Horizontal N-S	MTS Temposonic	± 8.2 in. (208 mm)	$2.5 \cdot 10^{-4}$ in. (6.4 μm)	Center of top of frame
D_east	Displacement	Horizontal N-S	MTS Temposonic	± 8.2 in. (208 mm)	$2.5 \cdot 10^{-4}$ in. (6.4 μm)	East side of top of frame
D_base	Displacement	Horizontal N-S	MTS Temposonic	± 5.1 in. (130 mm)	$1.5 \cdot 10^{-4}$ in. (3.8 μm)	Center of the north side of base of frame
Abase_NS	Acceleration	Horizontal N-S	Sensotec	± 16.8g	0.009g	Center of the simulator, below concrete platform
Abase_V	Acceleration	Vertical	Sensotec	± 6.6g	0.017g	Center of the simulator, below concrete platform
Abase_EW	Acceleration	Horizontal E-W	Sensotec	± 15.2g	0.036g	Center of the simulator, below concrete platform
Afram_NS	Acceleration	Horizontal N-S	Kulite	± 25.5g	0.01g	Center of the roof of testing frame
Afram_V	Acceleration	Vertical	Kulite	± 10g	0.004g	Center of the roof of testing frame
Afram_EW	Acceleration	Horizontal E-W	Kulite	± 10.3g	0.003g	Center of the roof of testing frame
Table_H	Acceleration	Horizontal N-S	Endevco	± 2g	$6.25 \cdot 10^{-5}$g	Actuator of simulator platform (horizontal control acceleration)
Table_V	Acceleration	Vertical	Endevco	± 4g	$1.25 \cdot 10^{-4}$g	Actuator of simulator platform (vertical control acceleration)
AfrmTSNS	Acceleration	Horizontal N-S	Kulite	± 10.2g	$3.12 \cdot 10^{-4}$g	Middle of the south side of top of frame
AfrmTSV	Acceleration	Vertical	Kulite	± 10.2g	$3.12 \cdot 10^{-4}$g	Middle of the south side of top of frame
AfrmTWEW	Acceleration	Horizontal E-W	Kulite	± 10.2g	$3.12 \cdot 10^{-4}$g	Middle of the west side of top of frame
AfrmTW_V	Acceleration	Vertical	Sensotec	± 10.2g	$3.12 \cdot 10^{-4}$g	Middle of the west side of top of frame
AsideNS	Acceleration	Horizontal N-S	Square Sensotec	± 10.2g	$3.12 \cdot 10^{-4}$g	Middle of intermediate angle of the south side of frame
AsideEW	Acceleration	Horizontal E-W	Square Sensotec	± 10.2g	$3.12 \cdot 10^{-4}$g	Middle of intermediate angle of the west side of frame
Agrid_NS	Acceleration	Horizontal N-S	Square Sensotec	± 10.2g	$3.12 \cdot 10^{-4}$g	Bottom of the compression post in suspension system
Agrid_V	Acceleration	Vertical	Square Sensotec	± 10.2g	$3.12 \cdot 10^{-4}$g	Bottom of the compression post in suspension system

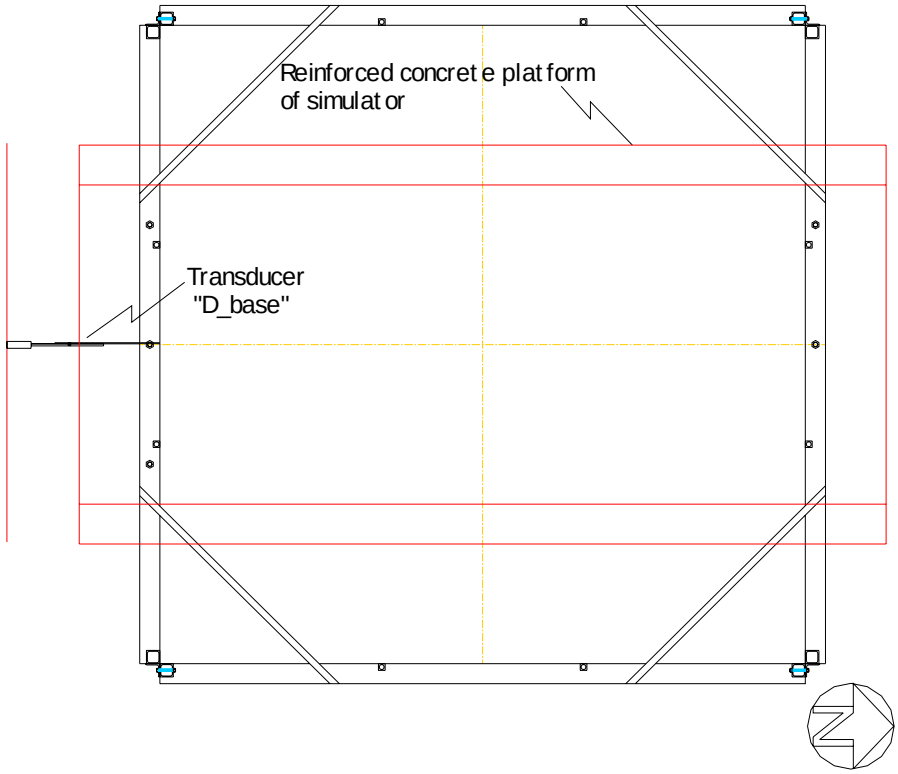

Figure 2–13a. Location of displacement transducers at the base of the testing frame.

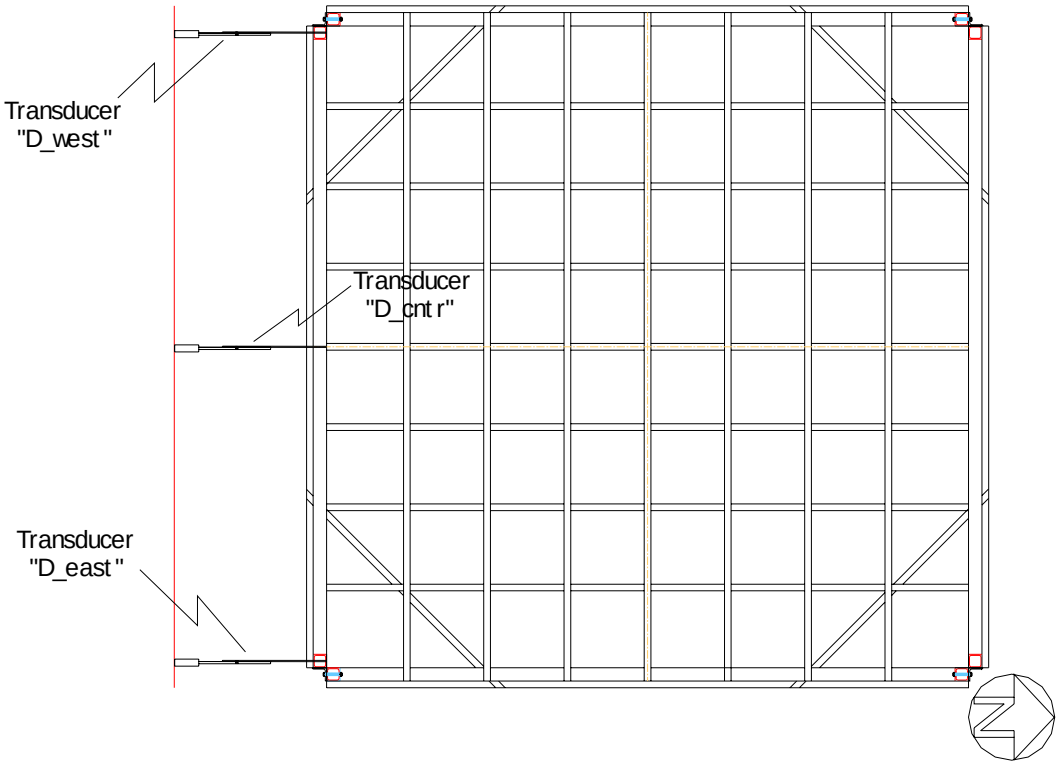

Figure 2–13b. Location of displacement transducers at the top of the testing frame.

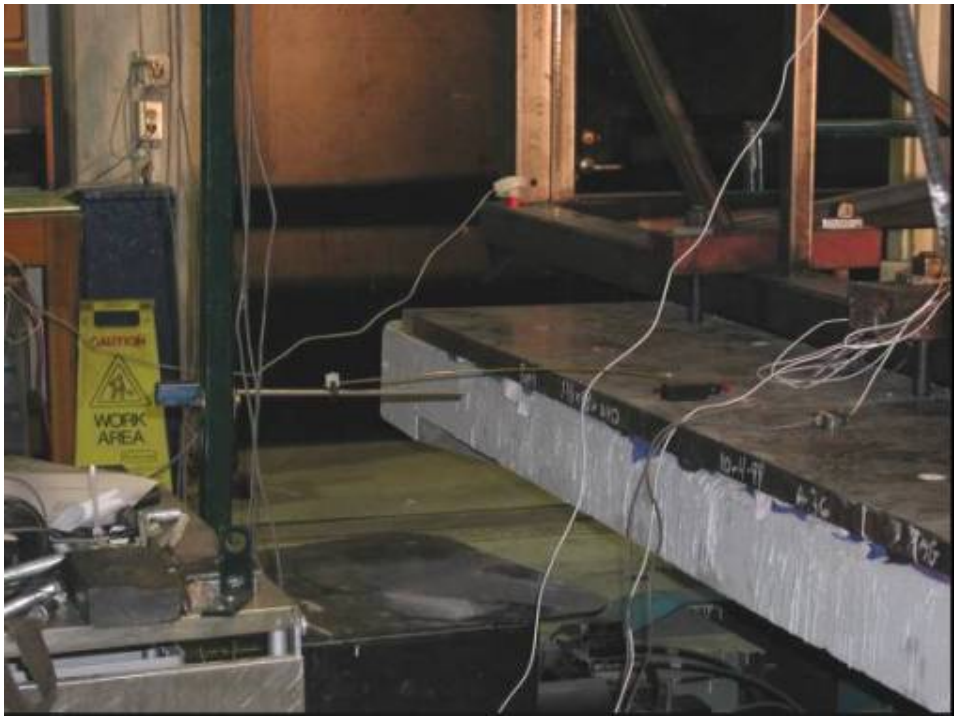

Source: NIST.

Figure 2–14a. Displacement transducers mounted on the base of the testing frame.

Source: NIST.

Figure 2–14b. Displacement transducers mounted on the top of the testing frame.

2.3 TEST SPECIMENS

2.3.1 Suspension Systems

Four different suspension systems were tested. While Systems 1 and 3 are close replicates of the systems used in the core areas of the WTC buildings, the original systems for the tenant spaces used 20 in. square tiles. These were manufactured only for the WTC towers and are no longer available. Systems 2 and 4 are similar systems using 24 in. square tiles, and might have been present in many tenant spaces on September 11, 2001.

The following subsections present the specifications and summary information for each of the four suspension systems. These four systems had many similarities that are summarized in this introduction. Systems 1 and 3, and 2 and 4 were identical except for differences arising from their different orientations with respect to the horizontal (longitudinal) axis of the simulator. Systems 1 and 3 were constructed to support 12 in. (0.30 m) square tiles on a concealed suspension system; systems 2 and 4 were constructed to support 24 in. (0.61 m) square lay-in tiles on an exposed tee bar grid system. Systems 1 and 2 had five cold rolled channel sections spanning in the east-west direction, while systems 3 and 4 had four cold rolled channel sections spanning in the north-south direction. The location of the pencil rods was identical for the four suspension systems. Each of the four suspension systems was constructed to support two light fixtures. Information on the locations of the fixtures is provided in Section 2.3.3, which describes the ceiling systems. The sections below provide a more detailed description of the member locations, connections, and materials used to construct the four suspension systems.

Suspension System 1

Table 2–3 presents summary information on each component of suspension system 1. Suspension system 1 consisted of no. 16 gauge 1½ in. (38 mm) deep cold rolled channel sections spanning in the east-west direction, which were hung by ¼ in. (6 mm) pencil rods. There were a total of five cold rolled channels. The first channel was installed 6 in. (0.15 m) from the southern edge of the test frame. The next three cold rolled channel sections were spaced at 4 ft (1.22 m) centers. The last channel was positioned 18 in. (0.46 m) from the northern edge of the test frame. The Z-bars were hung from the 16 gauge 1½ in. (38 mm) channel runners and spanned the north-south direction on 2 ft (0.61 m) centers. There were a total of eight Z-bars. The first Z-bar was located 6 in. (125 mm) from the western edge of the test frame. The next six Z-bars were spaced at 2 ft (0.61 m) on center. The final Z-bar was positioned 18 in. (0.46 m) from the eastern edge of the test frame. Two ft (0.61 m) tee splines spanned in the east-west direction between the Z-bar sections and were spaced every 12 in. (0.30 m). Breather splines were installed in every tile that was supported between tee splines.

The cold rolled channel sections were hung from ¼ in. (6 mm) pencil rods, which were connected to the top of the test frame. There were a total of 20 pencil rods, which were spaced at 4 ft (1.22 m) centers. Each pencil rod was connected to the top of the test frame using CADDY[4] fasteners as shown in Fig. 2–15. The CADDY fasteners were secured to the test frame using 4 in. (0.10 m) C-clamps as shown in Fig. 2–16. The pencil rod was attached to the cold rolled channel main runners using a CADDY side mount channel clamp, similar that used to connect the pencil rod to the top of the test frame, and is shown

[4] CADDY is a trademark of ERICO Products, Inc.

in Fig. 2–17. The Z-bar cross runners were hung from the cold rolled channel runners by C-15 wire Z-bar clamps (Figs. 2–18 and 2–19). The cold rolled channel section runners were secured to the edge of the test frame using XTAC clips, which were screwed to the channel and the edge of the test frame (Figs. 2–20 and 2–21). Figure 2–22 is a photograph of a breather spline.

Table 2–3. Summary information on components of suspension systems 1 and 3.

Component	Item no.	Description	Dimensions (in., mm)	Comments
Channel section	NA	Cold rolled channel	1½, 38	Channel runner was hung from pencil rods.
Z-bar beams	7300	Z section runners	NA	Z-bar beam splices were staggered; spanned along cold rolled channel.
Two-foot tee splines	S-392	T section spline	2, 51	Spanned between Z-bar runners and spaced at 1 ft. (305 mm) centers.
Breather splines	7486	Spline strip	11½, 292	Strips installed into each panels; spanned between two-foot tee splines.
¼ in. pencil rod	NA	Rod suspension support	¼ × 36, 6 × 914	Supported cold rolled channel section runners; spaced at 4 ft. (1.22 m) centers.
4 in. C-clamp	NA	Adjustable clamp	NA	Connected CADDY to test frame.
CADDY 708AB	708AB	Angle bracket support	NA	Connected top of pencil rod to test frame.
CADDY 4B15LS	B15LS	Side mount channel clamp	NA	Connected bottom of pencil rod to cold rolled channel runner.
Cross-tee adapter clip	XTAC	C-channel connector	NA	Connected cold rolled channel section runners to edge of test frame.
C-15 wire Z-bar clamps	C15	Wire connection bracket	NA	Connected cold rolled channel section runners to Z-bars.
Channel molding	7830	Hemmed angle molding	15/16 × 1 15/16 × 120, 13 × 49 × 3050	Hemmed angle molding with pre-finished exposed flanges.

Source: NIST.

Figure 2–15. Top (left) and bottom (right) CADDY fasteners in suspension system 1.

Source: NIST.

Figure 2–16. C-clamp and top CADDY fastener in suspension system 1.

Source: NIST.

Figure 2–17. Bottom CADDY fastener in suspension system 1.

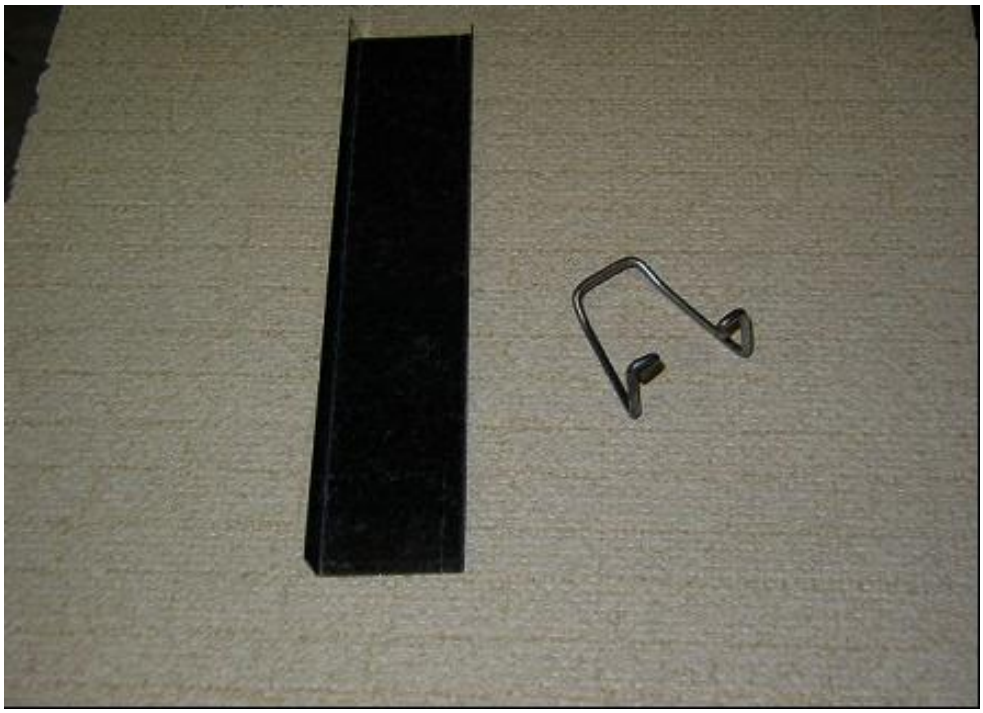

Source: NIST.

Figure 2–18. Z-bar section (left) and C-15 wire clip (right) in suspension system 1.

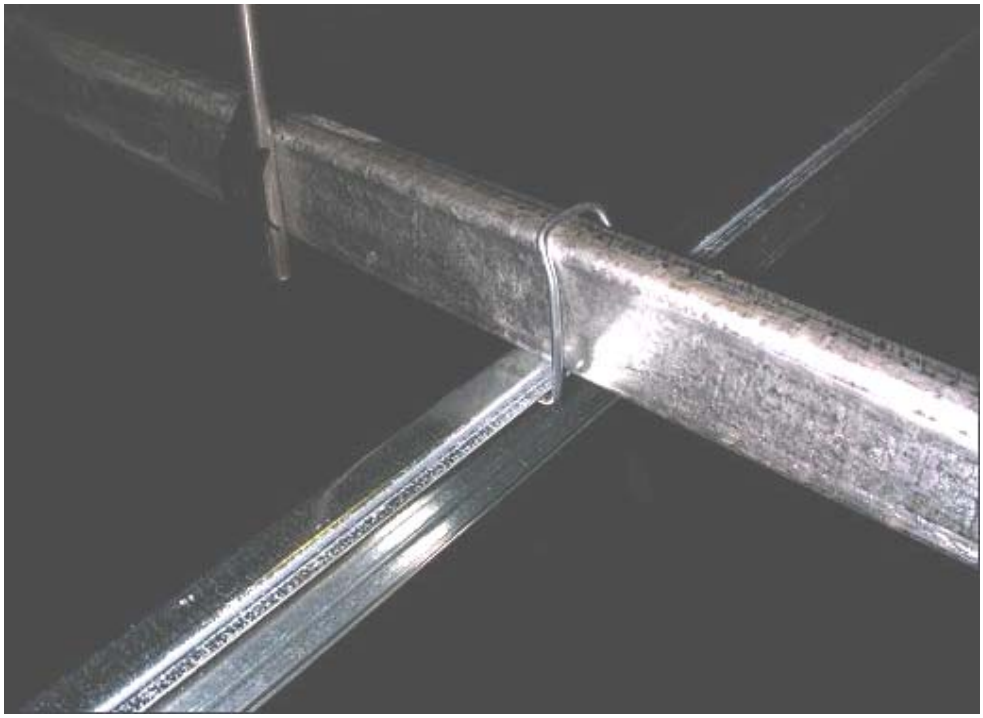

Source: NIST.

Figure 2–19. Channel section runner connection to Z-bar in suspension system 1.

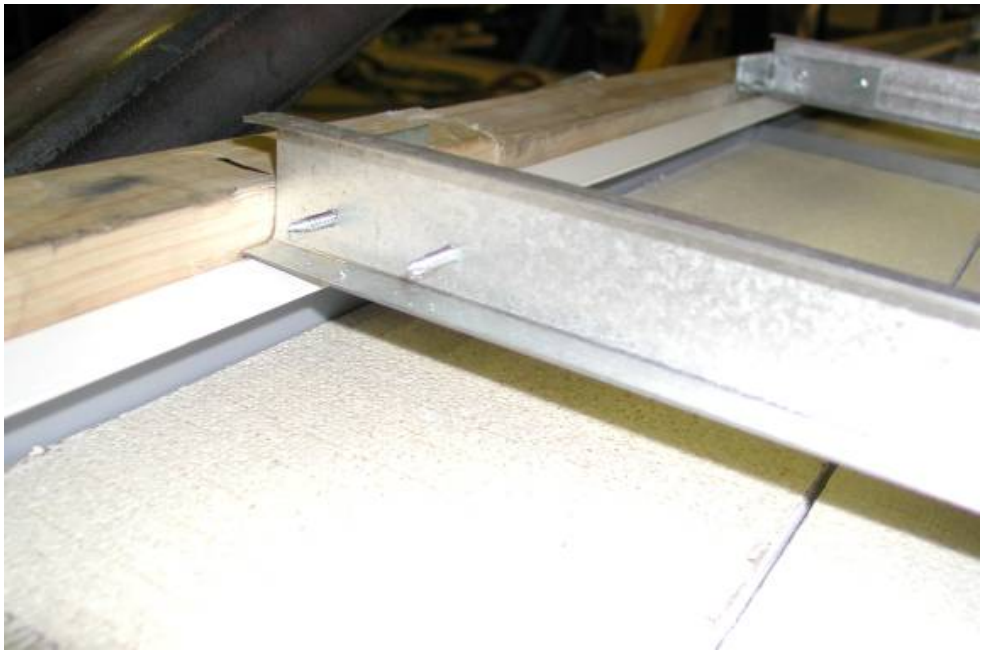

Source: NIST.

Figure 2–20. Channel section runner connection to edge of test frame in suspension system 1.

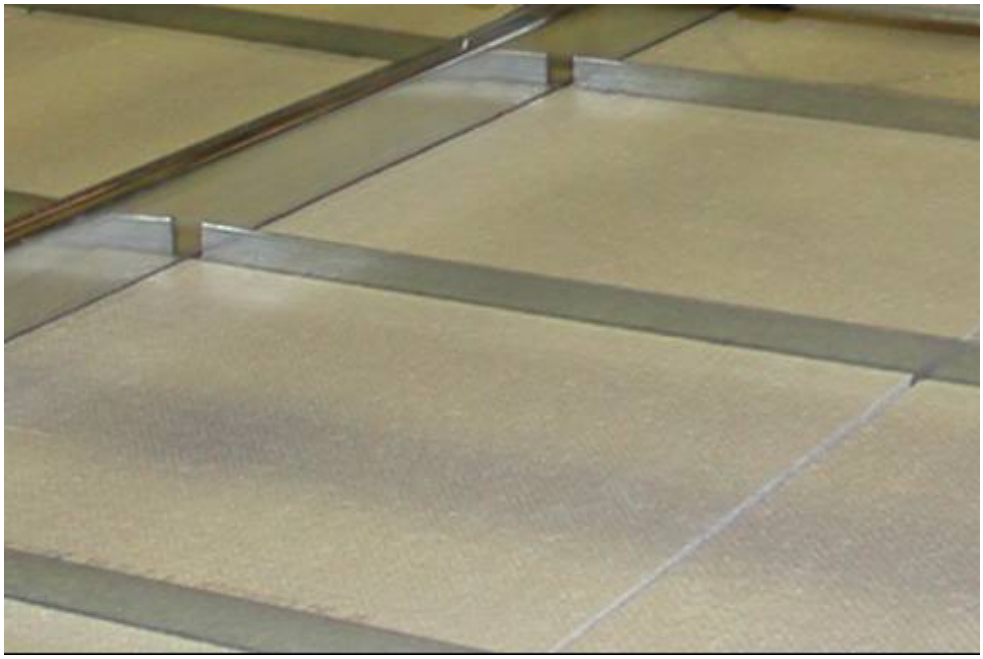

Source: NIST.

Figure 2–21. Two ft (0.61 m) cross tee used in suspension system 1.

Source: NIST.

Figure 2–22. Breather spline used in suspension system 1.

Suspension System 2

Table 2–4 presents summary information on each component of suspension system 2. Suspension system 2 consisted of 1½ in. (38 mm) deep cold rolled channel sections spanning in the east-west direction, which were hung by ¼ in. (6 mm) pencil rods. There were a total of five cold rolled channels. The first channel was installed 18 in. (0.46 m) from the southern edge of the test frame. The next three cold rolled channel sections were spaced at 4 ft (1.22 m) centers. The last channel was positioned 6 in. (0.15 m) from the northern edge of the test frame. Prelude main runners were hung from the 16 gauge 1½ in. (38 mm) deep cold rolled channels and spanned in the north-south direction at 4 ft (0.61 m) centers. There were a total of four main runners. The first main runner was installed 36 in. (0.91 m) from the western edge of the test frame. The next two main runners were spaced on 4 ft (1.22 m) centers. The final main runner was positioned 1 ft (0.305 m) from the eastern edge of the test frame. Four ft (1.22 m) cross tees spanned in the east-west direction between the main runner sections and were spaced every 2 ft (0.61 m). Two ft (0.61 m) cross tees spanned north-south between the 4 ft (1.22 m) cross tee sections and were spaced at 24 in. (0.61 m) on center.

The cold rolled channels were hung from ¼ in. (6 mm) pencil rods, which were connected to the top of the test frame. There were a total of 20 pencil rods, which were spaced at 4 ft (1.22 m) centers. The pencil rod was connected to the top of the test frame using CADDY clips. The CADDY clips were secured to the test frame using two 4 in. (0.10 m) C-clamps as shown in Fig. 2–23. One clamp was positioned to fasten the CADDY clip to the test frame. The other clamp was positioned to fasten the pencil rod to the test frame to prevent upward movement during testing. The pencil rod was attached to the cold rolled channels using a CADDY side mount channel clamp. The main runners were hung from the cold rolled channels by CBS clips (Fig. 2–24). Cold rolled channel sections were secured to the edge of the test frame using XTAC clips, which were screwed to the channel and the test frame edge.

Table 2–4. Summary information on components of suspension systems 2 and 4.

Component	Item no.	Description	Dimensions (in., mm)	Comments
Cold rolled channels	NA	C-channel	1½, 38	Hung from pencil rods.
Main beams	7300	Heavy duty main runner	1 5/16 × 1 11/16, 33 × 43	Double web with peaked roof top bulb and bottom flange with pre-finished steel capping. Main beam splices were staggered.
48 in. cross tees	XL7342	4 ft long cross tee	48 × 15/16 × 1 3/8, 1220 × 33 × 35	Double web with peaked roof top bulb, bottom flange with pre-finished steel cap and override at each end.
24 in. cross tees	XL7328	2 ft long cross tee	24 × 1 5/16 × 1 3/8, 610 × 33 × 35	Double web with peaked roof top bulb, bottom flange with pre-finished steel cap and override at each end.
¼ in. pencil rod	NA	Rod suspension support	¼ × 36, 6.4 × 914	Supported cold rolled channel sections. Spaced at 4 ft (1.22 m) centers.
4 in. C-clamp	NA	Adjustable connection clamp	NA	Connected CADDY to test frame. Two clamps used at each connection.
CADDY 708AB	708AB	Angle bracket support	NA	Connected top of pencil rod to test frame.
CADDY 4B15LS	4B15LS	Side mount channel clamp	NA	Connected bottom of pencil rod to cold rolled channel sections.
Cross-tee adapter clip	XTAC	C-channel connector	NA	Connected cold rolled channel sections to edge of test frame.
6 in. channel beam splice	CB56	Clip to main runners	NA	Connected cold rolled channel sections to main runners.
7/8 in. wall molding	7800	Hemmed angle molding	7/8 × 7/8 × 144, 22 × 22 × 3660	Hemmed angle molding with pre-finished exposed flanges.

Source: NIST.

Figure 2–23. C-clamps and top CADDY clip in suspension system 2.

Source: NIST.

Figure 2–24. CBS clip connecting channel to main runner in suspension system 2.

Suspension System 3

Suspension system 3 was similar to suspension system 1. Suspension system 3 consisted of no. 16 gauge 1½ in. (38 mm) deep cold rolled channel sections spanning in the north-south direction. These channel sections were hung by ¼ in. (6 mm) pencil rods from the test frame. There were a total of four cold rolled channel section runners. The first channel runner was located 2 ft (0.61 m) from the eastern edge of the test frame. The next two channel runners were spaced at 4 ft (1.22 m) centers. The fourth channel runner was located 2 ft (0.61 m) from the western edge of the test frame. The Z-bars were hung from the 16 gauge 1½ in. (38 mm) deep channel runners and spanned in the east-west direction at 2 ft (0.61 m) centers. There were a total of eight Z-bars. The first Z-bar was located 1.5 ft (457 mm) from the southern edge of the test frame. The next six Z-bars were spaced at 2 ft (0.61 m) on center. The final Z-bar was located 6 in. (0.15 m) from the northern edge of the test frame. Two ft (0.61 m) tee splines spanned in the north-south direction between the Z-bar sections and were spaced every 1 ft (0.30 m). Breather splines were installed in every tile that was supported between tee splines.

The cold rolled channel sections were hung from ¼ in. (6 mm) pencil rods, which were connected to the top of the test frame. There were a total of 20 pencil rods, which were spaced at 4 ft (1.22 m) centers. The pencil rod was connected to the top of the test frame using CADDY clips. The CADDY clips were secured to the test frame using of 4 in. (0.10 m) C-clamps. One clamp was positioned to fasten the CADDY clip to the test frame. The other clamp was positioned to fasten the pencil rod to the test frame to prevent upward movement during testing. The pencil rod was attached to the cold rolled channel main runners using a CADDY side mount channel clamp similar to that used to connect the pencil rod to the top of the test frame. The Z-bar cross runners were hung from the cold rolled channel runners by C-15 wire Z-bar clamps. The cold rolled channel section runners were secured to the edge of the test frame using XTAC clips, which were screwed to the channel and the edge of the test frame. Table 2–3 presents summary information on each component of suspension system 3.

Suspension System 4

Suspension system 4 was similar to suspension system 2. This suspension system consisted of 1½ in. (38 mm) deep cold rolled channel sections spanning in the north-south direction, which were hung from ¼ in. (6 mm) pencil rods. There were a total of four cold rolled channels. The first channel was 2 ft (0.45 m) from the eastern edge of the test frame. The next two cold rolled channels were spaced on 4 ft (1.22 m) centers. The last channel was positioned 2 ft (0.61 m) from the western edge of the test frame. Prelude main runners were hung from the 16 gauge, 1½ in. (38 mm) deep cold rolled channels and spanned the east-west direction on 4 ft (0.61 m) centers. There were a total of four main runners. The first main runner was installed 3 ft (0.91 m) from the northern edge of the test frame. The next two main runners were spaced at 4 ft (1.22 m) centers. The fourth main runner was located 1 ft (0.30 m) from the southern edge of the test frame. Four ft (1.22 m) cross tees spanned in the north-south direction between the main runner sections and were spaced at 2 ft (0.61 m) centers. Two ft (0.61 m) cross tees spanned in the east-west direction between the 4 ft (1.22 m) cross tees sections and were spaced at 2 ft (0.61 m) centers.

The cold rolled channels were hung from ¼ in. (6 mm) pencil rods, which were connected to the top of the test frame. There were a total of 20 pencil rods, which were spaced at 4 ft (1.22 m) centers. The pencil rod was connected to the top of the test frame using CADDY clips. The CADDY clips were

secured to the test frame through the use of two 4 in. (0.10 m) C-clamps. One clamp was positioned to fasten the CADDY clip to the test frame. The other clamp was positioned to fasten the pencil rod to the test frame to prevent upward movement during testing. The pencil rod was attached to the cold rolled channels using a CADDY side mount channel clamp. The main runners were hung from the cold rolled channels by CBS clips. Cold rolled channel sections were secured to the edge of the test frame using XTAC clips, which were screwed to the channel and the test frame edge. Table 2–4 presents summary information on each component of suspension system 4.

2.3.2 Tiles

Table 2–5 presents summary information on the two types of ceiling tiles examined in this study.

Table 2–5. Tile specifications.

Tile ID	Panel name	Description	Panel Dimensions (in., m) Breadth, Depth, Thickness	Approximate Weight (lb/ft^2)
1	K4C4	Beveled edge tile (Armstrong Item No. BF 592A)	12, 12, NA, 0.305, 0.305, NA	1.00
2	Ultima Beveled Tegular Humigard Plus	Acoustical mineral fiber tile (Armstrong Item No. 1911A)	24, 24, 3/4, 0.61, 0.61, 0.019	1.00

2.3.3 Ceiling Systems

This section provides information on each of the four ceiling systems tested in this study. Table 2–6 lists summary information on components of each ceiling system.

Table 2–6. Configuration of ceiling systems.

Test Series	Ceiling System ID	Suspension System ID[a]	Tile ID[b]	Figure No.[c]	Comments
TS1	CS1	1	1	2–25 to 2–31	System with cold rolled sections spanning in the east-west direction. Tiles were 12 in. (0.30 m) square.
TS2	CS2	2	2	2–32 to 2–35	System with cold rolled sections spanning in the east-west direction. Tiles were 24 in. (0.61 m) square.
TS3	CS3	3	1	2–36 to 2–41	System with cold rolled sections spanning in the north-south direction. Tiles were 12 in. (0.30 m) square.
TS4	CS4	4	2	2–42 to 2–43	System with cold rolled sections spanning in the north-south direction. Tiles were 24 in. (0.61 m) square.

a. See Section 2.3.2 for suspension system ID number.
b. See Table 2–5 for tile ID number.
c. Refers to a figure number in this report.

Ceiling System CS1

System CS1 was composed of suspension system 1 and tile 1. Figures 2–25 through 2–29 are photographs of system CS1. There were 16 panels spanning in both the east-west and north-south directions. The ceiling system was constructed flush to the edge of the test frame on all sides. Six in. (0.15 m) perimeter tiles had perimeter spring clips installed between the tile and the edge of the test frame. The total ceiling area was approximately 256 ft^2 (23.8 m^2): 16 ft (4.87 m) in the east-west direction by 16 ft (4.87 m) in the north-south direction. Figures 2–30 and 2–31 show the ceiling system layout for ceiling system CS1. Two 1 ft (0.30 m) by 4 ft (1.22 m) light fixtures were installed in the ceiling with light clips and two safety wires. The lights were supported on the grid by four swinging arms.

Ceiling System CS2

System CS2 was composed of suspension system 2 and tile 2. Figures 2–32 through 2–34 are photographs of system CS2. There were seven full panels and two half panels spanning in both the east-west and north-south directions. The ceiling system was constructed flush to all edges of the test frame. The total ceiling area was approximately 256 ft^2 (23.8 m^2): 16 ft (4.87 m) in the east-west direction by 16 ft (4.87 m) in the north-south direction. Figure 2–35 shows the ceiling system layout for ceiling system S2. Two 2 ft (0.61 m) by 4 ft (1.22 m) light fixtures were installed in the ceiling with light clips and two safety wires.

Source: NIST.

Figure 2–25. Bottom view of ceiling system CS1.

Source: NIST.

Figure 2–26. Close-up of top view of ceiling system CS1.

Source: NIST.

Figure 2–27. Top view of ceiling system CS1.

Source: NIST.

Figure 2–28. 12 in. by 48 in. (0.30 m by 1.22 m) fixture with safety clip and wires in ceiling system CS1.

Source: NIST.

Figure 2–29. Panel perimeter spring clips in ceiling system CS1.

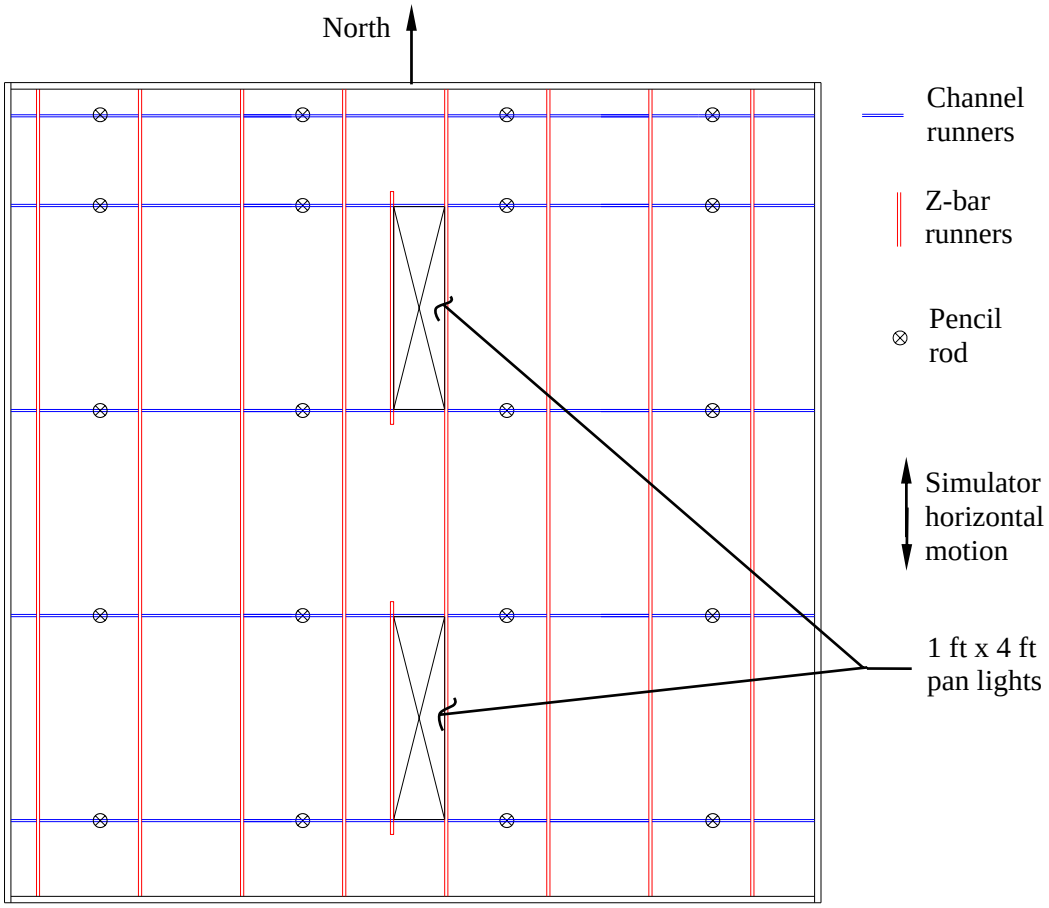

Figure 2–30. Layout of main supporting members in ceiling system CS1.

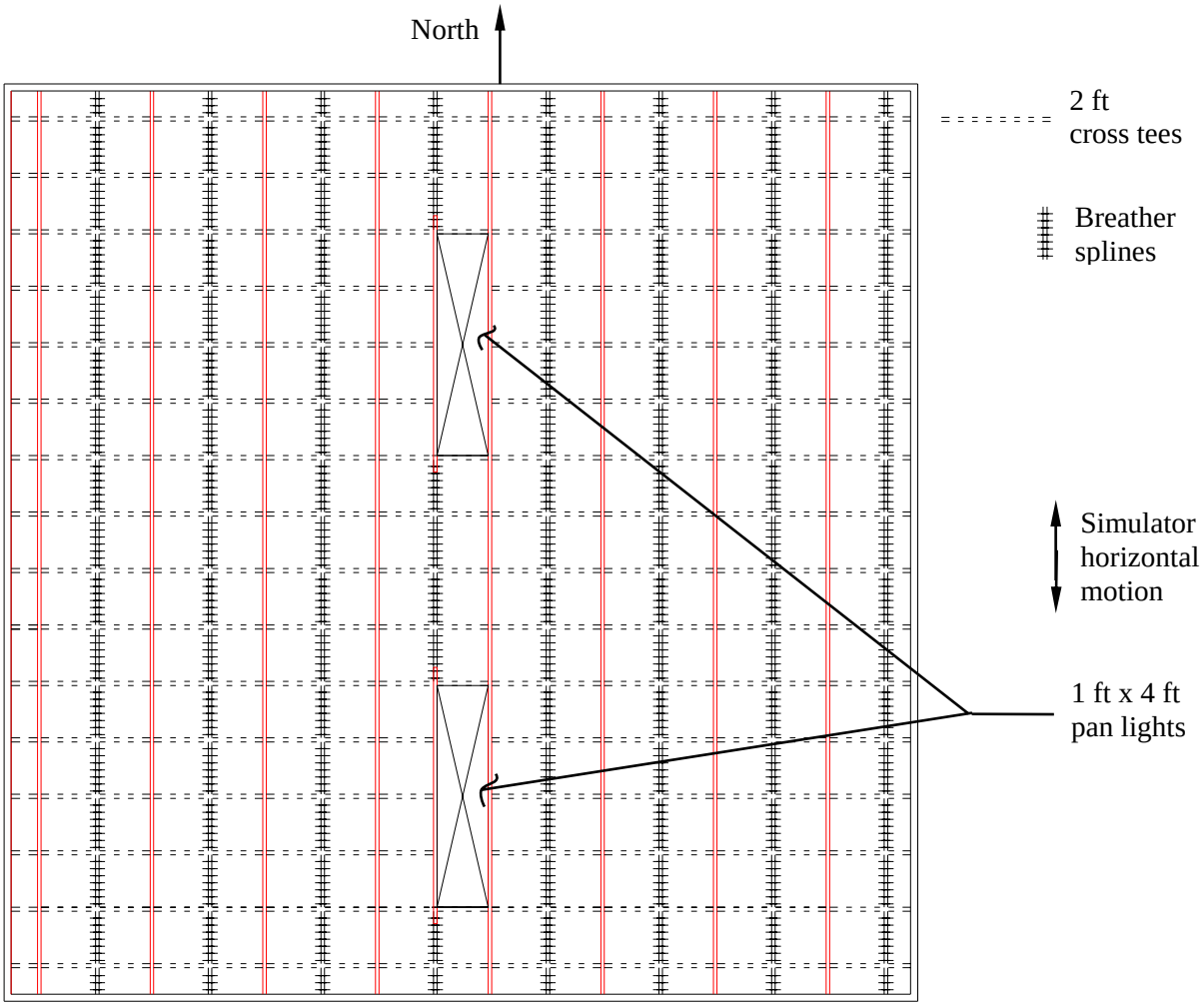

Figure 2–31. Layout of splines and cross tees in ceiling system CS1.

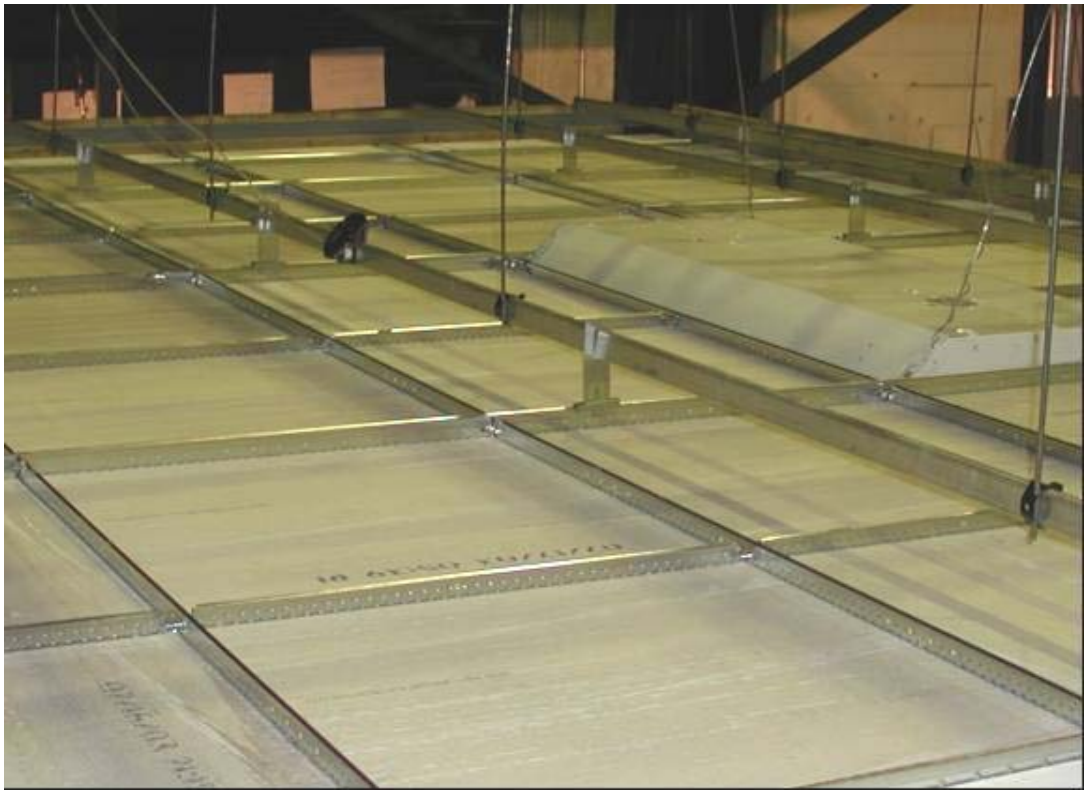

Source: NIST.

Figure 2–32. Top view of ceiling system CS2.

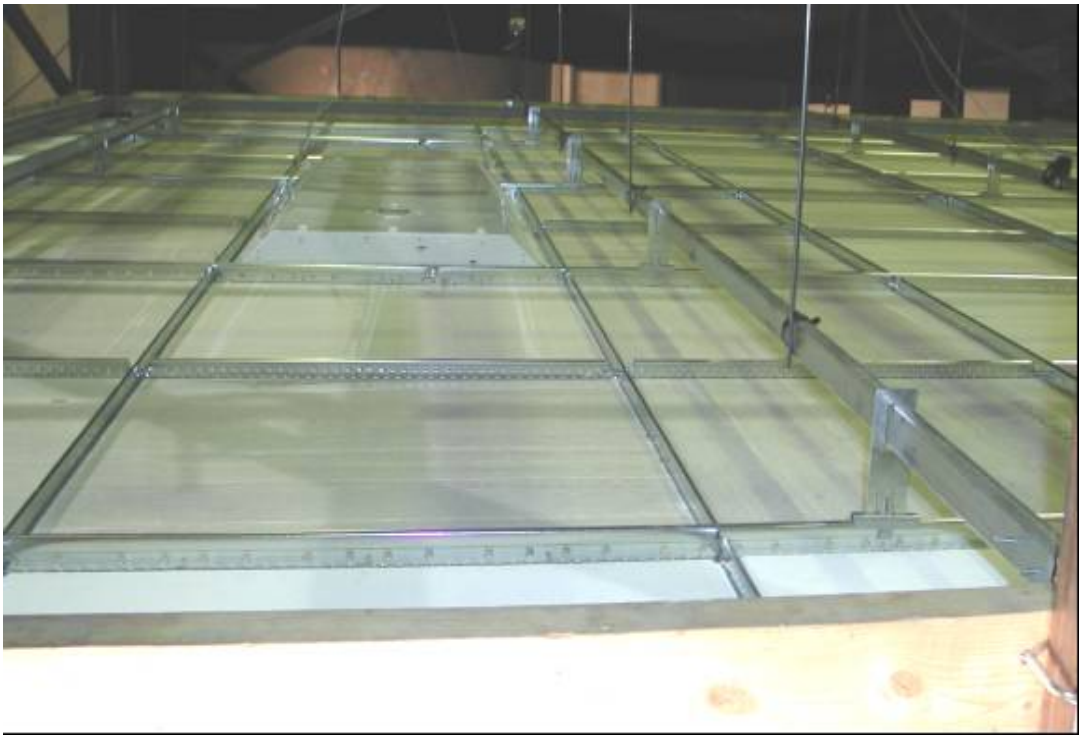

Source: NIST.

Figure 2–33. Top view of ceiling system CS2.

Source: NIST.

Figure 2–34. Bottom view of ceiling system CS2.

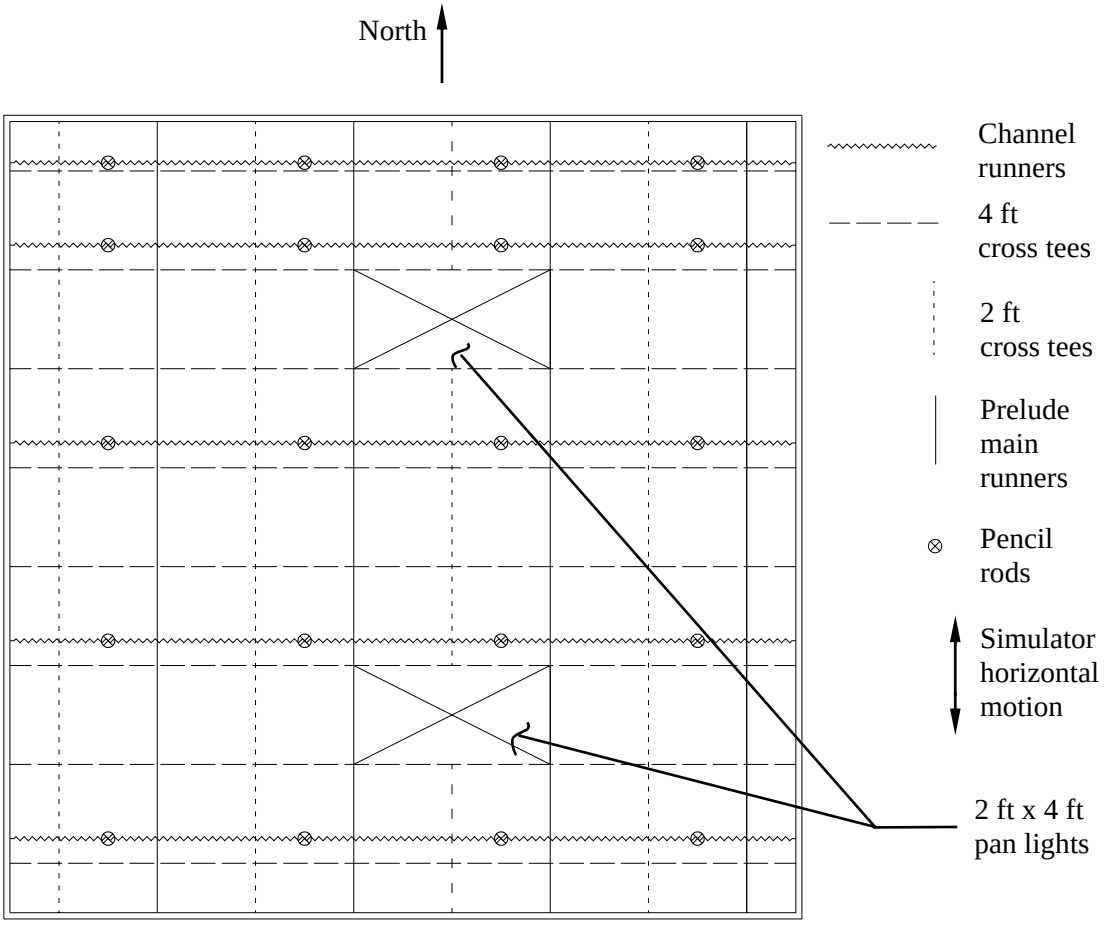

Figure 2–35. Layout for ceiling system CS2.

Ceiling System CS3

System CS3 was composed of suspension system 3 and tile 1. Ceiling system CS3 was similar to ceiling system CS1 except that this system had channel sections spanning in the north-south direction. Figures 2–36 and 2–37 are photographs of system CS3. There were 16 panels spanning in both the east-west and north-south directions. The ceiling system was constructed flush to the edge of the test frame on all sides. Six in. (1.52 m) perimeter tiles had perimeter spring clips installed between the tile and the edge of the test frame. The total ceiling area was approximately 256 ft^2 (23.8 m^2): 16 ft (4.87 m) in the east-west direction by 16 ft (4.87 m) in the north-south direction. Figures 2–38 and 2–39 show the ceiling system layout for ceiling system CS3. Two 1 ft (0.30 m) by 4 ft (1.22 m) light fixtures were installed in the ceiling with light clips and two safety wires. The lights were supported on the grid by four swinging arms.

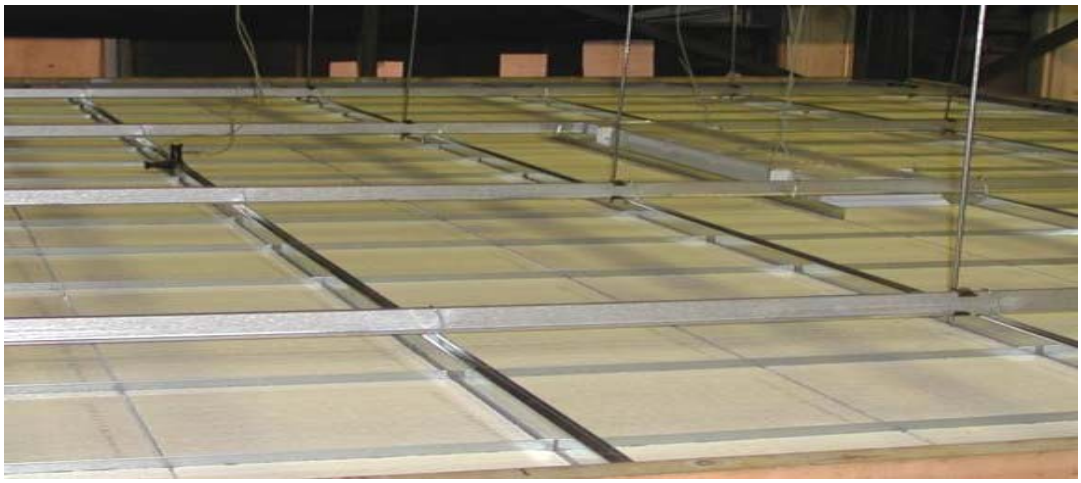

Source: NIST.

Figure 2–36. Top view of ceiling system CS3.

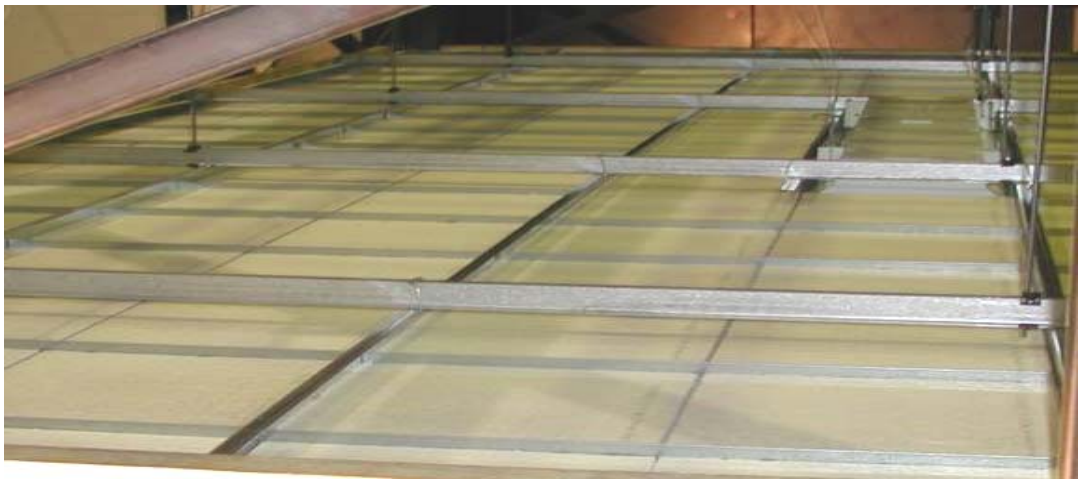

Source: NIST.

Figure 2–37. Top view of ceiling system CS3.

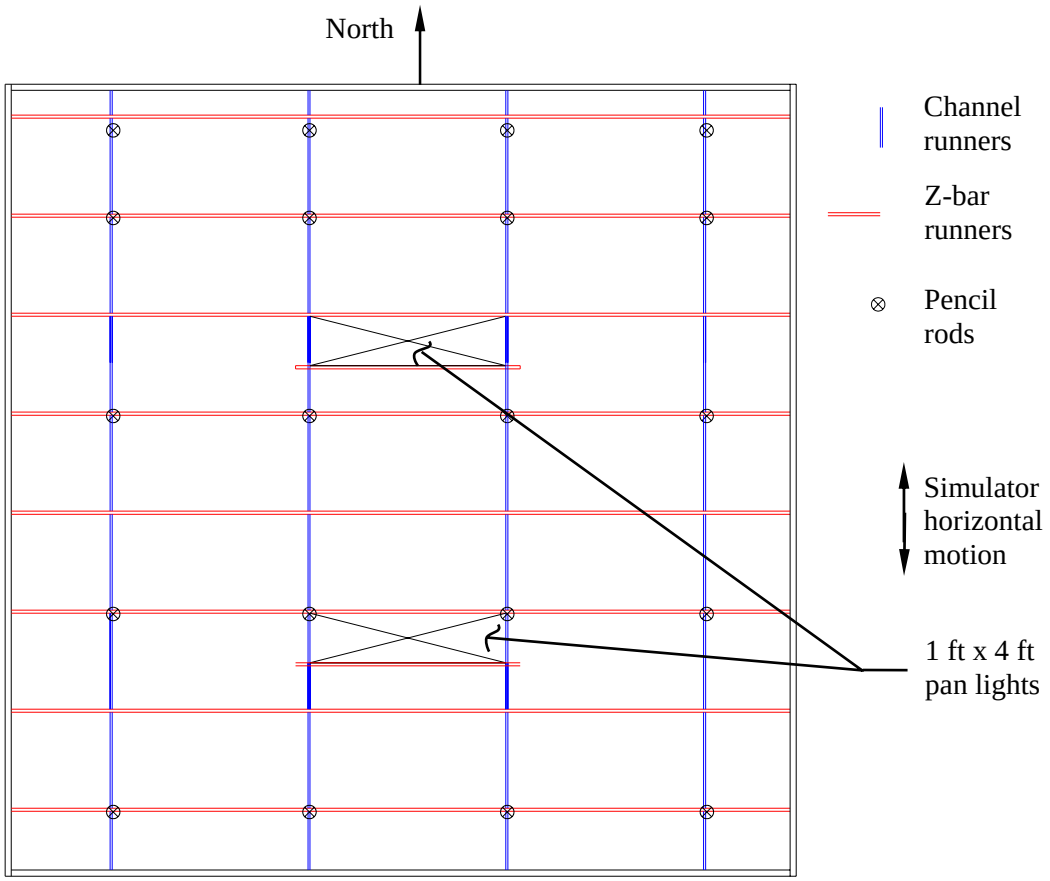

Figure 2–38. Layout of main supporting members in ceiling system CS3.

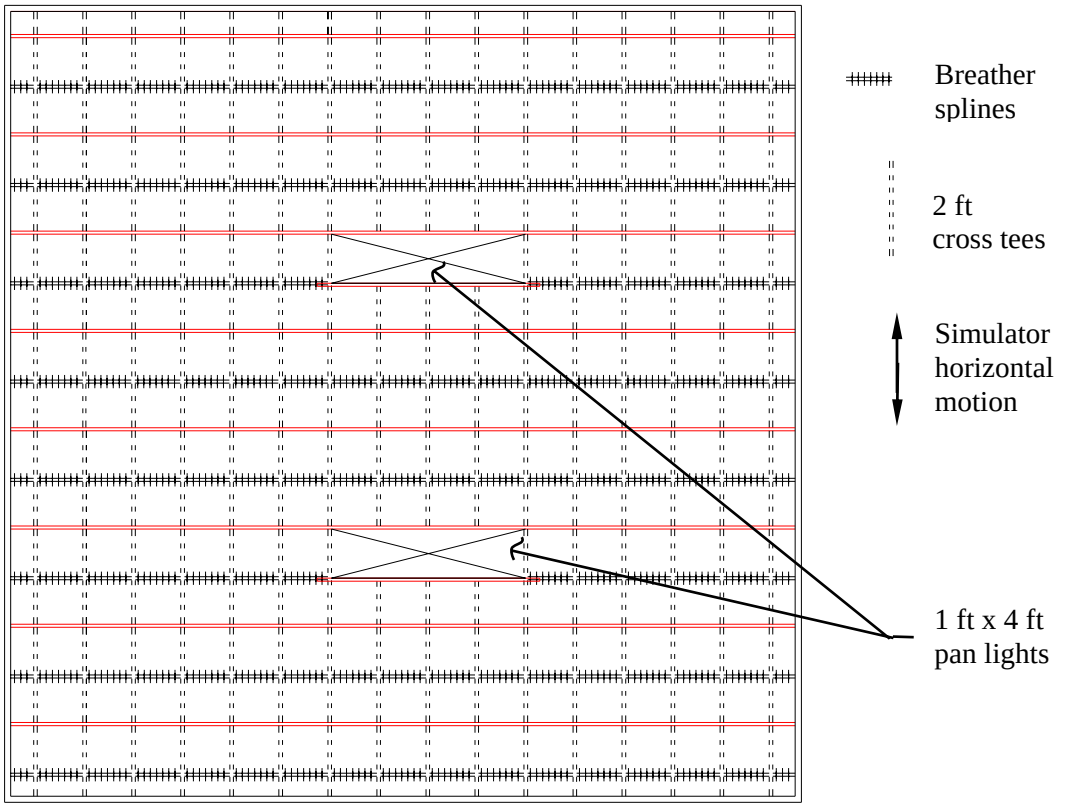

Figure 2–39. Layout of splines and cross tees in ceiling system CS3.

Ceiling System 4

System CS4 was composed of suspension system 4 and tile 2. Ceiling system CS4 was similar to ceiling system CS2 except that this system had prelude main runners spanning the east-west direction. Figure 2–40 is a photograph of system CS4. There were seven full panels and two half panels spanning in both the east-west and north-south directions. The ceiling system was constructed flush to all edges of the test frame. The total ceiling area was approximately 256 ft^2 (23.8 m^2): 16 ft (4.87 m) in the east-west direction by 16 ft (4.87 m) in the north-south direction. Figure 2–41 shows the ceiling system layout for ceiling system CS4. Two 2 ft (0.61 m) by 4 ft (1.22 m) light fixtures were mounted with light clips and two safety wires.

Source: NIST.

Figure 2–40. Bottom view of ceiling system CS4.

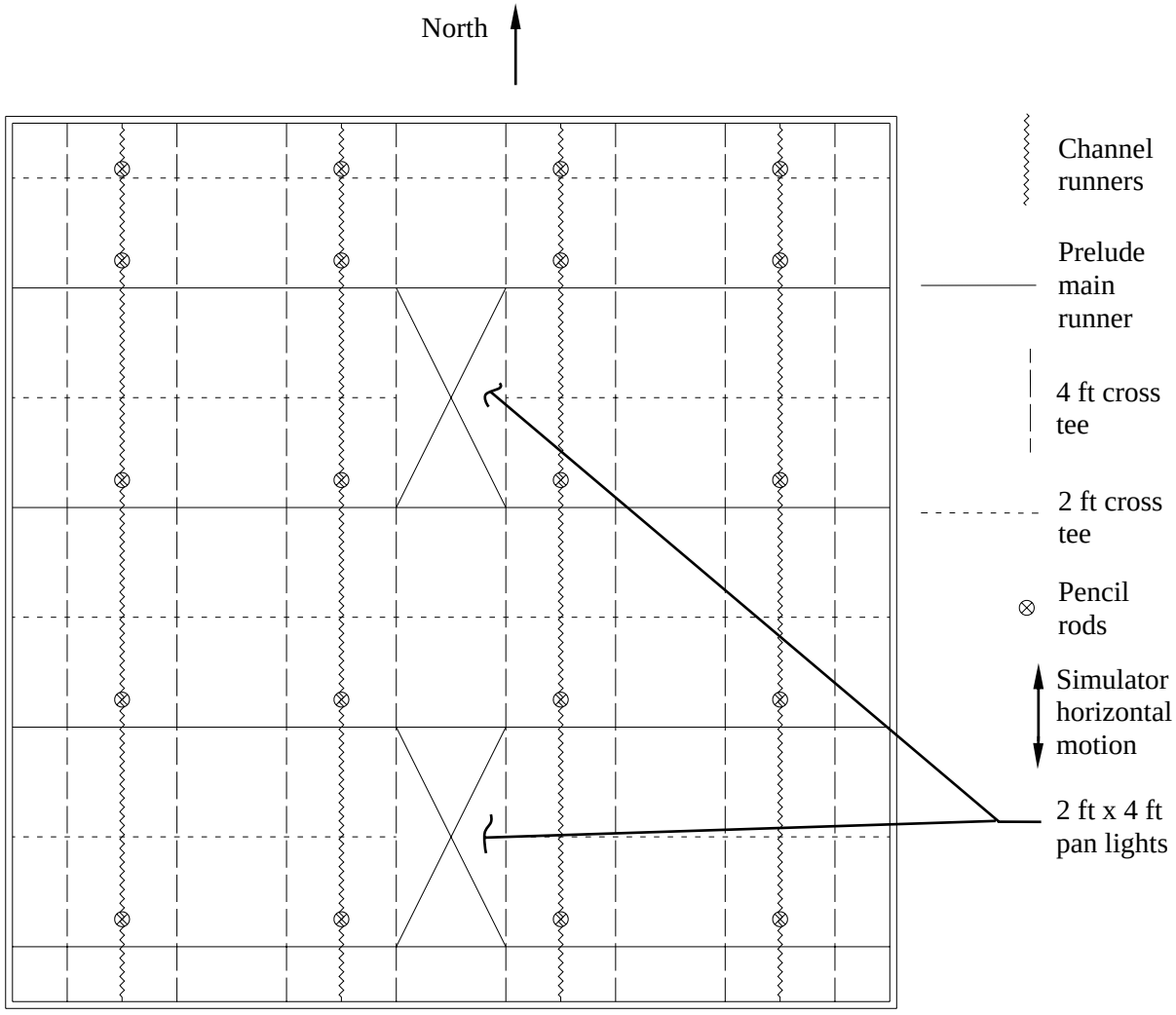

Figure 2–41. Layout for ceiling system CS4.

2.4 SYSTEM EXCITATION PATTERNS

2.4.1 General

Estimation of the forces and accelerations that occurred in the WTC towers was difficult due to the large number of unknown or poorly known parameters affecting the response, and because at the time of these tests there was little information available on the forces generated during such an impact. Limited information was available from tests involving military aircraft impacting soil or nearly rigid walls (Attaway et al. 2003), but no information was available for large aircraft impacting relatively flexible structures at high speed.

The project team thus conducted tests under a variety of excitations, hypothesizing that from the test results a pattern would emerge that would enable reasonable extrapolation to the behavior of the actual ceiling tile systems on September 11, 2001. Each of the four ceiling tile systems was subjected to a series of single impulses or blasts, the rationale for and nature of which are described in Section 2.4.3. The intensities of the impulses are listed Table 2–7, which appears in Section 2.5. In addition, the ceiling tile systems were subjected to a standard earthquake simulation that is a sequence of complex impulses. This is described in Section 2.4.4. The intensities of the earthquake excitations are listed in Table 2–8, which also appears in Section 2.5.

2.4.2 White Noise

White noise was used to find the natural frequencies of the test frame and the ceiling systems. The natural frequencies for the horizontal and vertical directions of each test specimen were obtained by finding the frequency associated with the peak in the acceleration transfer function (Clough and Penzien 1993). Figures 2–42 and 2–43 show the histories and the Fourier amplitude spectrum, respectively, of the white noise used in this study to calculate the natural frequencies of the test frame and test assemblies. The 60 Hz peak in the Fourier spectrum is associated with oil-column resonance in the vertical actuators of the simulator and falls well outside the testing range of interest: 1 to 33 Hz.

2.4.3 Single Impulse Excitations

Accurate estimation of the tower's motion during the airplane impact required detailed knowledge of the geometry, weight distribution, and impact velocity of the aircraft, as well as detailed knowledge of the geometry, weight distribution, and structural strength of the tower. At the time of this test series (fall 2003), much of this information was unknown, and the impact motion could only be roughly estimated. To allow this estimate to be made quickly, many simplifying assumptions were made regarding the nature of the impact.

Idealized Impact Waveform

Creating the profile of building motion as a result of the airplane impact involved both simplifying assumptions and estimation of many of the response parameters. First, a simple impact waveform was chosen based on the limited information available as of fall 2003. For simplicity, the same waveform was used for both towers. It was anticipated that ongoing numerical studies of the airplane impact would provide a much more accurate representation of the motion that occurred; however, the simplified

estimation described below provided a reasonable estimation that could be used for the experimental study and with the available test facility at the time that facility was available.

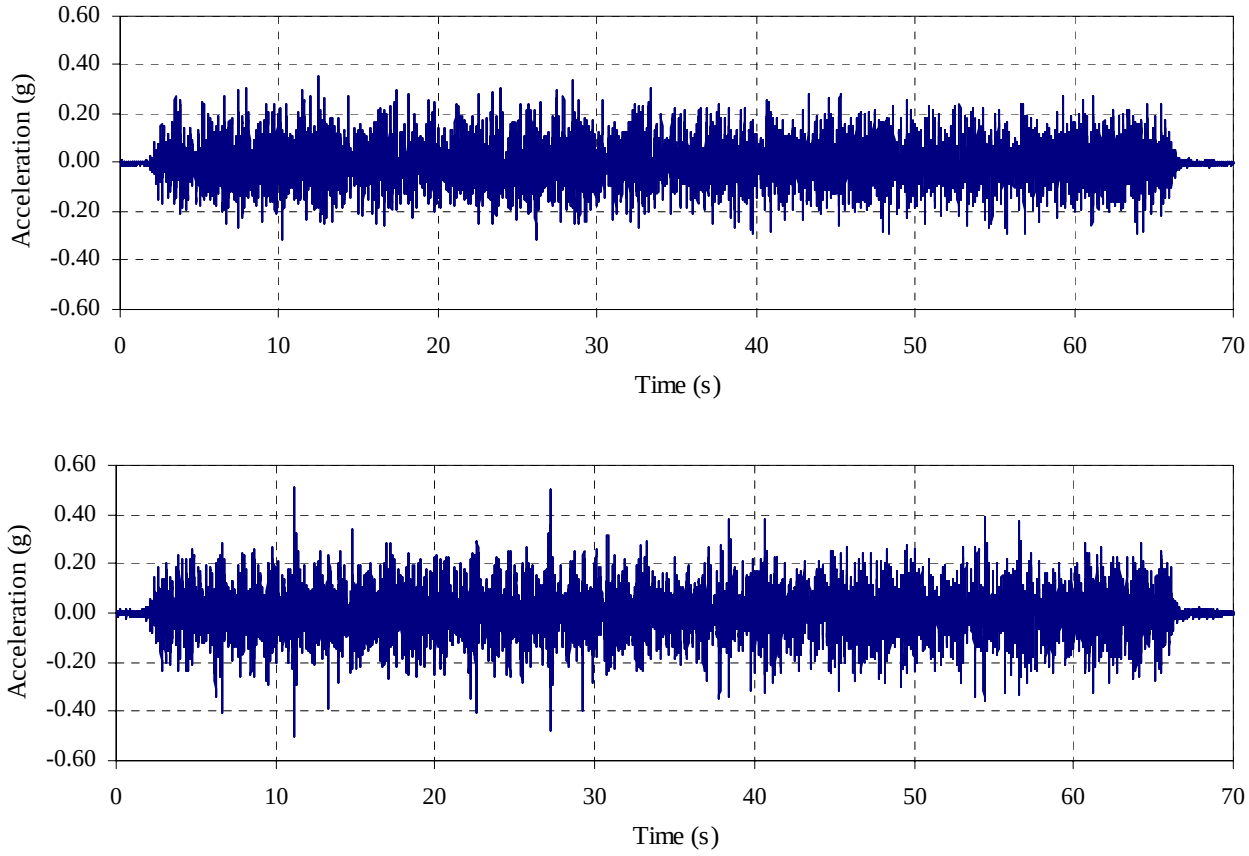

Figure 2–42. White noise histories; top: horizontal direction, bottom: vertical direction.

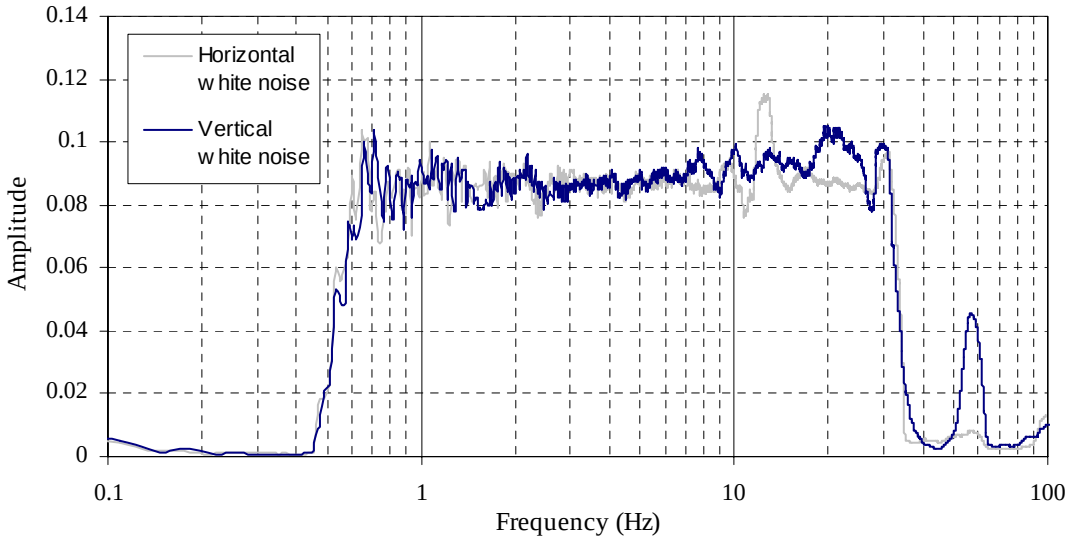

Figure 2–43. Fourier amplitude spectrum of horizontal and vertical white noise.

Based on the limited information available on aircraft impact (Attaway et al. 2003) and general information on blast loads, two possible waveforms were initially considered:

- The first waveform had a tower acceleration component that rose instantly to a maximum value, maintained this maximum response for a short duration, and then decreased to zero over a longer duration. This waveform corresponded to a large acceleration as the nose of the aircraft penetrated the tower, and was sustained as the forward portion of the fuselage, landing gear, engines, and wings penetrated. The acceleration then diminished as the portion of the aircraft within the building came to a stop and the tail penetrated the tower. While the actual motion was certainly much more complicated, for the purpose of simplifying the analysis, the acceleration was simplified to a constant value for the first quarter of the impact time, followed by a steady ramp to zero over the remainder of the time history. This waveform is shown in Figure 2–44.

- The second assumed waveform was similar except that the acceleration rose from zero to the maximum over the short duration, and then immediately began to decrease to zero. This waveform was simplified to an acceleration increasing with a constant slope for the first quarter of the history, and then decreasing with a constant slope over the remainder of the history.

When the two waveforms were modified for use on the UB shaking table, as described below, the difference between them was seen to be small, and the second waveform was removed from consideration. For this reason, the analysis with this second waveform is not described.

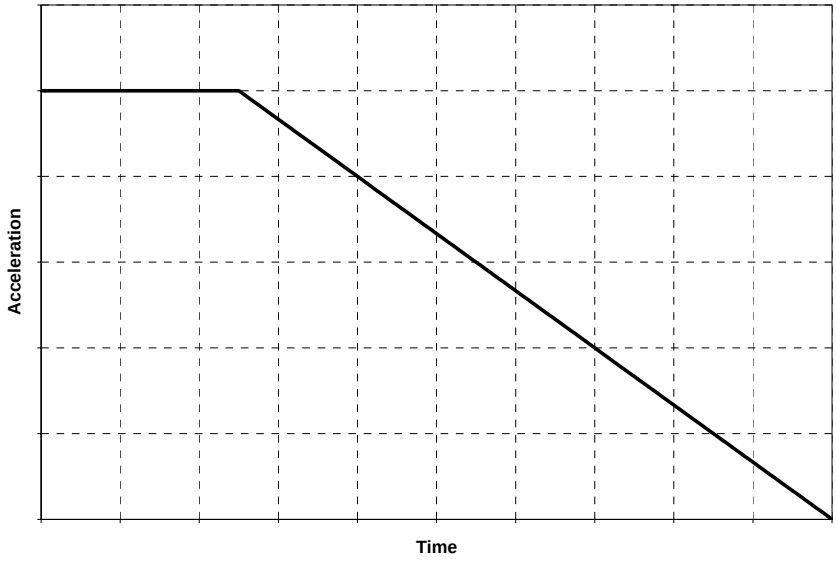

Figure 2–44. Generic acceleration waveform.

Estimation of Acceleration Magnitude and Duration

Once the shape of the acceleration response was assumed, the magnitude and duration of the acceleration was estimated from basic mechanics and some simplifying assumptions regarding the tower response. Basic information about the airplane included:

- The velocity of the airplane at the start of the impact, $V_p(0)$. This was assumed to be 560 mph (250 m/s). This value was based on verbal discussions with NIST investigators who were in the process of accurately determining the aircraft velocity based on video evidence (NIST NCSTAR 1-5A).[5] This value is slightly smaller than the 590 mph (264 m/s) that was reported by FEMA for the aircraft that hit WTC 2 (McAllister 2002).

- The mass of the airplane, m_p. This was assumed to be to be 8,500 slugs (124×10^3 kg), which was approximated by estimates of the masses of the aircraft itself, the estimated jet fuel on board, the passengers and their luggage, and the cargo. This was about 70 percent of the maximum takeoff mass of the airplane (McAllister 2002).

- The length of the airplane, l_p. A value of 159 ft (48.5 m) was used (Badrocke and Gunston 1998).

One important unknown parameter that influenced the impact motion is how far the airplane traveled into the building. The greater this distance, the longer the deceleration time would have been, which would reduce the peak acceleration accordingly. Based on initial estimates of the internal damage, it was assumed that the airplane penetrated through the center of the core. Some of the airplane debris would not likely have traveled this far into the tower, while some parts of the plane and some of the fuel passed through the building and exited the far side. It was, therefore, assumed that the center of mass of the airplane penetrated slightly more than one-half of the tower's depth. Assuming that the center of mass of the airplane is located at approximately the center of its length, the center of mass of the airplane would have traveled approximately 197 ft (60 m) between when the nose impacted the face of the tower and when the airplane remnants came to rest.

The motion of the tower was also influenced by both its mass and the distribution of that mass; however, neither the actual mass nor its distribution is known. Based on information in the original WTC design documents provided to NIST by Leslie E. Robertson Associates (LERA) and the Port Authority of new York and New Jersey (PANYNJ), and baseline computer models of the WTC towers (NIST NCSTAR 1-2), the average load per unit area (including live and dead loads) of a typical floor was approximately 87 lb/ft^2 (4.17 kN/m^2). Based on a typical floor area of 42,200 ft^2 (3,900 m^2), each floor in the tower would have had a weight of approximately 3,675 kip (16,400 kN), which corresponds to a mass of 114×10^3 slugs (1.67×10^6 kg).

To keep these calculations reasonably simple, the reference computer models assumed that the airplane and towers act as lumped, rigid masses. However, the towers were quite flexible with their mass distributed over their height. To account for this without making the analysis much more complicated,

[5] Subsequent analysis (NIST NCSTAR 1-5A) estimated the impact velocities as 466 mph ± 34 mph for WTC 1 and 545 mph ± 18 mph for WTC 2. The difference is of little significance since, as noted in the next section, the resulting shaking table velocity and displacement exceeded the table capability and had to be reduced.

only a portion of the tower's mass was assumed to participate. In this regard, the motion of the towers would have been greatest at the floors of impact, with the peak accelerations decreasing with the distance above or below the impact zone, until there would have been very little motion at the base. In addition, this study was less concerned with the accelerations on the impact floors, since flying debris would likely have damaged or destroyed most of the ceiling tiles there. Instead, the concern was for the floors just above or below the impact zone, which were not directly damaged by the airplane, but had significant fires after the impact. These floors would have likely seen somewhat less intense motion than the actual impact floors. After considering the above, it was estimated that about one-sixth of the tower's floors should be considered to be participating in the dynamic response for a lumped mass model of the vibrations. Therefore, the participating mass of the tower, m_t, was estimated to be 2.1×10^6 slugs (31×10^6 kg).

To assess the response of the tower at the end of the impact, it was necessary to consider the kinetic energy transferred from the airplane to the tower. Not all of the energy from the plane would have been transferred, but the efficiency of the impact could not be accurately estimated without extensive and detailed analysis. It was assumed that two-thirds of the energy was transferred from the airplane to the structure.

Based on the above assumptions, an impact magnitude and duration were calculated that were consistent with the assumed waveform (Fig. 2–44). The transfer of energy during the impact was described as:

$$KE_t(t_f) + KE_p(t_f) = 0.66\left[KE_t(0) + KE_p(0)\right] \tag{2–1}$$

Here, $KE_t(t)$ and $KE_p(t)$ were the kinetic energies of the tower and airplane at time , respectively, t_f is the time of the end of the impact, and the factor 0.66 accounted for the energy lost as described above. Expanding this equation yielded:

$$\frac{1}{2}\left(m_t + m_p\right)V_t(t_f)^2 = 0.66\left[\frac{1}{2}m_p V_p(0)^2\right] \tag{2–2}$$

Here, $V_t(t_f)$ was the velocity of the tower at the end of impact. It was assumed that at this time, both the tower and the airplane debris were moving together at the same velocity. Inserting the values determined above, $V_t(t_f)$ was found to be 42.3 ft/s (12.9 m/s).

Given the acceleration time history of the airplane in Fig. 2–46 and defining this as $A_p(t)$, which is a function of the acceleration magnitude, $A_{p,\max}$, and impact duration, t_f, then:

$$V_p(0) - V_p(t_f) = \int_0^{t_f} A_p(t)\,dt \tag{2–3}$$

and:

$$x_p(0) - x_p(t_f) = \iint_t A_p(t)\,dt \tag{2–4}$$

where, $x_p(t)$ was the position of the center of mass of the airplane at time t. Given the initial and final velocities of the airplane and the differential displacement, described above, Equations 2–3 and 2–4 were solved to determine the acceleration parameters. The estimated peak acceleration of the airplane was found to be –62g (–610 m/s^2), and the estimated duration of the impact was found to be 0.63 s. The resulting acceleration history is shown in Fig. 2–45.

Based on the airplane acceleration time history, the history of the impact force on the tower was calculated, and the peak force was determined to be 17 × 10^3 kip (75 × 10^3 kN). The force-time history is shown in Fig. 2–46. Figure 2–47 shows the history of the estimated tower acceleration. The peak acceleration is 0.25g (2.46 m/s^2). This acceleration history formed the basis for the modified history that was used in the experiments.

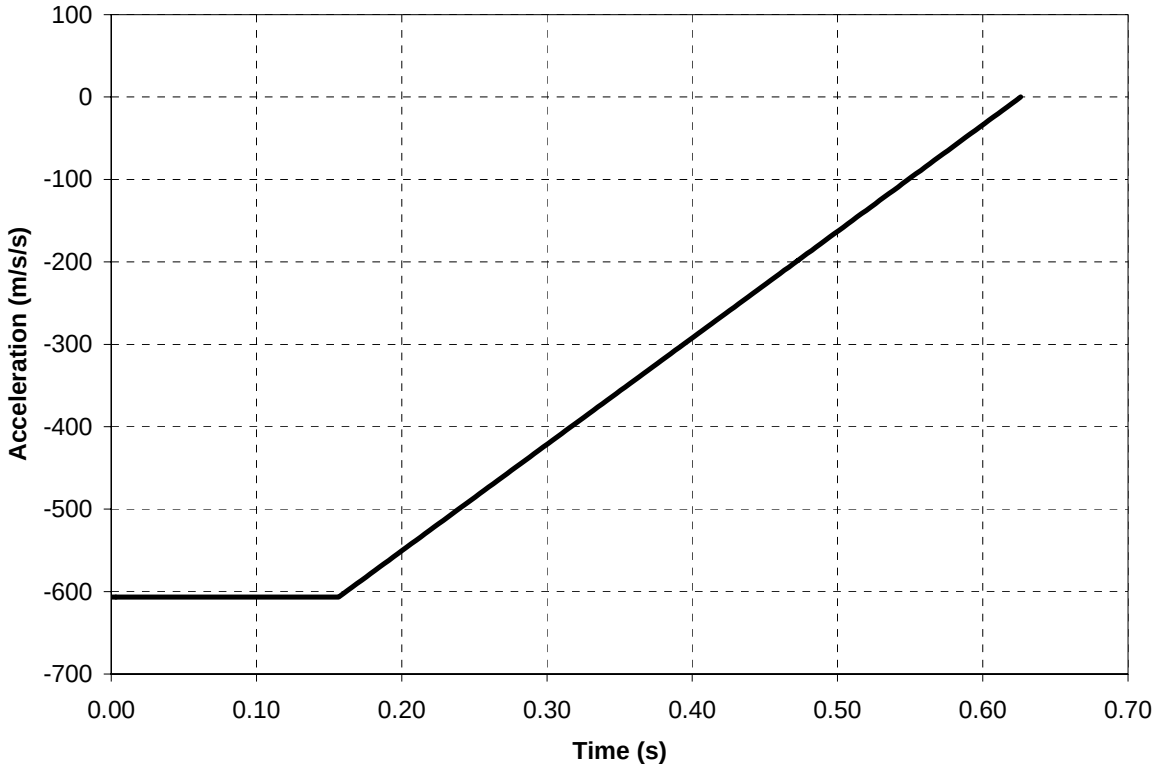

Figure 2–45. Estimated acceleration of airplane during impact.

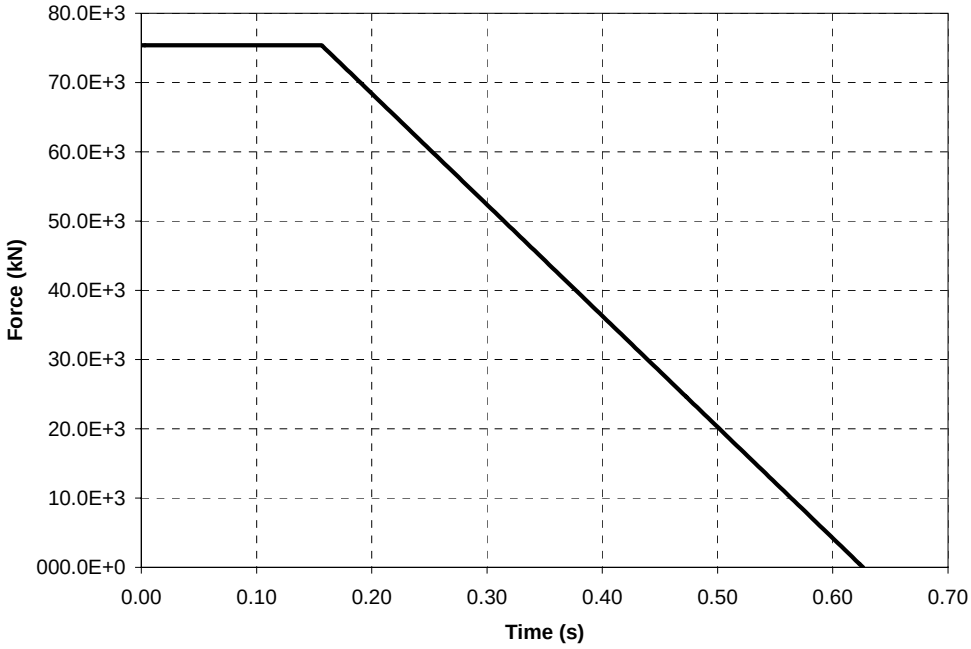

Figure 2–46. Estimated force on tower during impact.

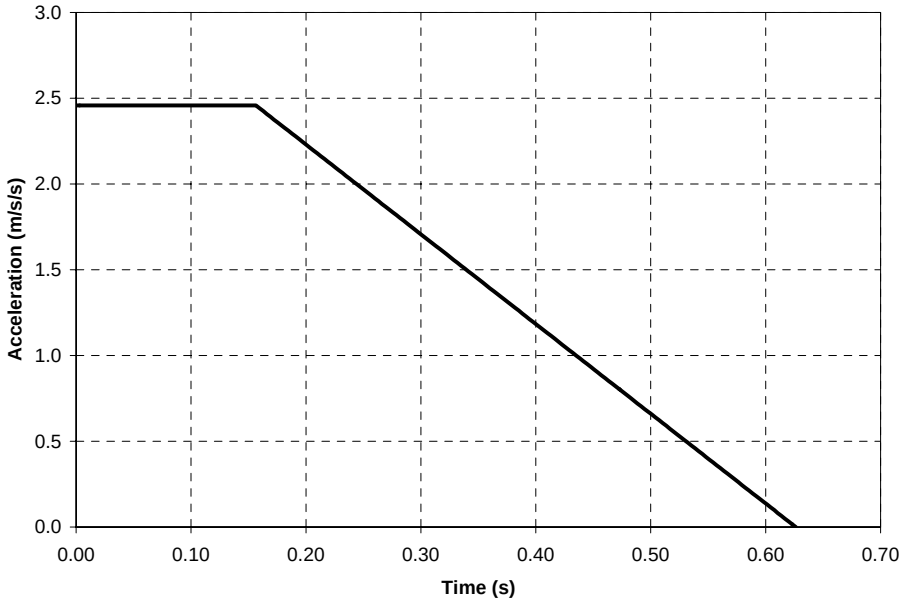

Figure 2–47. Estimated acceleration of tower during impact.

Development of Experimental Time History

The tower acceleration time history estimated above was considered to be a reasonable, simplified estimate of the actual tower acceleration. However, this motion had to be further refined before it could be used on the shaking table at UB. The peak acceleration of the history was not extreme, but the combination of the acceleration and the duration of the peak was problematic. The velocity and displacement resulting from this time history were well in excess of the shaking table capabilities.

To understand the necessary modifications to the time history, it was useful to understand the limitations of the shaking table. The specimen platform, essentially the tabletop, is driven by a series of servo-controlled hydraulic rams, which impose firm limits on the displacements, velocities, and accelerations that the table can generate. The piston area limits the force that each ram can produce, which in turn limits the peak acceleration that can be generated for a specimen of a particular mass. More important for the current tests is the ram stroke, which is limited to 1 ft (0.3 m) end to end. The hydraulic servovalves that control the rams have limited flow capacity and bandwidth. This limits the peak velocity of the shaking table to 1 ft/s (0.305 m/s) and limits the frequency of the motion to 50 Hz and less. These are all theoretical values, and additional physical and electronic limitations, as well as signal noise and mechanical limitations, prevent the table motion from reaching these limits.

A plot describing these limitations is shown in Fig. 2–48. Note that the response envelope slopes upward in the low frequency range, where the peak displacement limit tends to govern the response. In the middle frequency range, where the envelope is flat, the velocity limit governs, and in the higher frequency range, where the curve slopes downward, the acceleration limits govern. The gray line at approximately 0.9 Hz indicates the natural frequency of the towers.

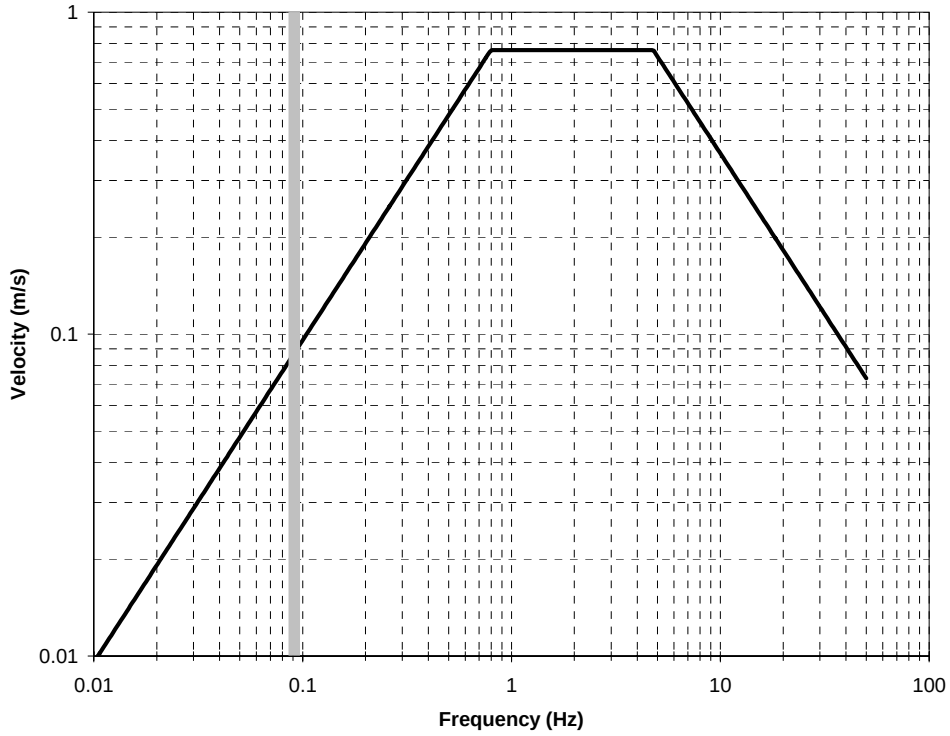

Figure 2–48. Theoretical peak response of the UB seismic simulator.

For the shaking table to be able to handle the impact history, three modifications had to be made to the waveform. First, the high frequency response components that occur at sharp transitions in the response had to be removed. Next, a deceleration component needed to be added to the history to return the velocity to zero. Finally, the entire waveform had to be scaled so that the peak velocity and displacement responses would remain within the table limits.

The first attempt at modifying the history consisted of filtering the signal with a low pass Butterworth filter to remove the unwanted, high frequency components. However, the phase shifts in some prominent frequencies, caused by filter during the removal of the high frequencies, significantly changed the nature of the history. Instead, the waveform was manually adjusted to remove the sharp transitions by replacing the transition areas with quarter sine and cosine functions, which had frequencies within the shaking table's response band. The result of this effort was that the two waveforms described in Section 2.4.2 converged toward a single result.

To decelerate the table before the displacement limits were reached, a pulse nearly as large and sharp as the primary impulse was required. This modification resulted in a history that varied significantly from the original desired waveform, but that could be scaled for use with the shaking table. Given that the intent was to have a single impulse approximation of the aircraft impact and that a more complex excitation was also to be used in the testing, it was accepted that this was a sufficient rendition for the purpose.

Acceleration signals for the simulator were then generated to produce the peak target accelerations listed in Table 2–8 (see Section 2.5). Signals for tests with peak target accelerations of between 0.05g and 0.085g were ramped displacement histories as shown in Fig. 2–49. Signals for tests exceeding a peak target acceleration of 0.085g were sinusoidal-type acceleration histories. The acceleration histories were identical for vertical and horizontal excitations. The acceleration histories used for these tests is provided in Fig. 2–50. The signals were generated and amplitude scaled using the program software STEX (MTS 1991).

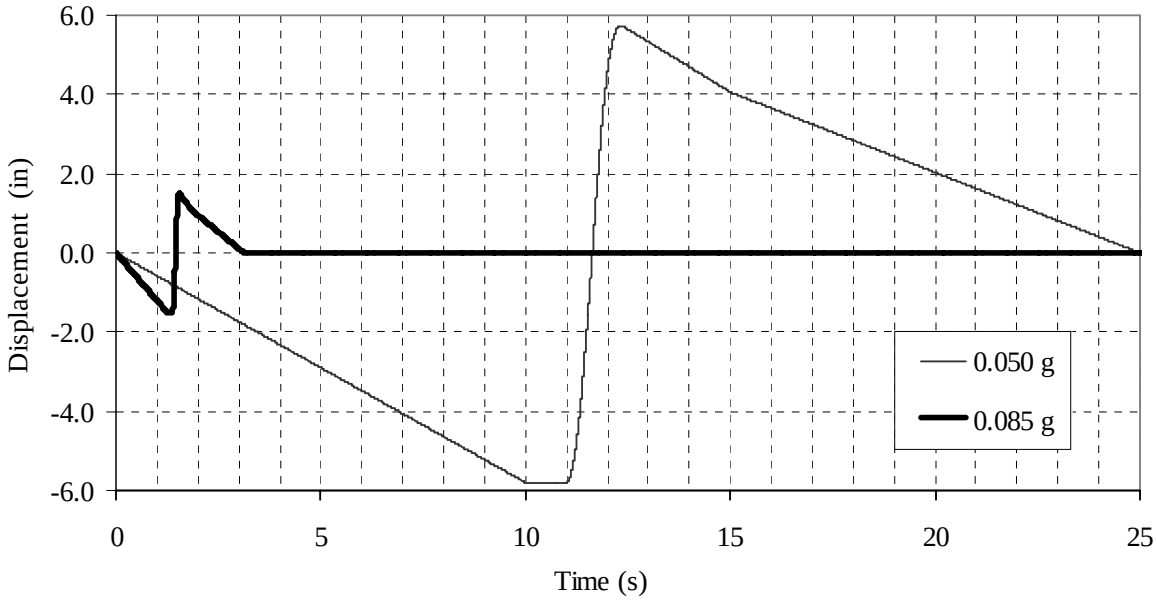

Figure 2–49. Displacement history inputs for tests 4 and 5.

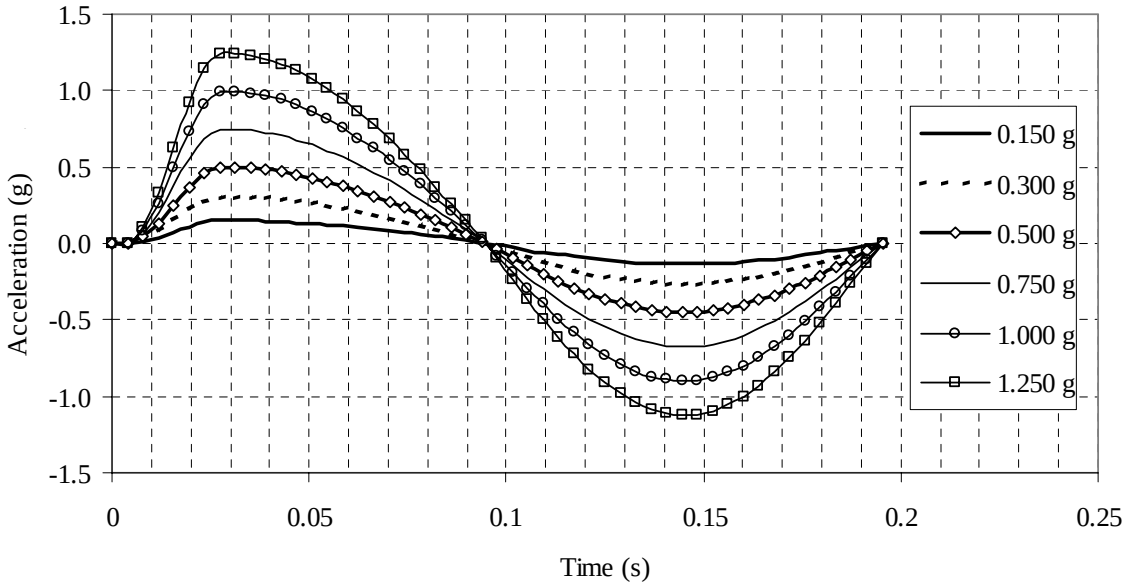

Figure 2–50. Horizontal and vertical acceleration history inputs into simulator for tests 6 through 23.

2.4.4 Multiple Impulse (Earthquake) Stimulation

To capture the effects of the multiple shocks reported by some of the tower occupants, ceiling systems CS2, CS3, and CS4 were also subjected to a set of combined horizontal and vertical excitations. Since the nature of the actual excitations is unknown, an available set was used. These were the excitations used to qualify a ceiling system according to ICBO-AC156, Acceptance Criteria for Seismic Qualification Testing of Nonstructural Components (ICBO 2000). The following text presents summary information on these histories, which involve both horizontal and vertical motion.

The required response spectrum (RRS) for horizontal shaking was developed using the normalized ICBO response spectrum shown in Fig. 2–51.

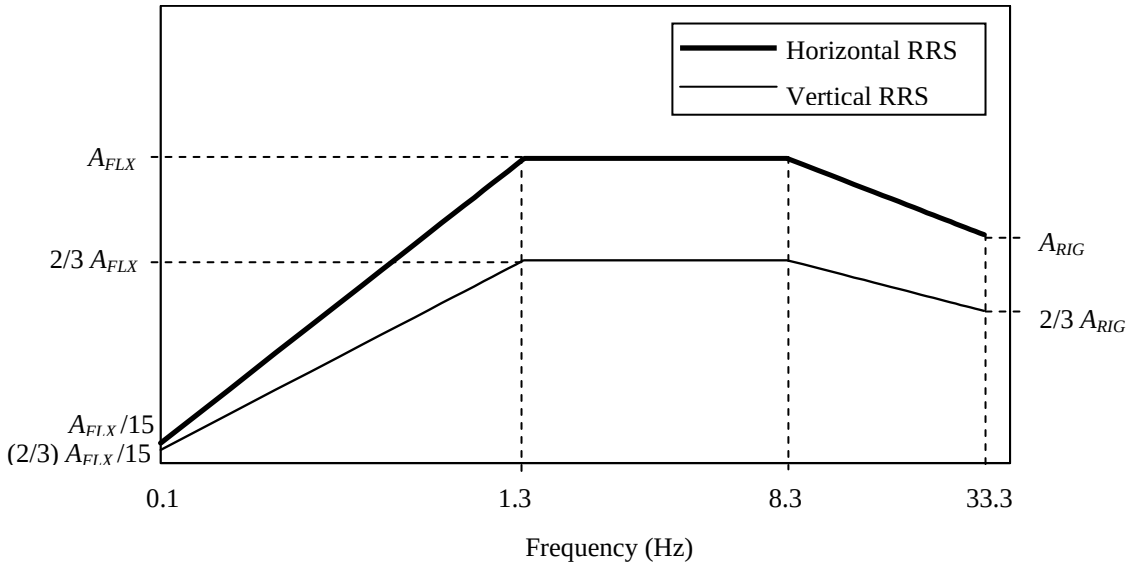

Figure 2–51. Required response spectra for horizontal and vertical shaking.

The values of the parameters A_{RIG} and A_{FLX} that define the ordinates of the horizontal spectrum were calculated with the following equations.

For horizontal design basis earthquake shaking, the International Building Code (ICC 2000) defines the short period design basis earthquake acceleration response as:

$$S_{DS} = \frac{2}{3} F_a S_S \tag{2–5}$$

where S_{DS} is the design spectral response acceleration at short periods, F_a is the site coefficient, and S_S is the mapped maximum earthquake spectral acceleration at short periods. Based on ICBO AC156, the spectral acceleration A_{RIG} of a rigid component (assumed to have a frequency $f \geq 33$ Hz) is given by Equation 2–6 and that of a flexible component A_{FLX} is given by Equation 2–7:

$$A_{RIG} = 0.4 \cdot S_{DS}(1 + 2\frac{z}{h}) \leq 1.2 \cdot S_{DS} \tag{2–6}$$

$$A_{FLX} = S_{DS}(1 + 2\frac{z}{h}) \leq 1.6 \cdot S_{DS} \tag{2–7}$$

where z is the height above the base of the building where the equipment or component is to be installed and h is the height of the building. If the equipment or component is to be installed in the roof of the building, $z/h = 1.0$. If the location of the equipment or component in a building is unknown, or if it is being qualified for a general use in buildings structures, it is conservative, but appropriate, to set $z = h$.

Table 2–7 shows the parameters used in this study to obtain the RRS for horizontal shaking for 5 percent damping for a mapped spectral acceleration at short period S_S equal between 0.25 and 1.75 with 1.0 highlighted. Figure 2–52 shows the RRS in the horizontal and vertical directions for 5 percent damping for a mapped spectral acceleration at short period, S_S =1.0g. The ordinates of the vertical RRS are given by ICBO as two-thirds (2/3) of those of the horizontal RRS, namely, A_{FLX} = 1.07, A_{RIG} = 0.80 for S_S = 1.0g.

Table 2–7. Parameters to calculate the horizontal RRS (z/h=1.0).

S_S	0.25	0.50	0.75	1.00	1.25	1.50	1.75
F_a	1.00	1.00	1.00	1.00	1.00	1.00	1.00
S_{DS}	0.17	0.33	0.50	0.67	0.83	1.00	1.17
A_{FLX}	0.27	0.53	0.80	1.07	1.33	1.60	1.87
$A_{FLX}/15$	0.02	0.04	0.05	0.07	0.09	0.11	0.12
A_{RIG}	0.20	0.40	0.60	0.80	1.00	1.20	1.40

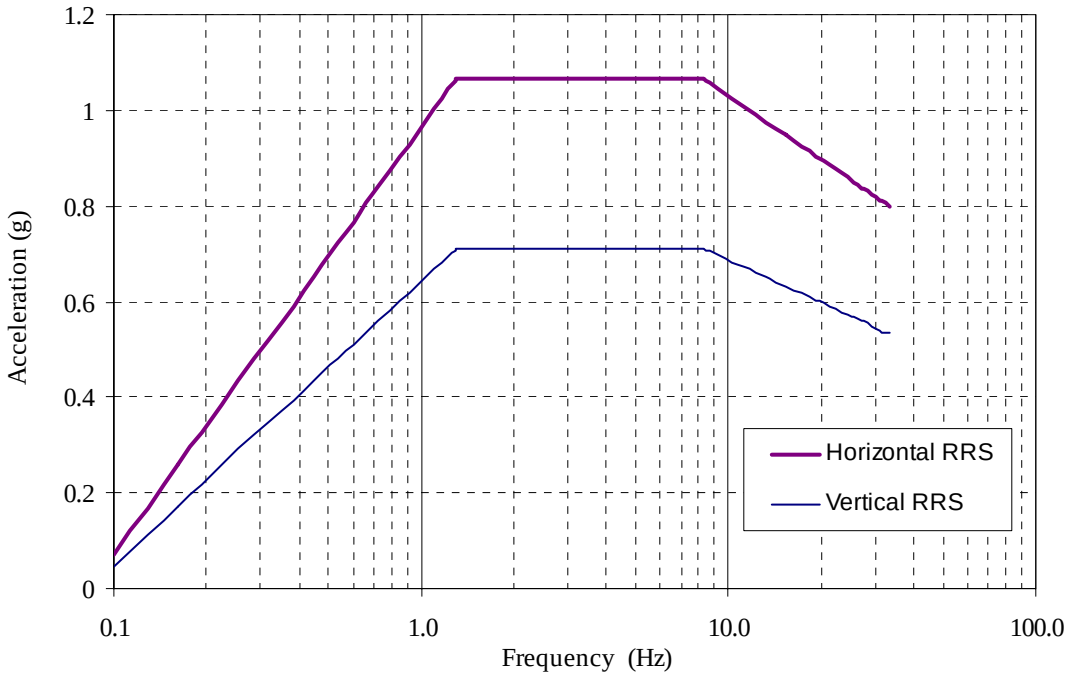

Figure 2–52. RRS for horizontal and vertical shaking for S_S=1.0.

Figure 2–53 presents 2000 National Earthquake Hazards Reduction Program (NEHRP) maximum considered earthquake (MCE) ground motion spectra and the ICBO-AC156 target qualification spectrum for seismic qualification for S_S = 1.0g and S_1 = 0.4g. The ground motion spectra are presented for NEHRP soil types A through E. The purpose of the presentation is to relate the qualification spectral demands that are assumed to apply anywhere in a building structure to the ground motion demands on a single degree of freedom representation of the building. The qualification spectrum envelops the MCE spectra (for S_S = 1.0g and S_1 = 0.4g) except in the short period range for site class D.

Figure 2–54 presents the 2000 NEHRP MCE and design basis earthquake (DBE) ground motion spectra and the ICBO-AC156 target qualification spectrum for seismic qualification for S_S = 1.0g and S_1 = 0.4g. The target qualification spectrum was developed for DBE shaking, and the difference between the NEHRP DBE spectrum and the target qualification spectrum (shown by the arrows in the figure) represents the assumed amplification of the DBE motion by a building framing system (into which the ceiling system would be installed).

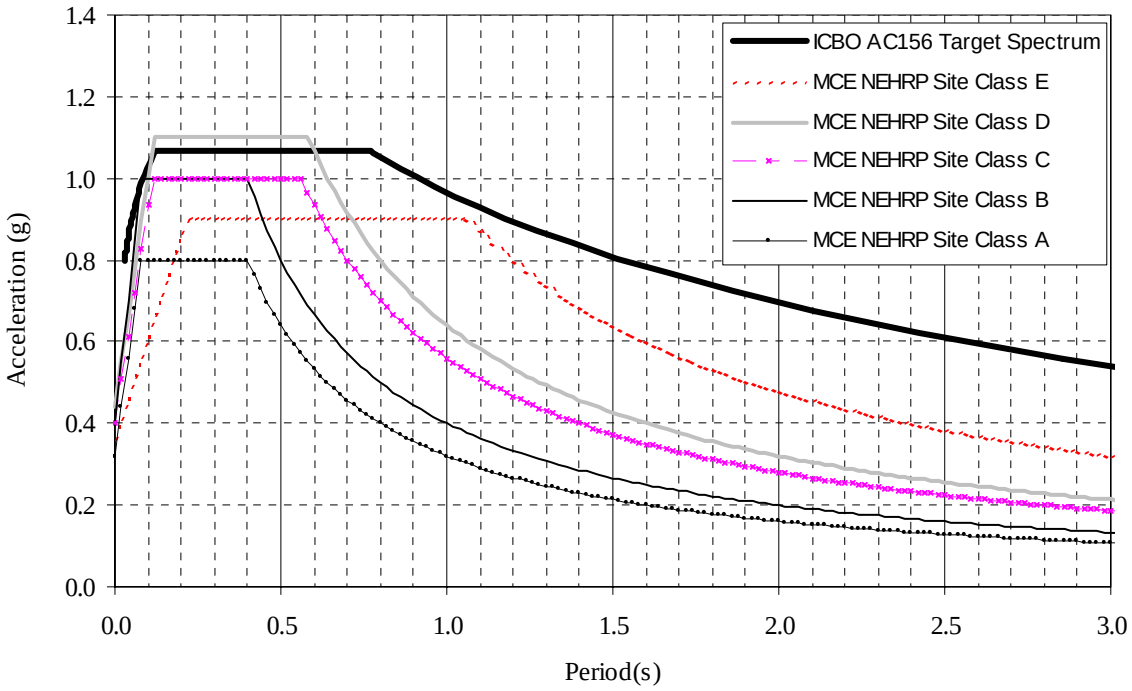

Figure 2–53. Relationship between MCE NEHRP spectra and target qualification spectrum (S_S=1.0g, S_1=0.4g).

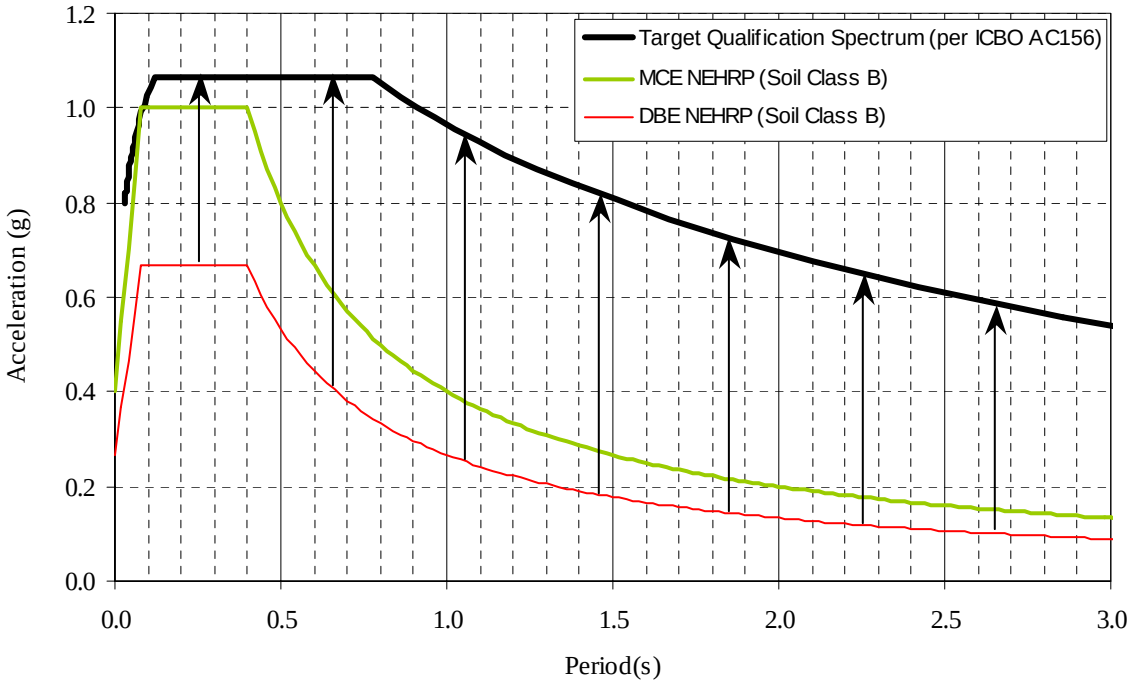

Figure 2–54. Relationship between NEHRP MCE and DBE spectra and target spectrum (S_S=1.0g, S_1=0.4g).

2.5 DESCRIPTION OF TEST SERIES

2.5.1 General

For the purpose of performance characterization, each of the four ceiling systems was subjected to a set of horizontal and vertical excitations. Each set included single-axis resonance search tests using white noise excitation along each (programmable) orthogonal axis of the simulation platform. The resonance search tests were undertaken to establish the natural frequency of the ceiling frame system. Following that, each set of excitations included either (a) a series of individual and biaxial impulsive excitations (Section 2.4.2) or (b) an earthquake excitation sequence (Section 2.4.3). The amplitude of the impact and earthquake excitations was varied from a relatively mild first level (0.015g), perhaps representing ceiling tiles at some distance from the airplane impact, up to the intensity limit of the shaking table (1.25g). The result of each test was characterized by certain criteria or limit states. If any distortion or damage to the system was experienced during a given test, the system was repaired before proceeding to the next test.

Table 2–8 lists the standard series of tests used for the impact excitations. The earthquake tests began with a white noise excitation and continued with intensities of 0.25g, 0.50g, 0.75g, 1.00g, 1.25g, 1.50g, 1.75g, and 2.50g.

2.5.2 Performance Criteria

The outcome of each test was verbally characterized by the extent of displacement of ceiling tiles and the degree of damage to the suspension system. For summary purposes, the outcome was also described in terms of limit states.

Definitions of two limit states of response were defined in a manner similar to those adopted in past studies using earthquake simulation (Badillo et al. 2002, 2003):

1. Loss of one or more tiles from the ceiling system.

2. Sufficient damage to one or more components of the suspension system such that repair or replacement of part or all of the suspension system would be required.

Table 2–8. Test sequence for a set of impact experiments for a single ceiling system.[a]

Test No.	Test Name	Target Peak Acceleration[b] (g)	Description
1	w1h	–	White noise excitation in the horizontal (N-S) direction
2	w1v	–	White noise excitation in the vertical direction
3	w1hv	–	White noise excitation in the horizontal and vertical directions
4	0050h	0.050	Motion in the horizontal (N-S) direction[c]
5	0085h	0.085	Motion in the horizontal (N-S) direction[c]
6	0150h	0.150	Motion in the horizontal (N-S) direction[d]
7	0150v	0.150	Motion in the vertical direction[d]
8	0150hv	0.150	Biaxial motion in the horizontal (N-S) and vertical directions[d]
9	0300h	0.300	Motion in the horizontal (N-S) direction[d]
10	0300v	0.300	Motion in the vertical direction[d]
11	0300hv	0.300	Biaxial motion in the horizontal (N-S) and vertical directions[d]
12	0500h	0.500	Motion in the horizontal (N-S) direction[d]
13	0500v	0.500	Motion in the vertical direction[d]
14	0500hv[e]	0.500	Biaxial motion in the horizontal (N-S) and vertical directions[d]
15	0750h	0.750	Motion in the horizontal (N-S) direction[d]
16	0750v	0.750	Motion in the vertical direction[d]
17	0750hv	0.750	Biaxial motion in the horizontal (N-S) and vertical directions[d]
18	1000h	1.000	Motion in the horizontal (N-S) direction[d]
19	1000v	1.000	Motion in the vertical direction[d]
20	1000hv[e]	1.000	Biaxial motion in the horizontal (N-S) and vertical directions[d]
21	1250h	1.250	Motion in the horizontal (N-S) direction[d]
22	1250v	1.250	Motion in the vertical direction[d]
23	1250hv[e]	1.250	Biaxial motion in the horizontal (N-S) and vertical directions[d]

a. For actual test sequences, see Table 3–1 and Table 3–2.
b. Peak target acceleration of the simulator platform.
c. For input histories, see Sec. 2.4.3; Fig. 2–51 shows the input displacement history.
d. For input histories, see Sec. 2.4.3; Fig. 2–52 shows the input acceleration history.
e. Results from tests presented in Chapter 3; see Appendix A.

2.6 REFERENCES

Attaway, S. W., J. G. Arguello, G. C. Bessette, R. G. Schmitt, P. Taylor, K. W. Gwinn, D. Crawford, S. Tieszen, and M. Baer. 2003. *Technology Overview for Analysis of Aircraft Impact*. SAND2003-1952, Sandia National Laboratories, Albuquerque, NM.

Badillo, H., D. Kusumastuti, A. S. Whittaker, and A. M. Reinhorn. 2002. "Seismic Qualification Tests of Ceiling Systems", Part I, Report No. UB CSEE/SEESL-2002-01, State University of New York at Buffalo, Buffalo, NY, April.

Badillo, H.. 2003. "Seismic Fragility Testing of Suspended Ceiling Systems," M.S. Thesis, Department of Civil, Structural, and Environmental Engineering, State University of New York at Buffalo, Buffalo, NY, August.

Badillo, H., A. S. Whittaker, and A. M. Reinhorn. 2003. "Seismic Qualification Tests of Ceiling Systems," Part III, Report No. UB CSEE/SEESL-2003-01, State University of New York at Buffalo, Buffalo, NY, February.

Badillo, H., A. S. Whittaker, and A. M. Reinhorn. 2003a. "Seismic Qualification Tests of Ceiling Systems," Part IV, Report No. UB CSEE/SEESL-2003-02, State University of New York at Buffalo, Buffalo, NY, May.

Badillo, H., A. S. Whittaker, and A. M. Reinhorn. 2003b. "Performance Characterization of Suspended Ceiling Systems," *Proceedings*, ATC-29-1 Seminar on Seismic Design, Performance, and Retrofit of Nonstructural Components in critical facilities, Applied Technology Council, Redwood City, CA, October.

Badrocke, M., and B. Gunston. 1998. *Boeing Aircraft Cutaways, The History of Boeing Aircraft Company*, Osprey Aviation, Wellingborough, UK.

Clough, R.W., and J. Penzien. 1993. *Dynamics of Structures*, 2nd ed., McGraw-Hill, NY.

ICBO (International Conference of Building Officials). 2000. Acceptance Criteria for Seismic Qualification Testing of Nonstructural Components. ICBO-AC156. Whittier, CA.

ICC (International Code Council). 2000. *International Building Code*. Falls Church, VA.

Kusumastuti, D., H. Badillo, A. S. Whittaker, and A. M. Reinhorn. 2002. "Seismic Qualification Tests Of Ceiling Systems," Part II, Report No. UB CSEE/SEESL-2002-02, State University of New York at Buffalo, Buffalo, NY, May.

McAllister, T., ed. 2002. *World Trade Center Building Performance Study: Data Collection, Preliminary Observations, and Recommendations.* FEMA 403. Federal Emergency Management Agency. Washington, DC, May.

MTS Systems Corp. 1991. STEX-Seismic Test Evaluation Software, MN.

Repp J. R., H. Badillo, A. S. Whittaker , and A. M. Reinhorn. 2003. "Seismic Qualification of Armstrong Suspended Ceiling Systems," Part V, Report No. UB CSEE/SEESL-2003-03, State University of New York at Buffalo, Buffalo, NY, September.

Repp J. R., H. Badillo, A. S. Whittaker , and A. M. Reinhorn, 2003a. "Seismic Qualification of Armstrong Suspended Ceiling Systems," Part VI, Report No. UB CSEE/SEESL-2003-04, State University of New York at Buffalo, Buffalo, NY, November.

Chapter 3
TEST RESULTS

3.1 COMPARISON OF PLATFORM SIMULATOR AND FRAME RESPONSES

The excitations described in Section 2.4 were used as the inputs to the earthquake simulator. The horizontal and vertical responses of the earthquake simulator and the frame were recorded with accelerometers and linear potentiometers. These responses were recorded for the purpose of comparing the input to the simulator and the response of the test frame including the ceiling systems. Accelerometers were placed at locations termed *Table* (shaking table acceleration control), *Abase* (on the center of the base of the frame), *Afram* (on the center of the roof of the frame), *AframTS* (on the side and top of the test frame), and *Agrid* (located toward the center of the suspension system) as noted in Section 2.2.3.

The figures in Appendix A show test results for each ceiling system for tests 0500hv, 1000hv, and 1250hv. These figures include acceleration histories and the response spectra for 5 percent damping for the five locations noted above and displacements histories from horizontal displacement transducers *Dbase* (at the bottom of the test frame) and *Dcntr* (at the top middle of the test frame).

As expected, there was virtually no difference between the histories and spectra calculated using the accelerometers *Table* and *Abase*. However, it is evident from comparing the spectra for *Afram* (the roof acceleration), *AframTS* (on the side and top of the test frame), and *Agrid* (suspension grid) with *Abase* (base acceleration), that the flexibility of the test frame amplified the horizontal and vertical excitation from the simulator platform to the ceiling systems. Such amplification must be placed in the context of impact characterization. Although characterization of ceiling systems should be established on the basis of the input histories to the ceiling system, because the spectra for *Afram* exceed those for *Table* across the entire period range, the characterization of the ceiling systems was conservatively based on spectra generated using the simulator platform histories (*Table*). Note that ceiling systems with fundamental periods ranging from 0.0 s through 0.4 s (bracketing the systems tested as part of this study) sustained demands substantially more severe than those estimated using the *Table* accelerometers.

3.2 SINGLE IMPULSE TESTS

Following each test, the ceiling suspension grid system was inspected visually. All connections, anchors, and hanging rods were examined.

Table 3–1 presents summary information of the resonance search tests performed on each ceiling system. The natural frequencies of each system are given for both directions of the test frame, the horizontal direction (f_x) and the vertical direction (f_y) using data from the white noise tests. Table 3–2 presents summary information on each test of each system. Listed are the test name, the test record, and the maximum accelerations in five different locations in the test fixture. The maximum horizontal response of the accelerometers at locations termed *Table* (shaking table acceleration control), *Abase* (on the center of the base of the frame), *Afram* (on the middle of the south side of the top of the frame), *AframTS* (on the

top and side of the frame) and *Agrid* (located near the center on the suspension system) are identified. Table 3–3 presents summary information of the damage to each ceiling system for each test. Figures 3–1 through 3–12 are photographs of some of the damage observed during testing.

Table 3–1. Results from resonance search tests.

Ceiling System	Test Record	Horizontal Frequency (Hz)	Vertical Frequency (Hz)
CS1 Date of test: 8/27/2003	S1w1h	f_x = 11.91 Hz	–
	S1w1v	–	f_y = 7.23Hz
	S1w1hv	f_x = 11.72 Hz	f_y = 7.03 Hz
CS2 Date of test: 8/27/2003	S2w1h	f_x = 11.91 Hz	–
	S2w1v	–	f_y = 6.45 Hz
	S2w1hv	f_x = 11.72 Hz	f_y = 6.45 Hz
CS3 Date of test: 8/28/2003	S3w1h	f_x = 11.13 Hz	–
	S3w1v	–	f_y = 7.23Hz
	S3w1hv	f_x = 11.33 Hz	f_y = 7.23Hz
CS4 Date of test: 8/29/2003	S4w1h	f_x = 11.91 Hz	–
	S4w1v	–	f_y = 6.64 Hz
	S4w1hv	f_x = 11.72 Hz	f_y = 6.45 Hz

Table 3–2. Measured acceleration values.

Ceiling System	Test Record	Maximum Recorded Horizontal Acceleration (g) [a,b]					Maximum Recorded Vertical Acceleration (g) [a,b]				
		Table	Abase	Afram	Agrid	Afram TSNS	Table	Abase	Afram	Agrid	Afram TSV
CS1 Date of test: 8/27/03	0050h	0.07	0.07	0.12	0.07	0.12	–	–	–	–	–
	0085h	0.10	0.10	0.22	0.07	0.21	–	–	–	–	–
	0150h	0.17	0.17	0.29	0.08	0.28	–	–	–	–	–
	0150v	–	–	–	–	–	0.15	0.16	0.44	0.26	0.16
	0150hv	0.17	0.18	0.29	0.68	0.28	0.15	0.15	0.43	0.40	0.21
	0300h	0.35	0.36	0.55	0.15	0.53	–	–	–	–	–
	0300v	–	–	–	–	–	0.32	0.31	0.97	0.58	0.38
	0300hv	0.34	0.36	0.72	1.46	0.68	0.32	0.32	1.07	1.42	0.48
	0500h	0.63	0.64	1.04	0.39	0.97	–	–	–	–	–
	0500v	–	–	–	–	–	0.61	0.62	1.59	0.78	0.73
	0500hv	0.57	0.60	1.45	3.39	1.35	0.61	0.60	1.71	3.84	0.94
	0750h	1.03	1.08	1.99	1.07	1.87	–	–	–	–	–
	0750v	–	–	–	–	–	1.11	1.18	3.12	1.73	1.34
	0750hv	0.95	0.92	2.14	5.76	1.97	1.12	1.15	2.98	3.93	1.77
	1000h	1.54	1.61	2.64	1.80	2.50	–	–	–	–	–
	1000v	–	–	–	–	–	1.85	2.05	5.35	2.47	2.26
	1000hv	1.42	1.29	2.19	4.20	2.04	1.72	2.06	5.19	5.75	2.73
	1250h	2.05	2.28	3.55	1.78	3.34	–	–	–	–	–
	1250v	–	–	–	–	–	2.54	3.06	6.99	11.12	3.30
CS2 Date of test: 8/27/03	0050h	0.09	0.07	0.14	0.08	0.14	–	–	–	–	–
	0085h	0.10	0.10	0.20	0.14	0.19	–	–	–	–	–
	0150h	0.16	0.16	0.29	0.12	0.27	–	–	–	–	–
	0150v	–	–	–	–	–	0.14	0.16	0.39	0.83	0.17
	0150hv	0.16	0.17	0.34	0.93	0.32	0.14	0.14	0.41	1.10	0.21
	0300h	0.33	0.34	0.57	0.39	0.55	–	–	–	–	–

Ceiling System	Test Record	Maximum Recorded Horizontal Acceleration (g) [a,b]					Maximum Recorded Vertical Acceleration (g) [a,b]				
		Table	Abase	Afram	Agrid	Afram TSNS	Table	Abase	Afram	Agrid	Afram TSV
	0300v	–	–	–	–	–	0.32	0.32	0.80	1.76	0.36
	0300hv	0.32	0.34	0.75	2.03	0.70	0.32	0.32	0.82	4.31	0.47
	0500h	0.59	0.62	0.62	0.77	0.96	–	–	–	–	–
	0500v	–	–	–	–	–	0.59	0.59	1.72	2.73	0.72
	0500hv	0.56	0.58	1.39	5.03	1.30	0.60	0.58	1.75	3.27	0.93
	0750h	1.00	1.05	2.05	2.92	1.95	–	–	–	–	–
	0750v	–	–	–	–	–	1.10	1.14	3.08	2.34	1.27
	0750hv	0.97	0.91	2.01	6.99	1.84	1.11	1.16	3.05	4.74	1.80
	1000h	1.51	1.59	2.70	5.34	2.57	–	–	–	–	–
	1000v	–	–	–	–	–	1.78	2.06	5.18	4.36	2.19
	1000hv	1.40	1.25	2.25	2.10	2.10	1.71	1.98	4.79	5.90	2.80
	1250h	2.05	2.24	3.47	6.83	3.30	–	–	–	–	–
	1250v	–	–	–	–	–	2.35	2.94	7.03	5.16	3.07
	1250hv	2.03	1.81	2.83	9.25	2.68	2.14	2.57	5.76	6.43	3.60
CS3 Date of test: 8/28/03	0050h	0.06	0.07	0.13	0.24	0.13	–	–	–	–	–
	0085h	0.10	0.10	0.20	0.29	0.19	–	–	–	–	–
	0150h	0.19	0.20	0.32	0.26	0.31	–	–	–	–	–
	0150v	–	–	–	–	–	0.15	0.15	0.43	0.36	0.16
	0150hv	0.19	0.20	0.35	0.99	0.33	0.15	0.14	0.44	0.60	0.22
	0300h	0.35	0.37	0.61	0.54	0.59	–	–	–	–	–
	0300v	–	–	–	–	–	0.32	0.32	0.97	1.70	0.37
	0300hv	0.33	0.36	0.73	3.02	0.68	0.32	0.31	1.01	1.54	0.48
	0500h	0.60	0.63	1.02	0.70	0.97	–	–	–	–	–
	0500v	–	–	–	–	–	0.59	0.59	1.93	2.27	0.70
	0500hv	0.57	0.60	1.48	5.47	1.39	0.61	0.59	2.00	3.75	0.93

Ceiling System	Test Record	Maximum Recorded Horizontal Acceleration (g) [a,b]					Maximum Recorded Vertical Acceleration (g) [a,b]				
		Table	Abase	Afram	Agrid	Afram TSNS	Table	Abase	Afram	Agrid	Afram TSV
	0750h	1.00	1.05	1.91	1.78	1.82	–	–	–	–	–
	0750v	–	–	–	–	–	1.10	1.20	2.73	3.51	1.31
	0750hv	0.95	0.92	2.12	8.63	1.97	1.08	1.13	2.69	3.89	1.73
	1000h	1.49	1.58	2.71	4.77	2.58	–	–	–	–	–
	1000v	–	–	–	–	–	1.71	2.04	3.63	4.69	2.12
	1000hv	1.40	1.26	2.42	12.35	2.31	1.67	1.96	3.52	6.80	2.72
	1250h	2.05	2.23	3.57	3.56	3.45	–	–	–	–	–
	1250v	–	–	–	–	–	2.34	2.99	6.5	4.29	3.12
	1250hv	2.03	1.80	2.82	11.07	2.72	2.17	2.68	5.01	4.65	3.64
CS4 Date of test: 8/29/03	0050h	0.06	0.07	0.14	0.13	0.14	–	–	–	–	–
	0085h	0.10	0.10	0.20	0.18	0.20	–	–	–	–	–
	0150h	0.14	0.14	0.24	0.31	0.23	–	–	–	–	–
	0150v	–	–	–	–	–	0.14	0.15	0.41	0.87	0.16
	0150hv	0.16	0.17	0.30	0.45	0.30	0.15	0.15	0.43	0.89	0.21
	0300h	0.33	0.33	0.53	1.12	0.51	–	–	–	–	–
	0300v	–	–	–	–	–	0.31	0.32	0.86	2.48	0.37
	0300hv	0.32	0.34	0.69	1.27	0.68	0.32	0.31	0.88	2.92	0.47
	0500h	0.58	0.61	1.08	1.78	1.04	–	–	–	–	–
	0500v	–	–	–	–	–	0.59	0.61	1.75	3.26	0.72
	0500hv	0.55	0.59	1.38	2.04	1.37	0.59	0.60	1.74	3.35	0.90
	0750h	1.00	1.05	2.08	3.39	1.99	–	–	–	–	–
	0750v	–	–	–	–	–	1.10	1.17	3.20	3.93	1.32
	0750hv	0.94	0.90	1.94	2.65	1.91	1.06	1.13	2.74	3.12	1.75
	1000h	1.47	1.56	2.67	5.77	2.57	–	–	–	–	–

Ceiling System	Test Record	Maximum Recorded Horizontal Acceleration (g) [a,b]					Maximum Recorded Vertical Acceleration (g) [a,b]				
		Table	Abase	Afram	Agrid	Afram TSNS	Table	Abase	Afram	Agrid	Afram TSV
	1000v	–	–	–	–	–	1.72	2.07	4.98	4.72	2.11
	1000hv	1.38	1.26	2.05	4.03	2.04	1.68	1.95	4.32	5.21	2.80
	1250h	2.05	2.20	3.44	6.37	3.23	–	–	–	–	–
	1250v	–	–	–	–	–	2.38	3.07	7.39	7.05	3.18
	1250hv	1.98	1.75	2.31	5.64	2.37	2.19	2.70	5.98	8.47	3.71

a. See Figs. 2–11 and 2–12 for accelerometer locations.
b. Unfiltered maximum recorded acceleration.

Table 3–3. Observed ceiling system damage from single impulse tests.

Ceiling System	Test Record	Summary Remarks on Observed Damages[a]
CS1 Date of test: 8/27/03	0050h	No damage to the suspension system or tiles.
	0085h	No damage to the suspension system or tiles.
	0150h	No damage to the suspension system or tiles.
	0150v	No damage to the suspension system or tiles.
	0150hv	No damage to the suspension system or tiles.
	0300h	No damage to the suspension system or tiles.
	0300v	No damage to the suspension system or tiles.
	0300hv	No damage to the suspension system or tiles.
	0500h	No damage to the suspension system or tiles.
	0500v	No damage to the suspension system or tiles.
	0500hv	No damage to the suspension system or tiles.
	0750h	No damage to the suspension system or tiles.
	0750v	No damage to the suspension system or tiles.
	0750hv	No damage to the suspension system or tiles.
	1000h	No damage to the suspension system or tiles.
	1000v	No damage to the suspension system or tiles.
	1000hv	One tile was damaged, which was replaced following testing. Two Z-bar clips were damaged and replaced following testing. Some perimeter tiles displaced above the perimeter clips.
	1250h	No damage to the suspension system or tiles.
	1250v	The light fixture on southern side of the ceiling system dislodged because the light support arm swung inward during testing. Many Z-bar clips we re dislodged near the fixtures and center of the ceiling system. The perimeter tiles displaced above perimeter spring clips along the northern edge of the ceiling system.
CS2 Date of test: 8/28/03	0050h	No damage to the suspension system or tiles.
	0085h	No damage to the suspension system or tiles.
	0150h	No damage to the suspension system or tiles.
	0150v	No damage to the suspension system or tiles.
	0150hv	No damage to the suspension system or tiles.
	0300h	No damage to the suspension system or tiles.

Ceiling System	Test Record	Summary Remarks on Observed Damages[a]
	0300v	No damage to the suspension system or tiles.
	0300hv	No damage to the suspension system or tiles.
	0500h	No damage to the suspension system or tiles.
	0500v	No damage to the suspension system or tiles.
	0500hv	One of the four swing arm supports for the south light fixture swung in leaving the corner of the fixture unsupported. No damage to the suspension system or tiles. The swing arm was repositioned following testing.
	0750h	One southern perimeter cross-tee spanning to the wall type molding dropped past the molding. The cross-tee was repositioned following testing.
	0750v	One tile dislodged up between the cross-tees and onto the grid but did not fall. No damage to the suspension system or tiles. The dislodged tiles were repositioned following testing.
	0750hv	One tile dislodged up between the cross-tees and onto the grid but did not fall. No damage to the suspension system or tiles. The dislodged tiles were repositioned following testing.
	1000h	One southern perimeter cross-tee spanning to the wall molding dropped past the molding. The cross-tee was repositioned following testing.
	1000v	Five tiles dislodged up between the cross-tees and onto the grid but did not fall. No damage to the suspension system or tiles. The dislodged tiles were repositioned following testing.
	1000hv	Seven tiles dislodged up between the cross-tees and onto the grid but did not fall. No damage to the suspension system or tiles. The dislodged tiles were repositioned following testing.
	1250h	Cross-tee connections located at the southern light fixture were disconnected and reconnected following testing. Five southern perimeter cross-tees spanning to the wall molding dropped past the molding. The cross-tees were replaced following testing.
	1250v	Ten tiles dislodged up between the cross-tees and onto the grid but did not fall. The corner of northern light fixture fell through the grid. No damage to the suspension system or tiles. The dislodged tiles were repositioned following testing.
	1250hv	Seven tiles dislodged up between the cross-tees and onto the grid but did not fall. The cross-tee connections located at the southern and northern light fixtures were disconnected. The connection tabs at these connections were bent inward. Four southern perimeter cross-tees spanning to the wall molding dropped past the molding.
CS3 Date of test: 8/28/03	0050h	No damage to the suspension system or tiles.
	0085h	No damage to the suspension system or tiles.
	0150h	No damage to the suspension system or tiles.
	0150v	No damage to the suspension system or tiles.

Ceiling System	Test Record	Summary Remarks on Observed Damages[a]
	0150hv	No damage to the suspension system or tiles.
	0300h	No damage to the suspension system or tiles.
	0300v	No damage to the suspension system or tiles.
	0300hv	No damage to the suspension system or tiles.
	0500h	No damage to the suspension system or tiles.
	0500v	No damage to the suspension system or tiles.
	0500hv	No damage to the suspension system or tiles.
	0750h	No damage to the suspension system or tiles.
	0750v	No damage to the suspension system or tiles.
	0750hv	No damage to the suspension system or tiles.
	1000h	No damage to the suspension system or tiles.
	1000v	No damage to the suspension system or tiles.
	1000hv	Three Z-bar clips were bent disconnecting the Z-bars and channel sections in the center of the ceiling system. This failure caused the middle of the ceiling system to sag between the runners. The Z-bar clips were replaced following testing.
	1250h	One Z-bar clip was disconnected in the center of the ceiling system. One southern perimeter cross-tee spanning to the wall molding dropped past the molding. The system was repositioned after testing.
	1250v	Five Z-bar clips were bent disconnecting the Z-bars and channel sections in the center of the ceiling system. These failures caused the middle of the ceiling system to sag between the runners. The Z-bar with the five disconnected Z-bar clips had a damaged and disconnected splice. The Z-bar splice was fixed and the five Z-bar clips were replaced after testing.
	1250hv	Four Z-bar clips were bent disconnecting the Z-bars and channel sections in the center of the ceiling system. These failures caused the middle of the ceiling system to sag between the runners. The Z-bar with the four disconnected Z-bar clips had a damaged and disconnected splice.
CS4 Date of test: 8/29/03	0050h	No damage to the suspension system or tiles.
	0085h	No damage to the suspension system or tiles.
	0150h	No damage to the suspension system or tiles.
	0150v	No damage to the suspension system or tiles.
	0150hv	No damage to the suspension system or tiles.
	0300h	No damage to the suspension system or tiles.

Ceiling System	Test Record	Summary Remarks on Observed Damages[a]
	0300v	No damage to the suspension system or tiles.
	0300hv	No damage to the suspension system or tiles.
	0500h	No damage to the suspension system or tiles.
	0500v	No damage to the suspension system or tiles.
	0500hv	No damage to the suspension system or tiles.
	0750h	No damage to the suspension system or tiles.
	0750v	One tile dislodged up between the cross-tees and onto the grid but did not fall. No damage to the suspension system or tiles. The dislodged tiles were repositioned following testing.
	0750hv	Six tiles dislodged up between the cross-tees and onto the grid but did not fall. No damage to the suspension system or tiles. The dislodged tiles were repositioned following testing.
	1000h	No damage to the suspension system or tiles.
	1000v	Five tiles dislodged up between the cross-tees and onto the grid but did not fall. No damage to the suspension system or tiles. The dislodged tiles were repositioned following testing.
	1000hv	Nineteen tiles dislodged up between the cross-tees and onto the grid but did not fall. One of the four swing arm supports for the south light fixture rotated in leaving the corner of the fixture unsupported. No damage to the suspension system or tiles. The swing arm and dislodged tiles were repositioned following testing.
	1250h	The cross-tee connections located at the northern light fixture were disconnected. The connection tabs at these connections were bent inward. The connection tabs were realigned following testing.
	1250v	Nine tiles dislodged up between the cross-tees and onto the grid but did not fall. No damage to the suspension system or tiles. The dislodged tiles were repositioned following testing.
	1250hv	Ten tiles dislodged up between the cross-tees and onto the grid but did not fall. Five northern perimeter cross-tees spanning to the wall molding dropped down past the wall-type molding. The grid connections on the northern perimeter of the ceiling systems between the light fixtures and ceiling system perimeter failed. One tile fell.

a. See Figs. 3–1 through 3–12 for photographs of representative damage to the ceiling system.

Source: NIST.

Figure 3–1. Displacement of perimeter tiles over perimeter spring clips following Test 20 for ceiling system CS1.

Source: NIST.

Figure 3–2. Bottom view of damage to ceiling system CS1 following Test 20.

Source: NIST.

Figure 3–3. Bottom view of damage to ceiling system CS1 following Test 20.

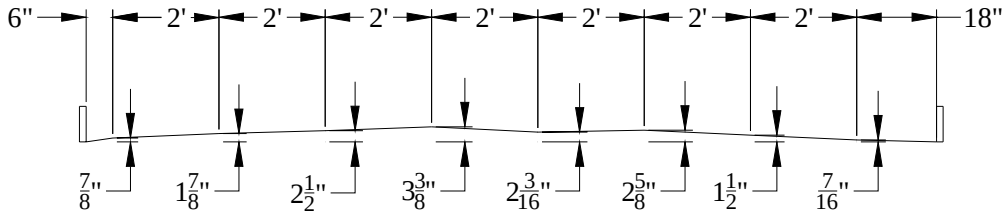

Figure 3–4. Permanent vertical displacements of Z-bars in the east-west direction following Test 20 for ceiling system CS1.

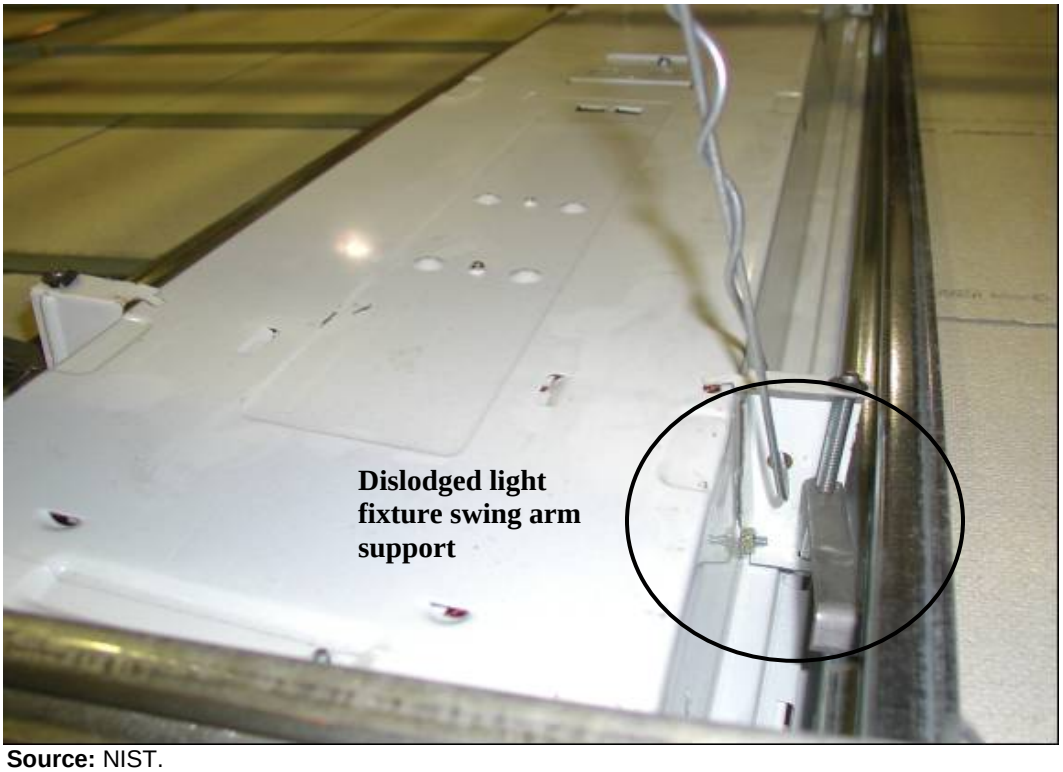

Source: NIST.

Figure 3–5. Light fixture swing arm support dislodged following Test 21 for ceiling system CS1.

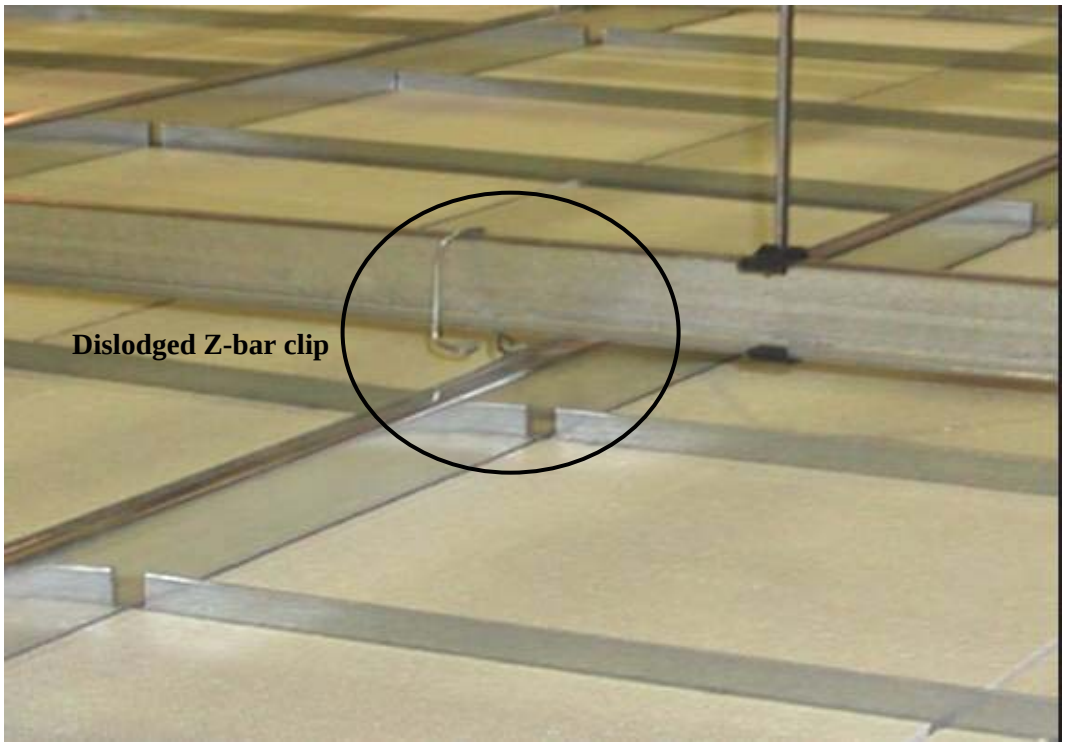

Source: NIST.

Figure 3–6. Dislodged Z-bar clip in ceiling system CS1 following Test 21.

Source: NIST.

Figure 3–7. Dislodged southern light fixture corner in ceiling system CS2 following Test 14.

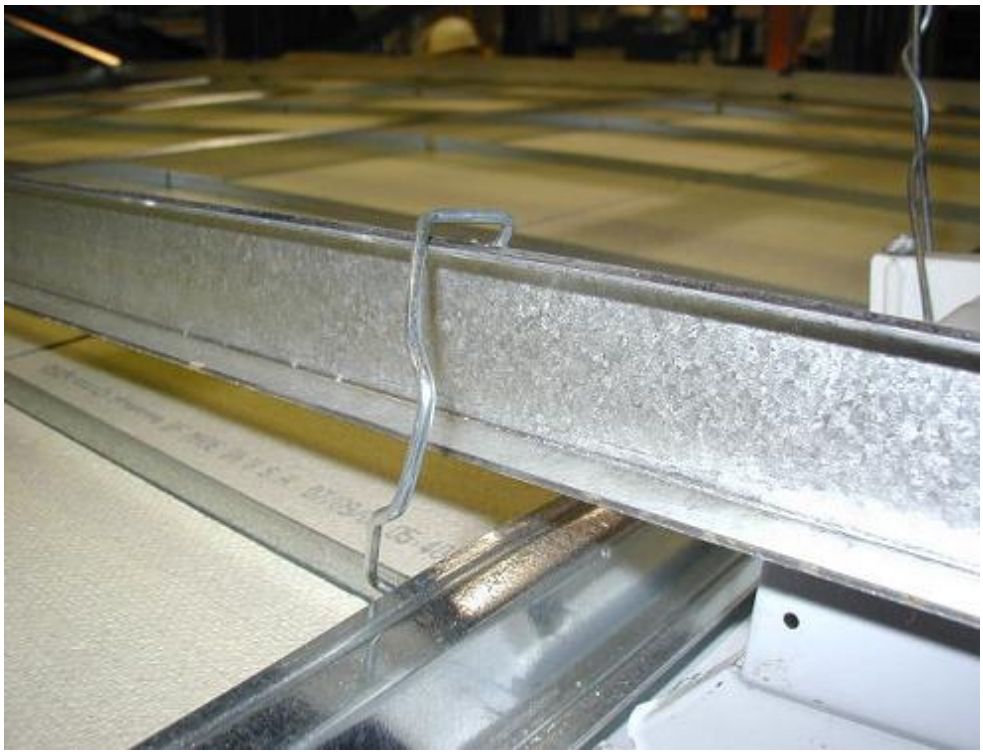

Source: NIST.

Figure 3–8. Stretching of Z-bar clips located at northern light fixture corner in ceiling system CS3 following Test 20.

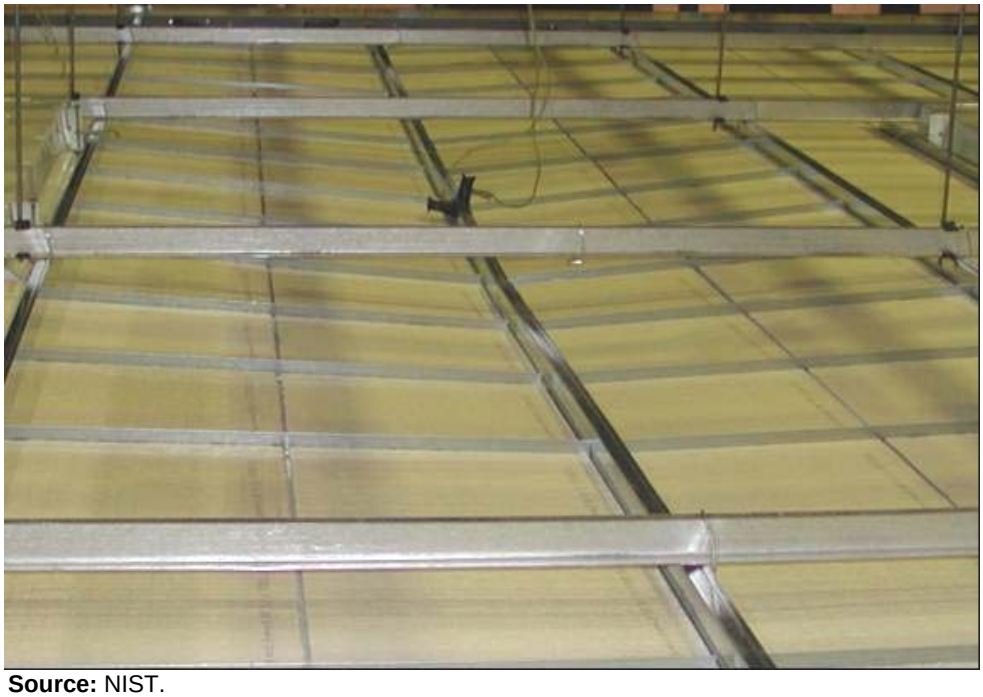

Source: NIST.

Figure 3–9. Damage to the center of ceiling system CS3 following Test 20.

Source: NIST.

Figure 3–10. Damage to the center of ceiling system CS3 following Test 23.

Source: NIST.

Figure 3–11. Damage to the northern perimeter of ceiling system CS4 following Test 23.

Source: NIST.

Figure 3–12. Damage to the northern perimeter of ceiling system CS4 following Test 23.

3.3 EARTHQUAKE TESTS

Earthquake testing was conducted for Ceiling Systems 2, 3, and 4. The earthquake response data are presented in Table 3–4. No tests were undertaken for Ceiling 1.

Table 3–4. Observed ceiling system damage from earthquake tests.

Ceiling System	Nominal Acceleration (g)	Summary Remarks on Observed Damages[a]
CS2 Date of test: 8/28/03	0.25	No damage to the suspension system or tiles.
	0.50	No damage to the suspension system or tiles.
	0.75	No damage to the suspension system or tiles.
	1.00	Tiles jumped and border tees dropped.
	1.25	Tiles jumped and border tees dropped.
	1.50	Tiles jumped and border tees dropped.
	1.75	Tiles jumped and border tees dropped.
	2.50	Three tiles fell and three were displaced upward. Tees were down at the light fixture.
CS3 Date of test: 8/28/03	0.25	No damage to the suspension system or tiles.
	0.50	No damage to the suspension system or tiles.
	0.75	No damage to the suspension system or tiles.
	1.00	No damage to the suspension system or tiles.
	1.25	Cut border came loose.
	1.50	No residual damage to the suspension system or tiles.
	1.75	Three Z clips dislodged in the center of the ceiling frame and the center of the frame was sagging.
	2.50	Major collapse of the system. See Fig. 3–13.
CS4 Date of test: 8/29/03	0.25	No damage to the suspension system or tiles.
	0.50	No damage to the suspension system or tiles.
	0.75	No damage to the suspension system or tiles.
	1.00	No damage to the suspension system or tiles.
	1.25	No damage to the suspension system or tiles.
	1.50	The north and south perimeters fell.
	1.75	Entire north perimeter fell. Significant damage to south perimeter. See Figs. 3–14 and 3–15.

a. See Figs. 3–13 through 3–15 for photographs of representative damage to the ceiling system.

Source: NIST.

Figure 3–13. Collapse of ceiling system CS3 after 2.5g earthquake excitation.

Source: NIST.

Figure 3–14. Damage to north perimeter of ceiling system CS4 after 1.75g earthquake excitation.

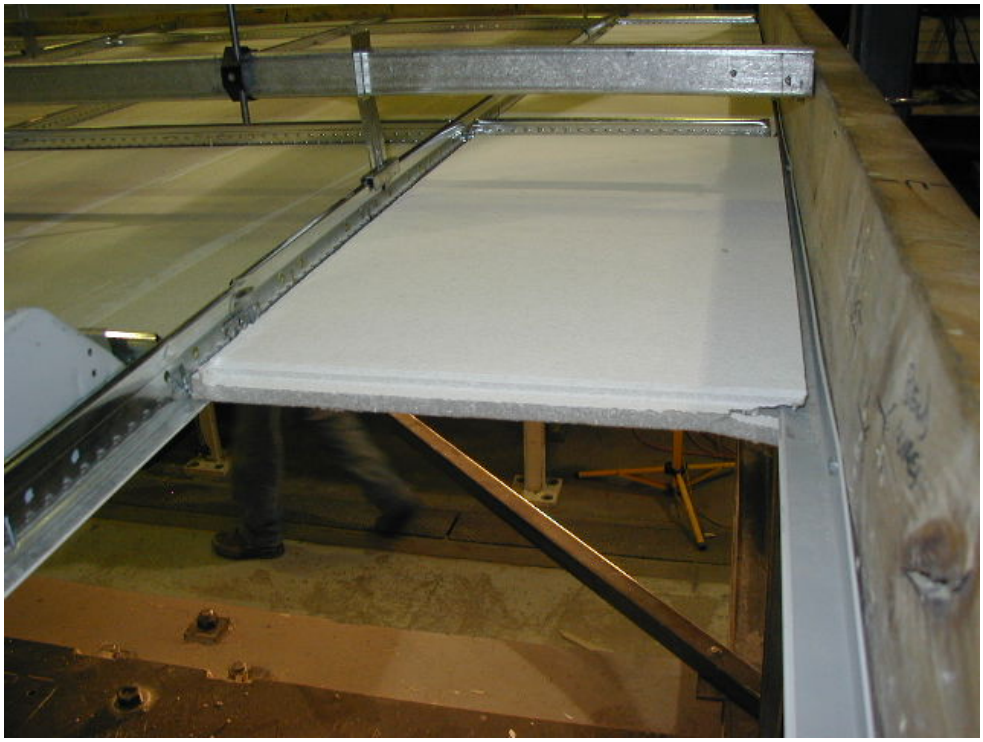

Source: NIST.

Figure 3–15. Damage to south perimeter of ceiling system CS4 after 1.75g earthquake excitation.

This page intentionally left blank.

Chapter 4
SUMMARY

4.1 SUMMARY OF TEST RESULTS

The motion of the test frame and suspension systems was considerably larger than the motion at the base of the test frame in the period range between 0.0 s and 0.5 s. The ratio of the spectral response of the ceiling system calculated using the frame (*Afram*) and simulator (*Abase*) acceleration histories, averaged over a frequency range of 5 Hz to 15 Hz, ranged between 1.5 and 3.0 for horizontal (H) shaking, and 2.3 and 3.2 for vertical (V) shaking.

The performance of the different types of ceiling systems is summarized in Table 4–1, where the performance for the two limit states of Section 3.2.2 is given in terms of target peak acceleration of the simulator.

Table 4–1. Performance of ceiling systems.

Testing Series	Ceiling System ID	System Description	Impulse	Qualification Level (g)	
				Limit State 1[a]	Limit State 2[b]
TS1	CS1	System with cold rolled sections spanning east-west direction. Tiles were 12 in. (305 mm) square.	H	>1.25	>1.25
			V	>1.25	>1.25
			H&V	>1.00	> 1.00
			EQ	–	–
TS2	CS2	System with cold rolled sections spanning east-west direction. Tiles were 24 in. (610 mm) square.	H	>1.25	>1.00
			V	>1.25	>1.25
			H&V	>1.25	1.00
			EQ	1.75	1.75
TS3	CS3	System with cold rolled sections spanning north-south direction. Tiles were 12 in. (305 mm) square.	H	>1.25	>1.00
			V	>1.25	1.00
			H&V	>1.25	0.75
			EQ	1.75	1.50
TS4	CS4	System with cold rolled sections spanning north-south direction. Tiles were 24 in. (610 mm) square.	H	>1.25	>1.25
			V	>1.25	>1.25
			H&V	1.25	1.25
			EQ	1.25	12.0

a. Limit state 1 is the loss of one or more tiles.
b. Limit state 2 is sufficient damage to one or more components of the suspension system such that repair or replacement of part or all of the suspension system would be required.
Key: EQ, earthquake; H, horizontal; V, vertical.

4.2 IMPLICATIONS OF TEST RESULTS

All four combinations of impulse direction and ceiling system resisted significant damage up to about 1g applied to the test platform, about 2.5g to 3g at the ceiling frame. Tile motion intensified with increasing impulse strength, and significant damage occurred (or began to occur) for relatively modest further increments in impulse strength. From analysis of this ascending effect for all systems under all the impulses suggests that their total failure would occur at values near the 1.75g to 2.5g (at the test platform) observed for the earthquake impulses. Qualitatively, this corresponds to about 4g to 5g at the ceiling frame.

Comparison of this magnitude with the results of the impact calculations must take into account that these tests are not exact replications of the initiating events on September 11, 2001:

- The installed ceiling tile systems had been in service for up to 30 years. During that time, the buildings had been subjected to wind forces that swayed the towers, and several occupants have reported that high winds resulted in falling ceiling tiles. Thus, the frames were not in the new condition of the systems tested here.

- The boundary conditions in the test frame were not identical to the service boundary conditions in the towers at the times of the aircraft impact. The tower frames were different from the test frame and the dimensions of the ceiling system were far larger.

Appendix A
TEST HISTORIES

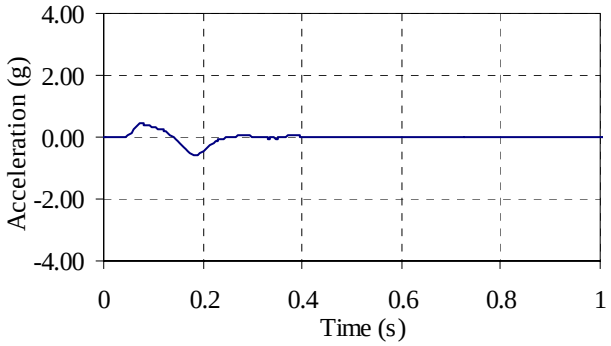

a) horizontal acceleration (*Table*)

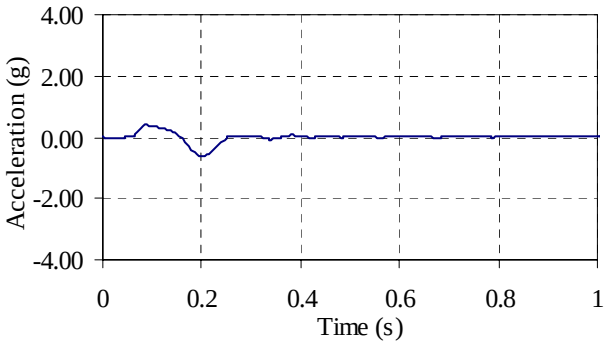

b) horizontal acceleration (*Abase*)

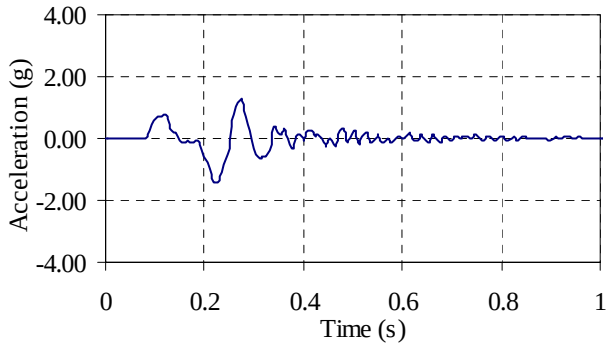

c) horizontal acceleration (*Afram*)

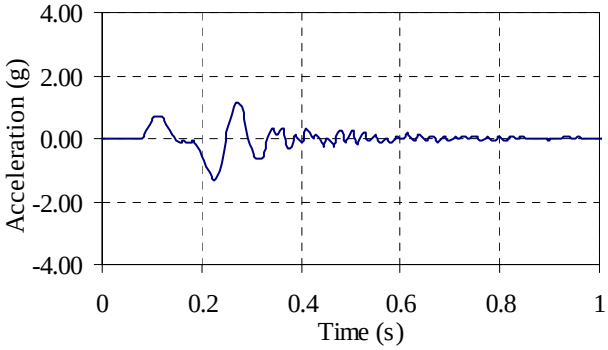

d) horizontal acceleration (*AframTS*)

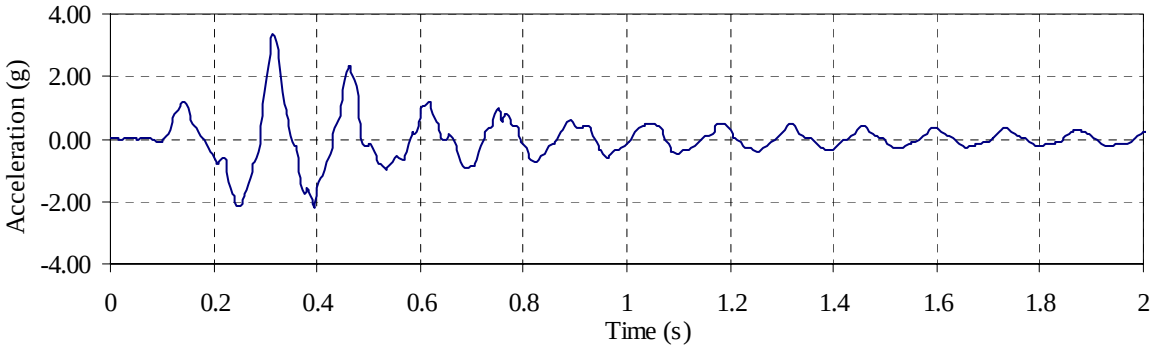

e) horizontal acceleration (*Agrid*)

Figure A–1. Horizontal displacement and acceleration histories for Test 14 on ceiling system CS1.

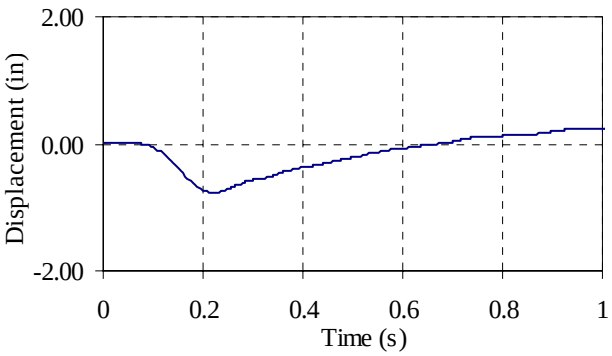

f) horizontal displacement (*Dbase*)

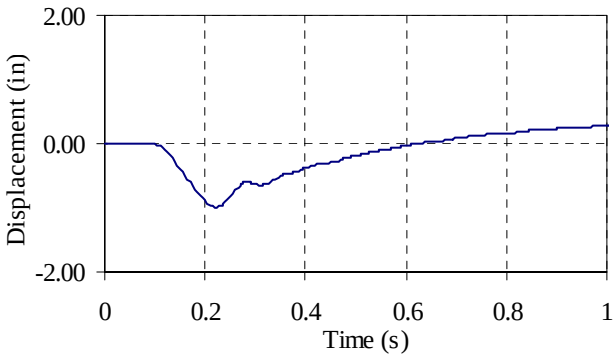

g) horizontal displacement (*Dcntr*)

Figure A–1. Horizontal displacement and acceleration histories for Test 14 on ceiling system CS1 (continued).

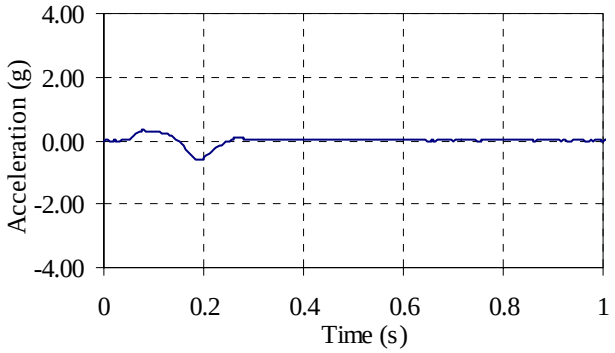

a) vertical acceleration (*Table*)

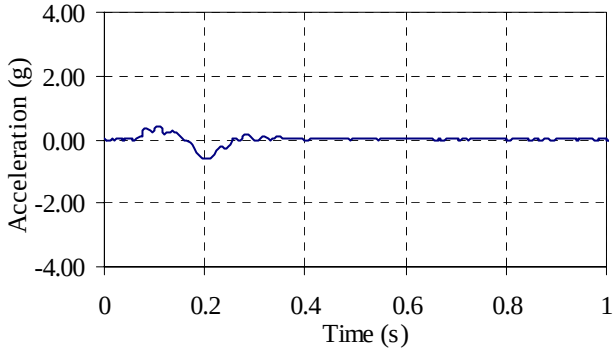

b) vertical acceleration (*Abase*)

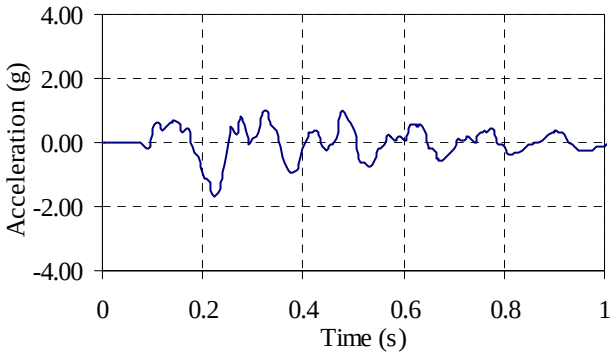

c) vertical acceleration (*Afram*)

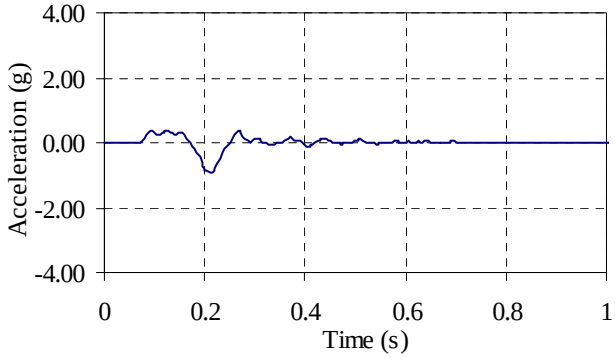

d) vertical acceleration (*AframTS*)

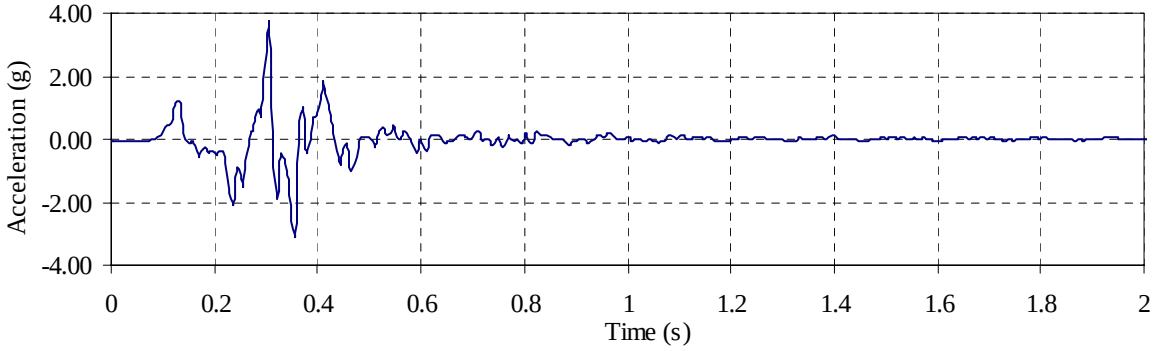

e) vertical acceleration (*Agrid*)

Figure A–2. Vertical acceleration histories for Test 14 on ceiling system CS1.

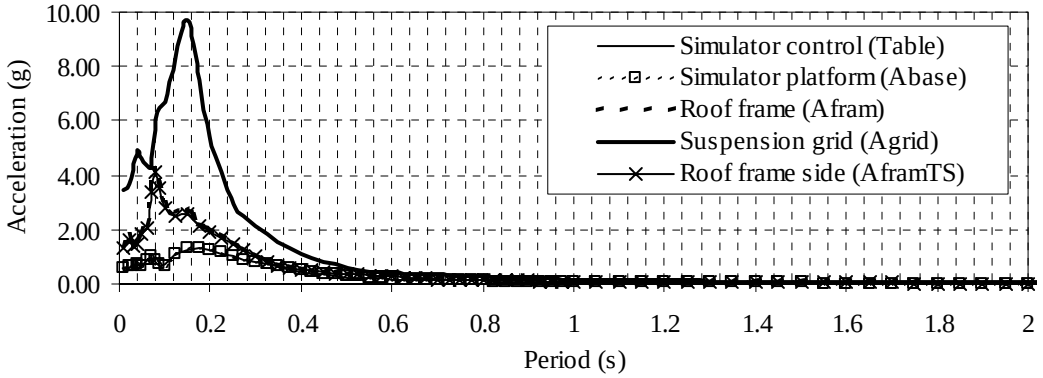

a) horizontal response spectra

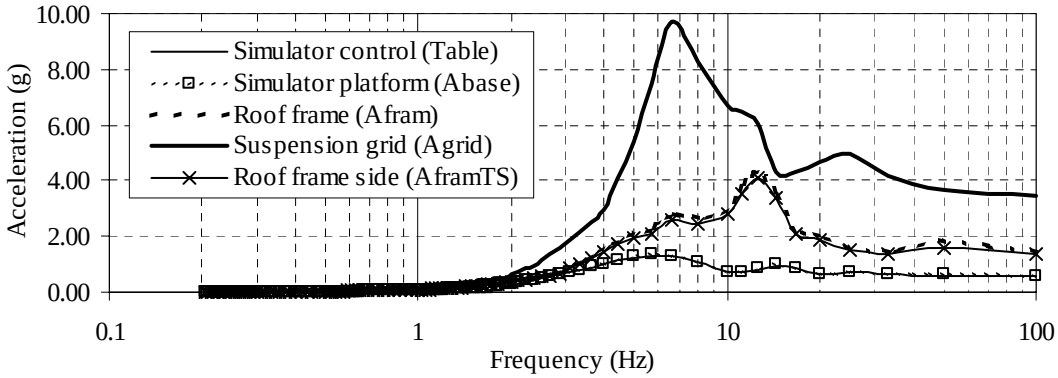

b) horizontal response spectra

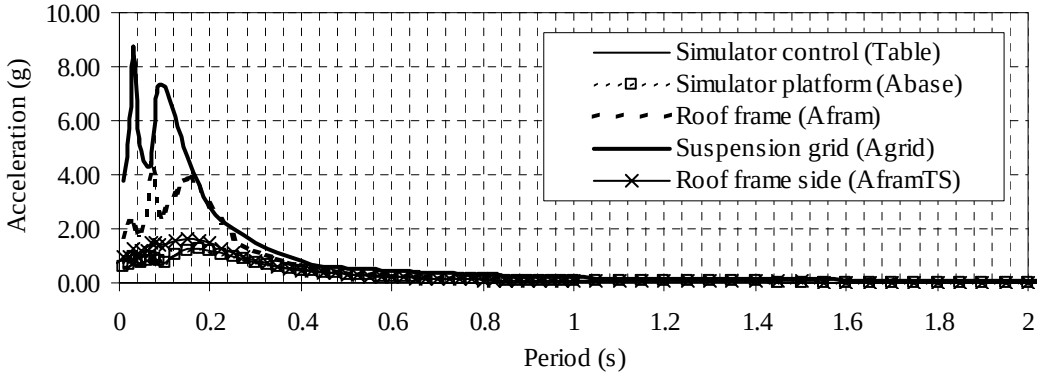

c) vertical response spectra

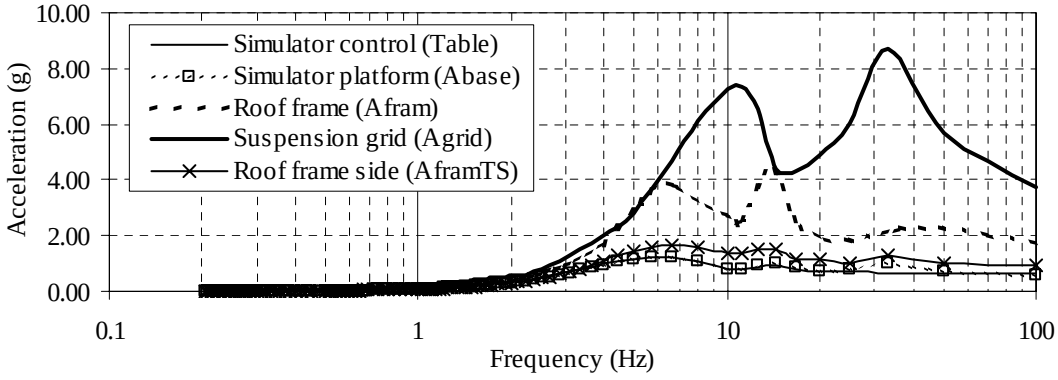

d) vertical response spectra

Figure A–3. Response spectra for Test 14 on ceiling system CS1.

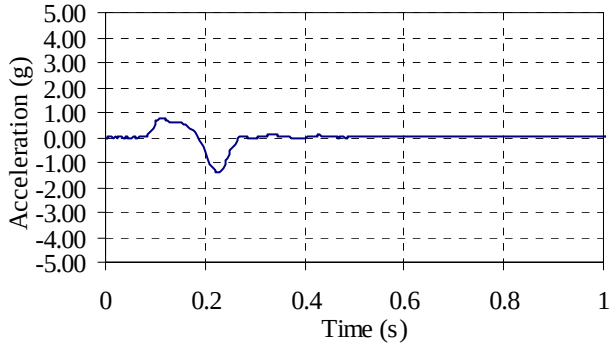

a) horizontal acceleration (*Table*)

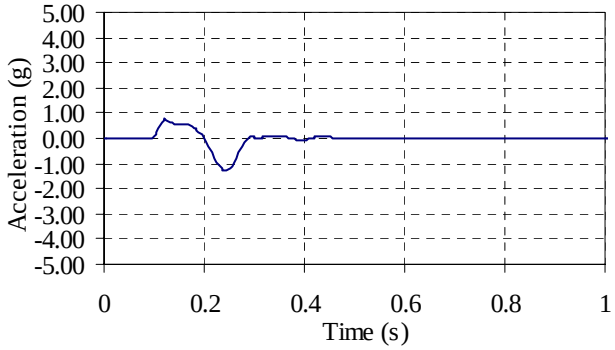

b) horizontal acceleration (*Abase*)

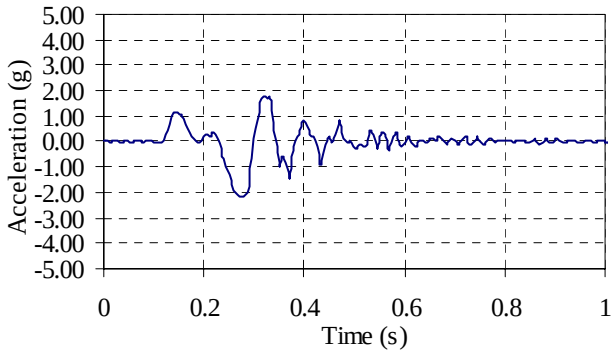

c) horizontal acceleration (*Afram*)

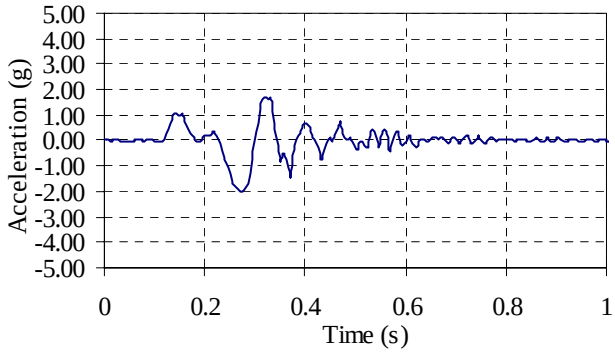

d) horizontal acceleration (*AframTS*)

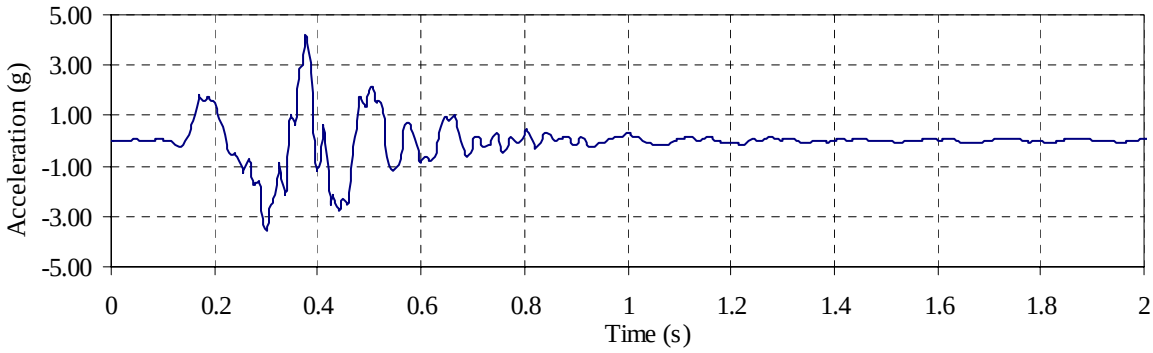

e) horizontal acceleration (*Agrid*)

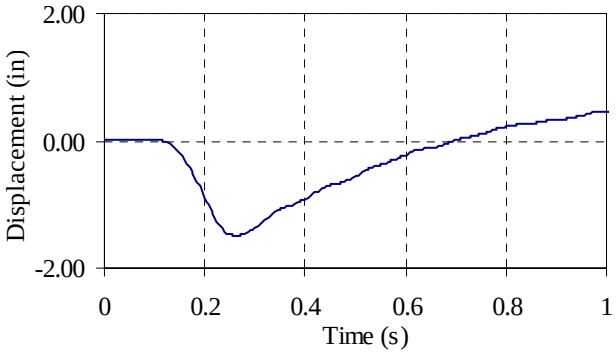

f) horizontal displacement (*Dbase*)

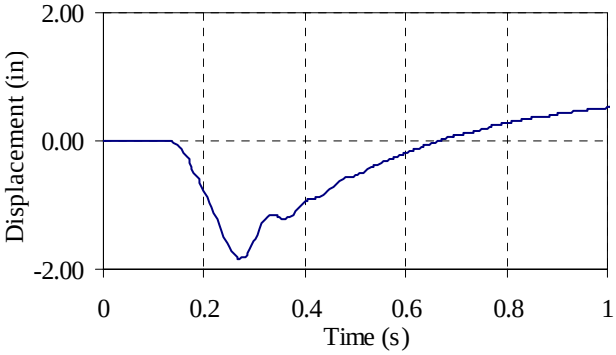

g) horizontal displacement (*Dcntr*)

Figure A–4. Horizontal displacement and acceleration histories for Test 20 on ceiling system CS1.

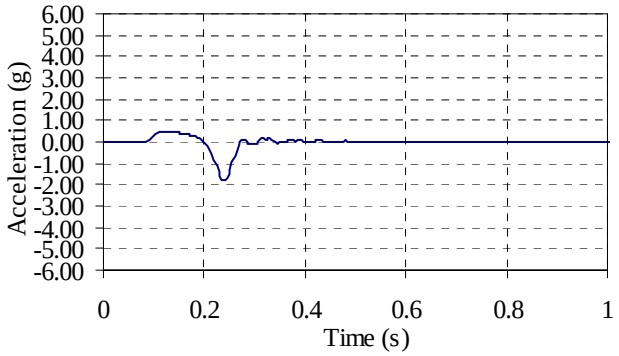

a) vertical acceleration (*Table*)

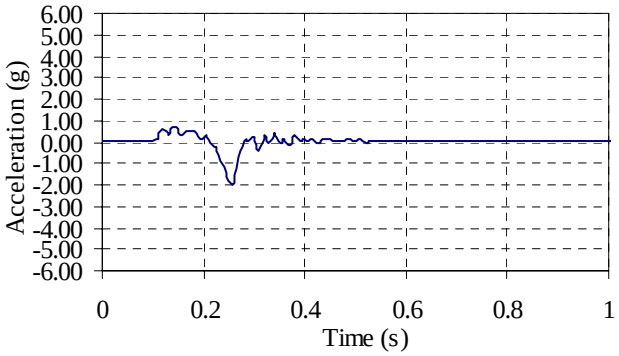

b) vertical acceleration (*Abase*)

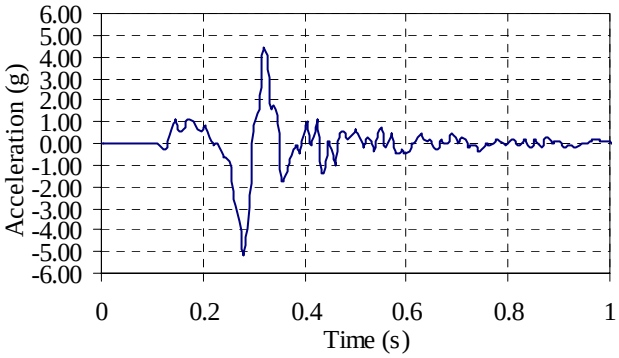

c) vertical acceleration (*Afram*)

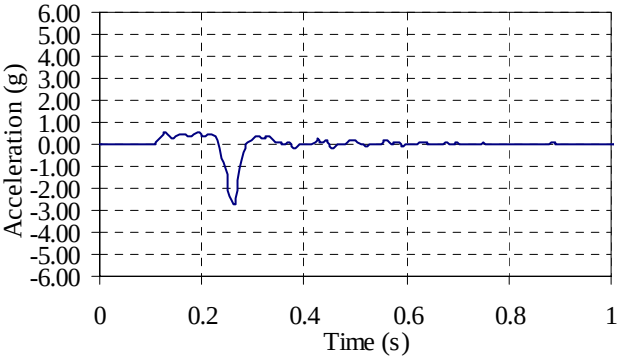

d) vertical acceleration (*AframTS*)

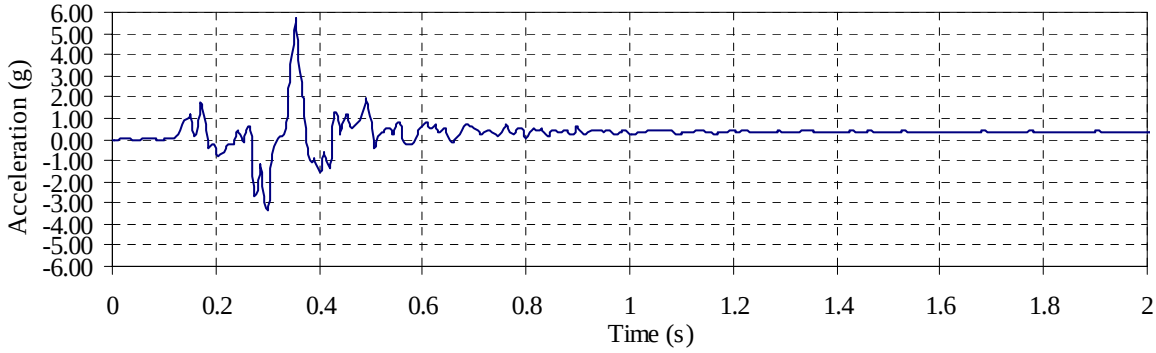

e) vertical acceleration (*Agrid*)

Figure A–5. Vertical acceleration histories for Test 20 on ceiling system CS1.

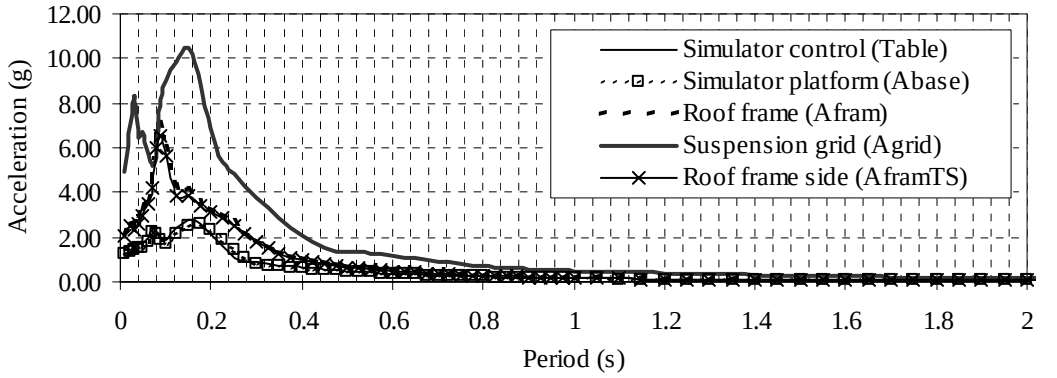

a) horizontal response spectra

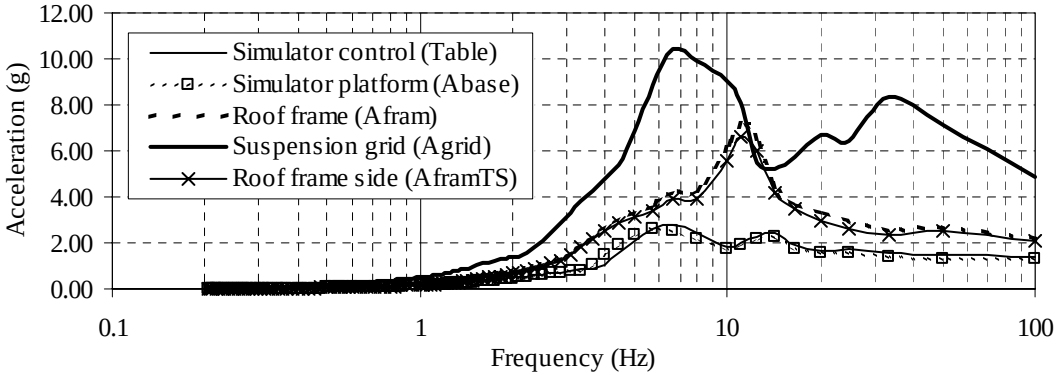

b) horizontal response spectra

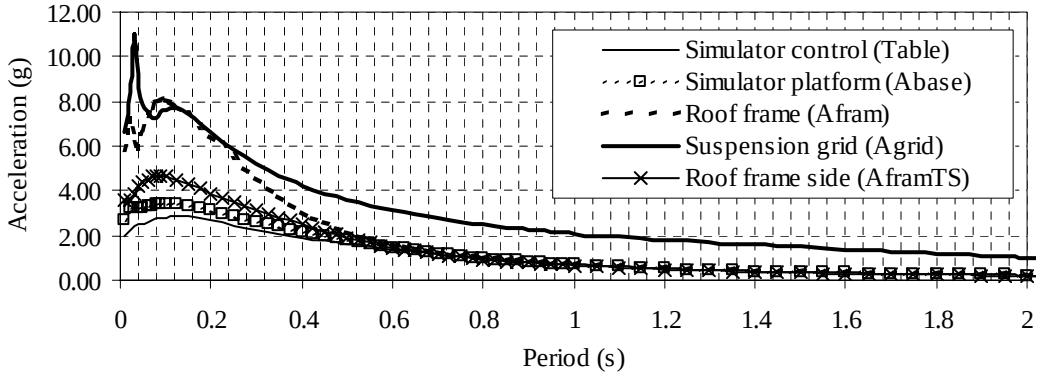

c) vertical response spectra

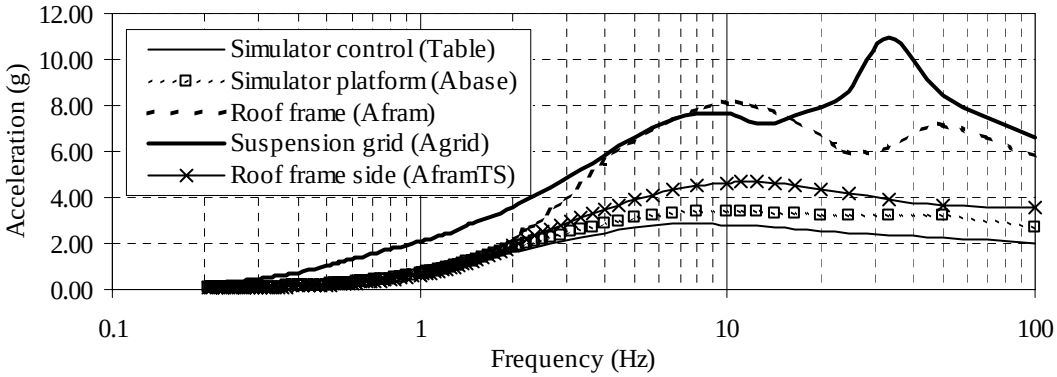

d) vertical response spectra

Figure A–6. Response spectra for Test 20 on ceiling system CS1.

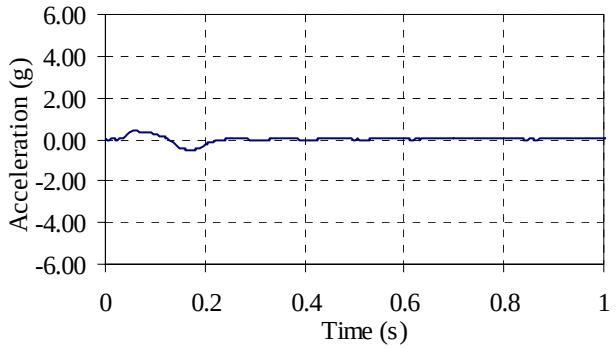

a) horizontal acceleration (*Table*)

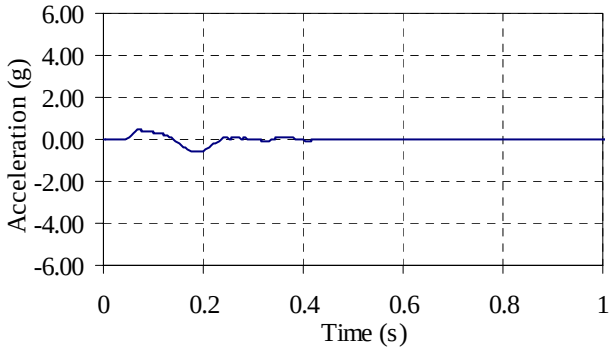

b) horizontal acceleration (*Abase*)

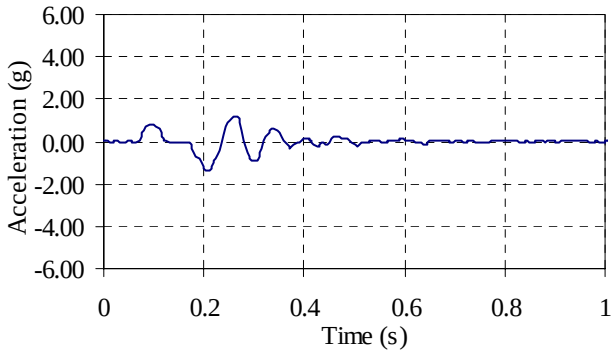

c) horizontal acceleration (*Afram*)

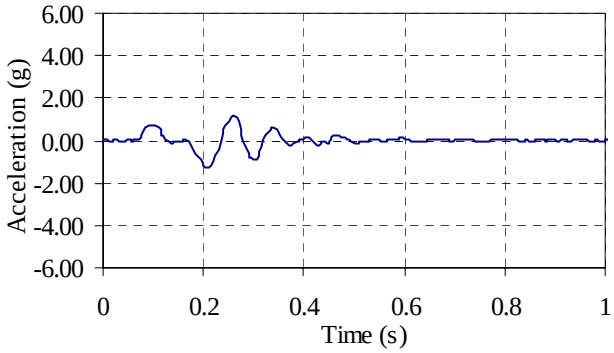

d) horizontal acceleration (*AframTS*)

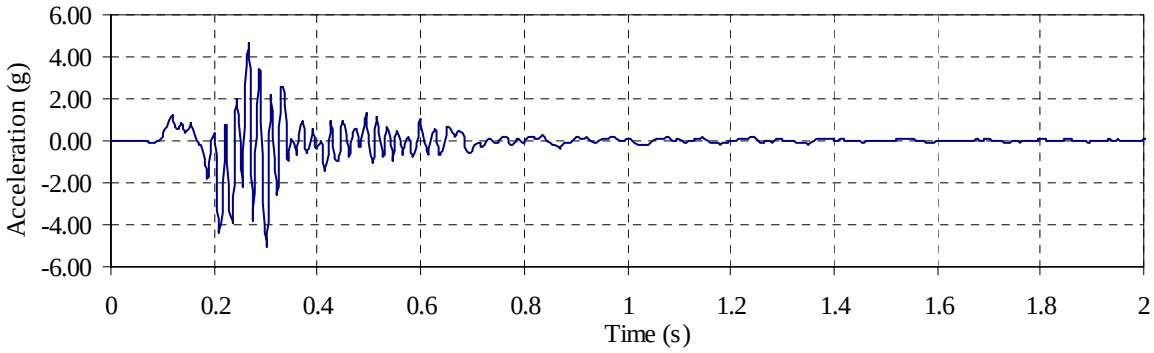

e) horizontal acceleration (*Agrid*)

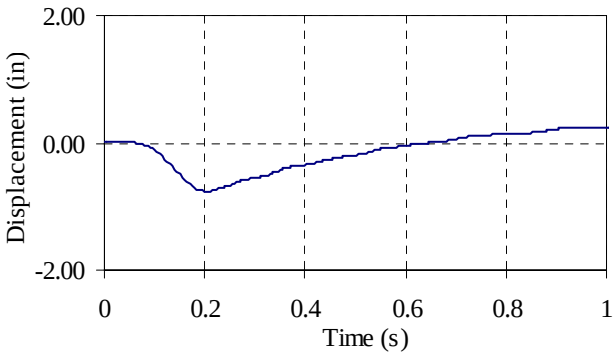

f) horizontal displacement (*Dbase*)

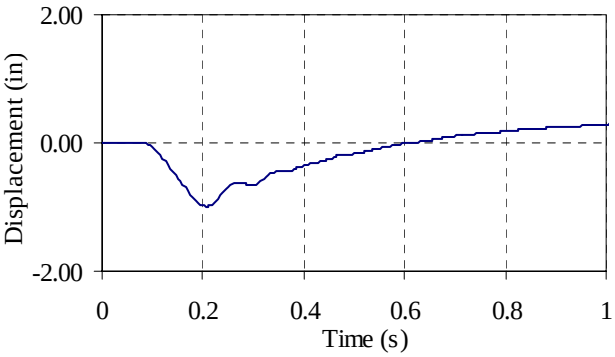

g) horizontal displacement (*Dcntr*)

Figure A–7. Horizontal displacement and acceleration histories for Test 14 on ceiling system CS2.

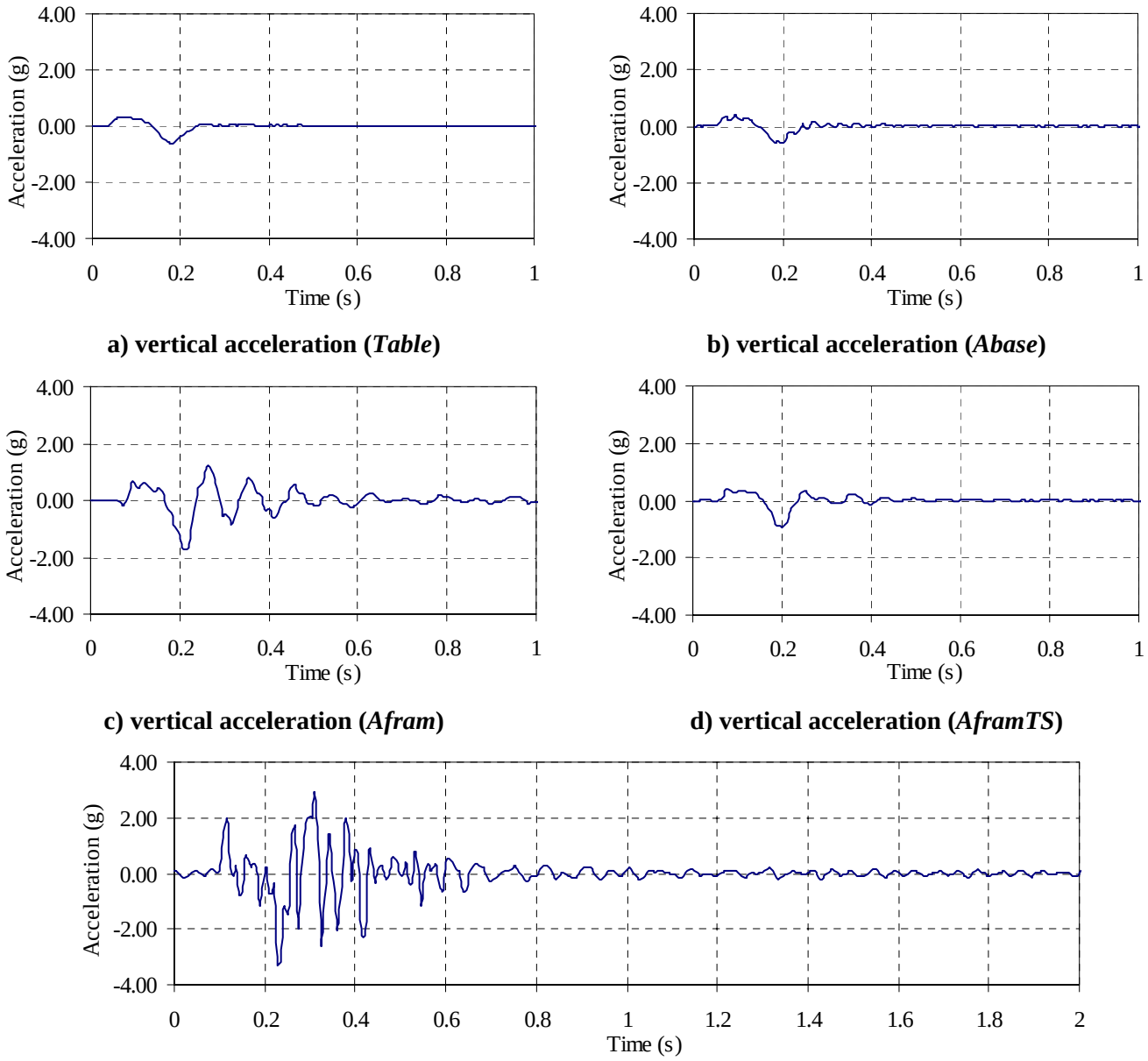

a) vertical acceleration (*Table*)

b) vertical acceleration (*Abase*)

c) vertical acceleration (*Afram*)

d) vertical acceleration (*AframTS*)

e) vertical acceleration (*Agrid*)

Figure A–8. Vertical acceleration histories for Test 14 on ceiling system CS2.

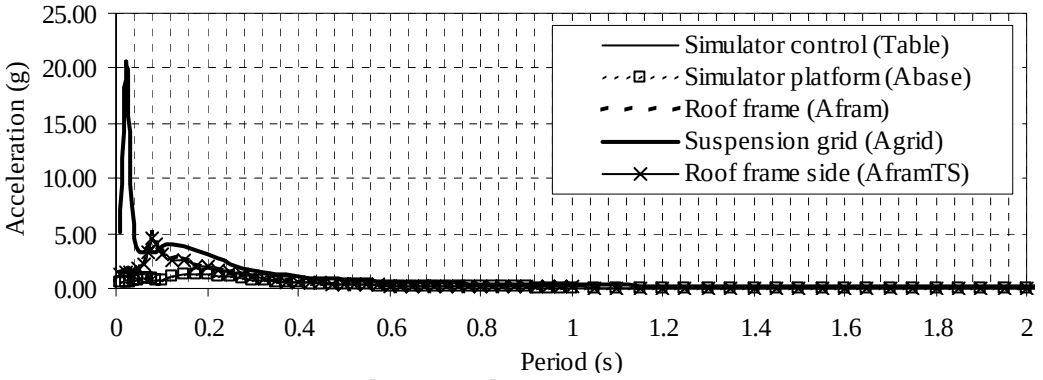

a) horizontal response spectra

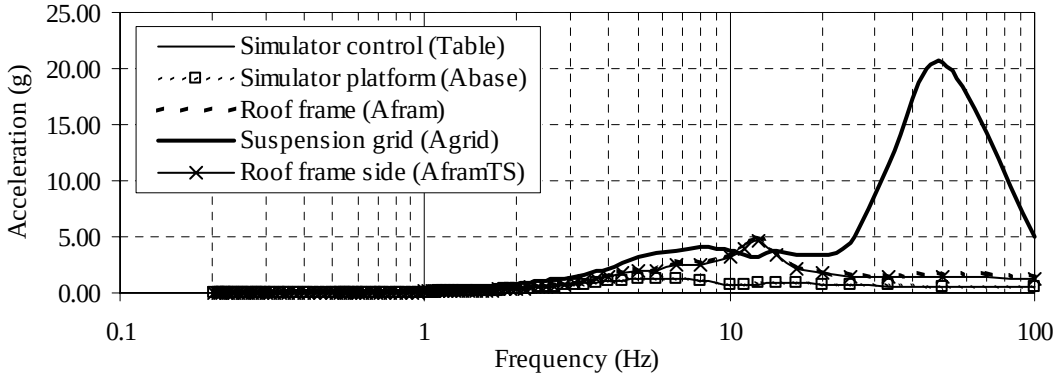

b) horizontal response spectra

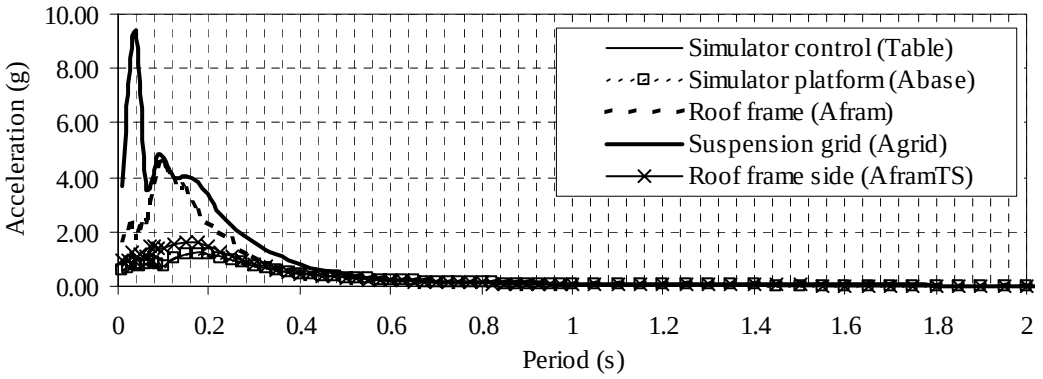

c) vertical response spectra

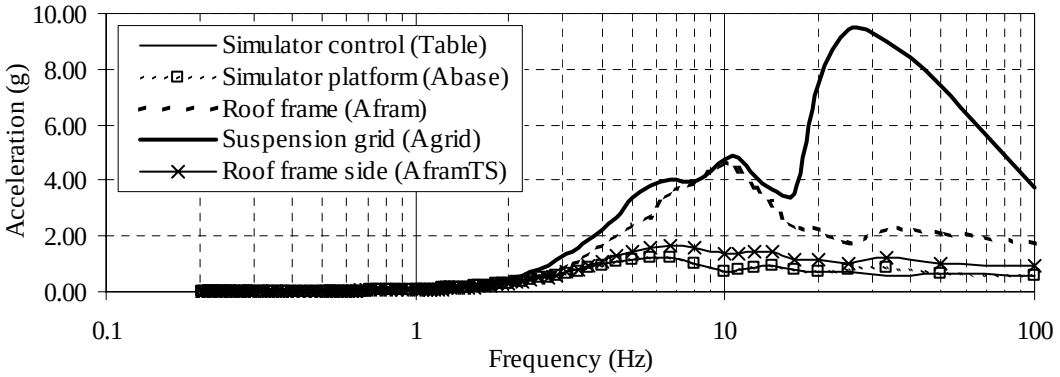

d) vertical response spectra

Figure A–9. Response spectra for Test 14 on ceiling system CS2.

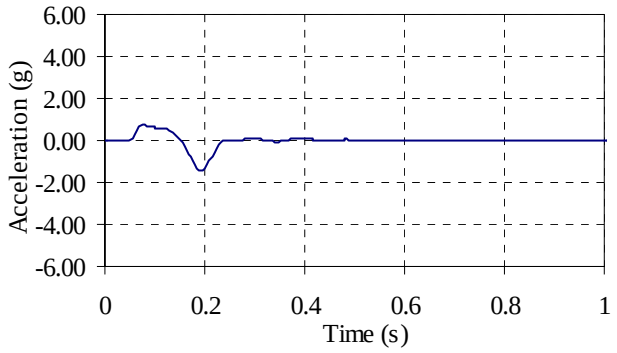

a) horizontal acceleration (*Table*)

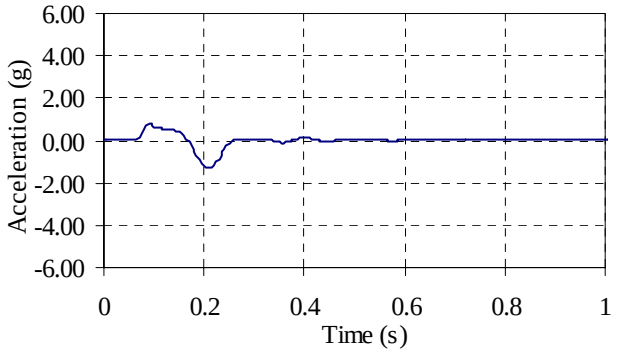

b) horizontal acceleration (*Abase*)

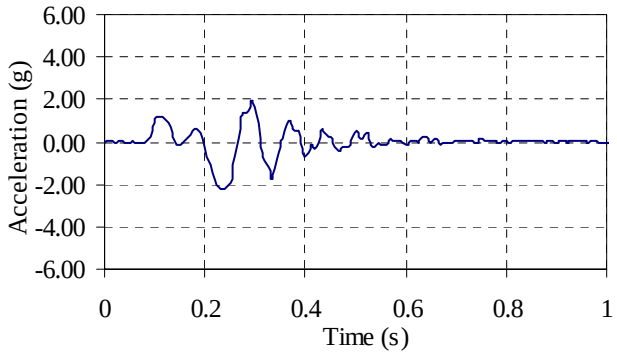

c) horizontal acceleration (*Afram*)

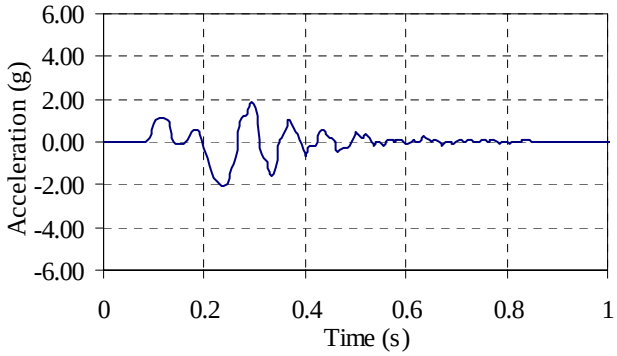

d) horizontal acceleration (*AframTS*)

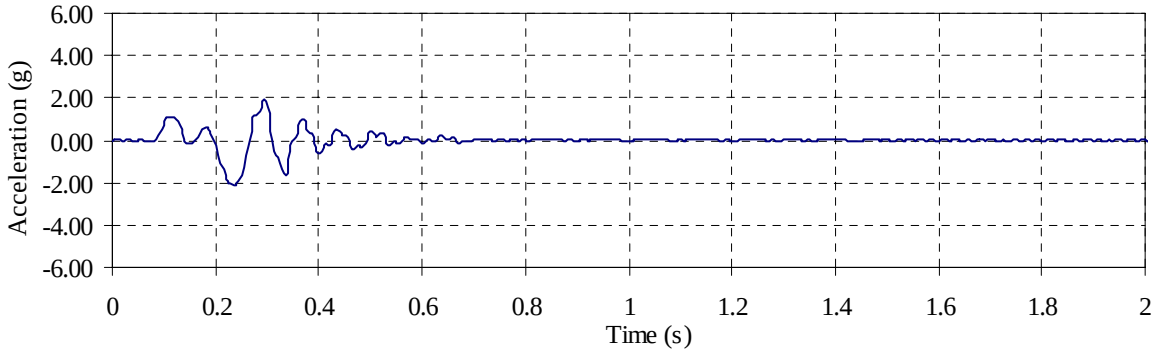

e) horizontal acceleration (*Agrid*)

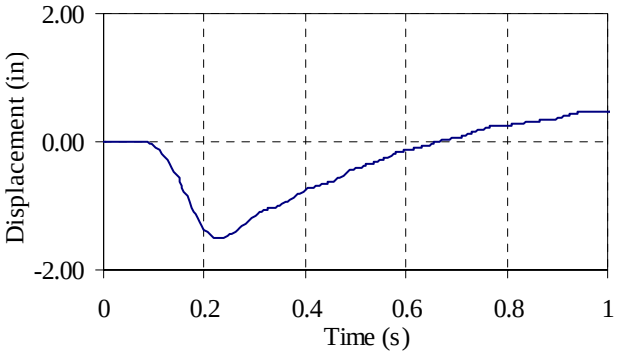

f) horizontal displacement (*Dbase*)

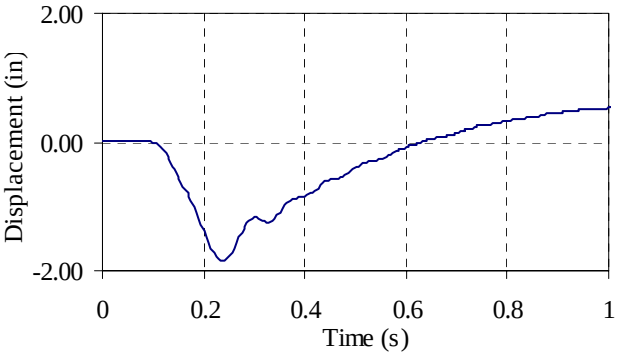

g) horizontal displacement (*Dcntr*)

Figure A–10. Horizontal displacement and acceleration histories for Test 20 on ceiling system CS2.

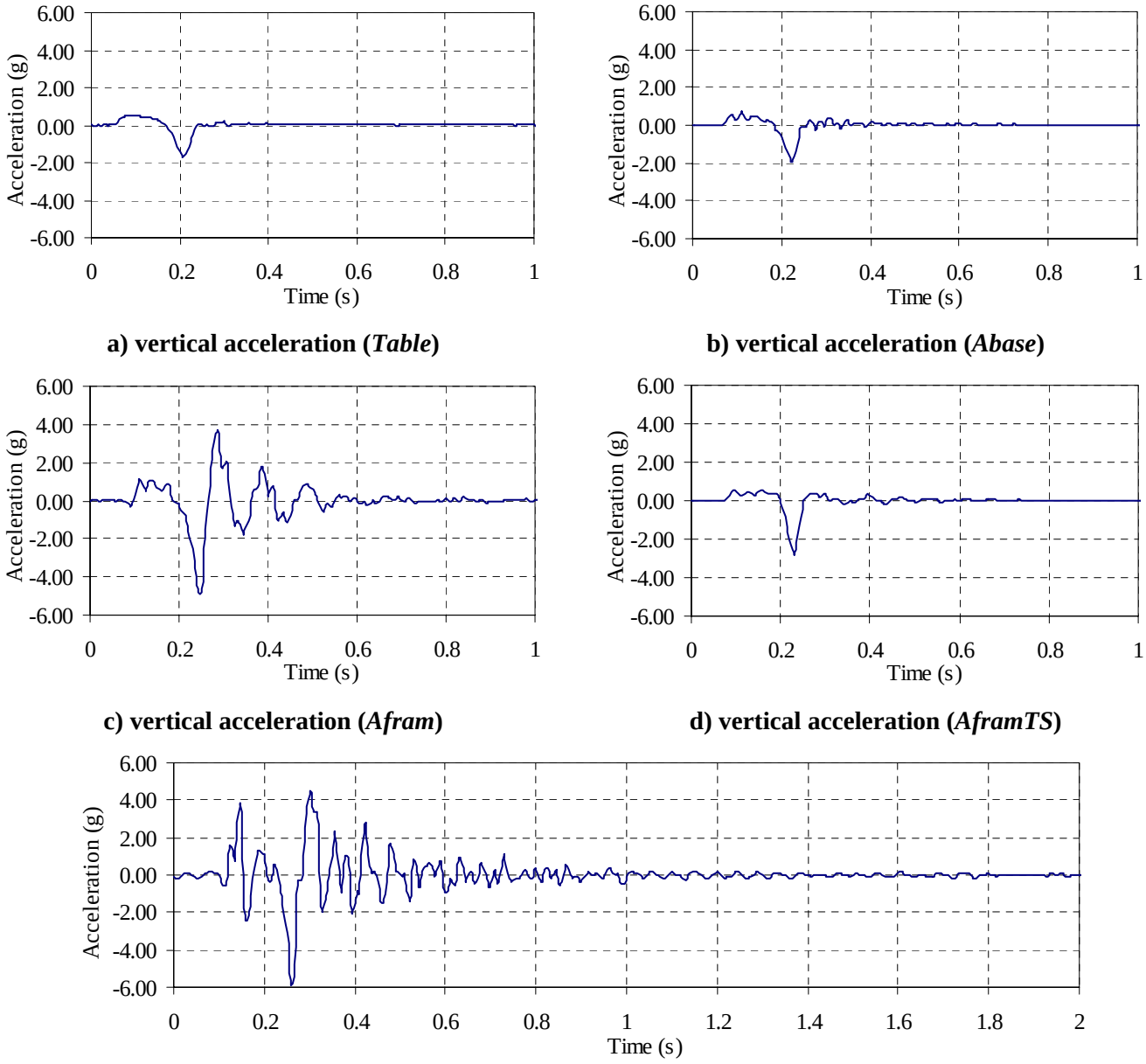

a) vertical acceleration (*Table*)

b) vertical acceleration (*Abase*)

c) vertical acceleration (*Afram*)

d) vertical acceleration (*AframTS*)

e) vertical acceleration (*Agrid*)

Figure A–11. Vertical acceleration histories for Test 20 on ceiling system CS2.

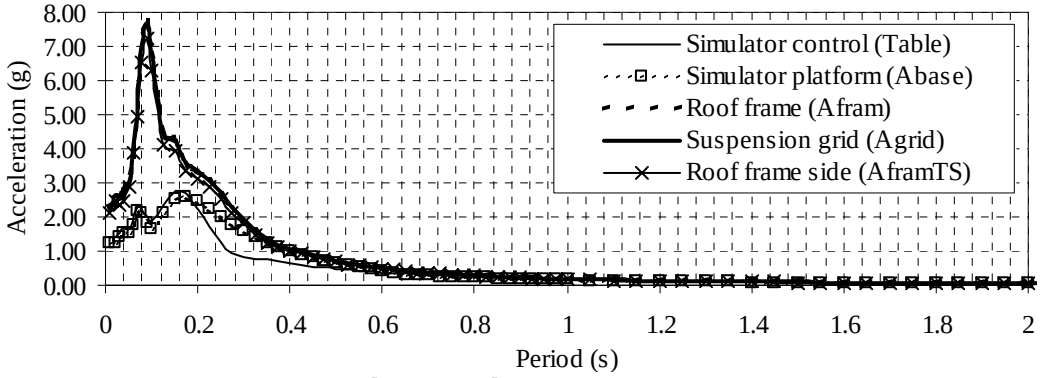

a) horizontal response spectra

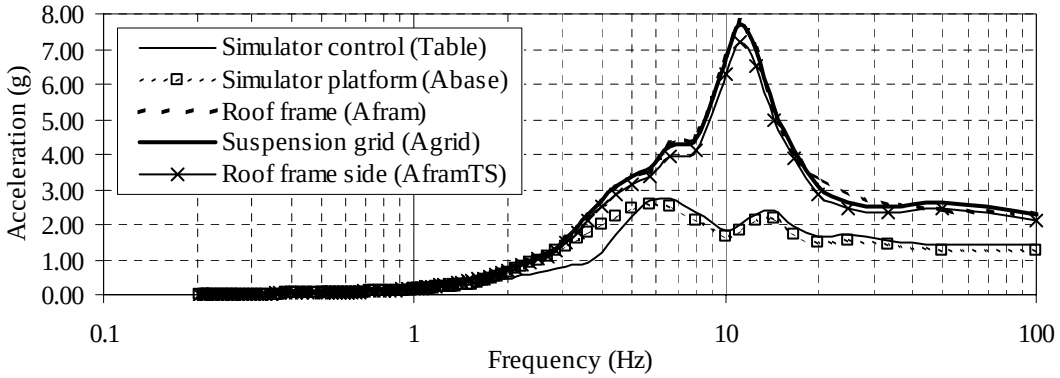

b) horizontal response spectra

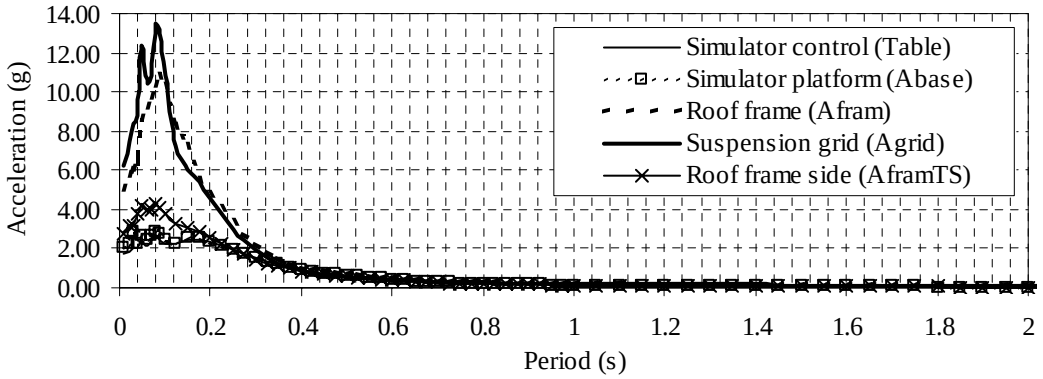

c) vertical response spectra

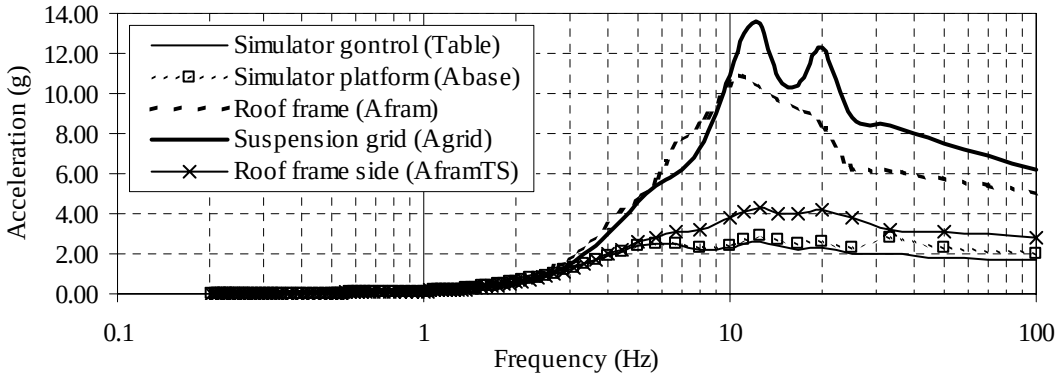

d) vertical response spectra

Figure A–12. Response spectra for Test 20 on ceiling system CS2.

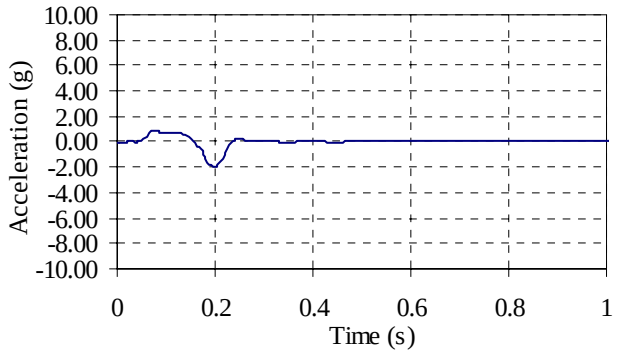

a) horizontal acceleration (*Table*)

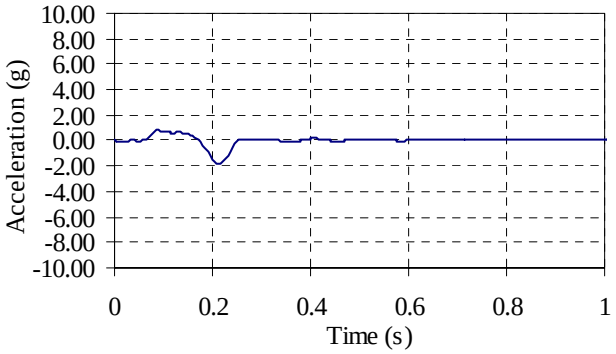

b) horizontal acceleration (*Abase*)

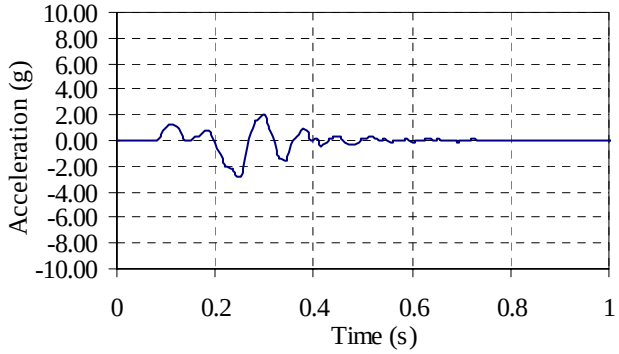

c) horizontal acceleration (*Afram*)

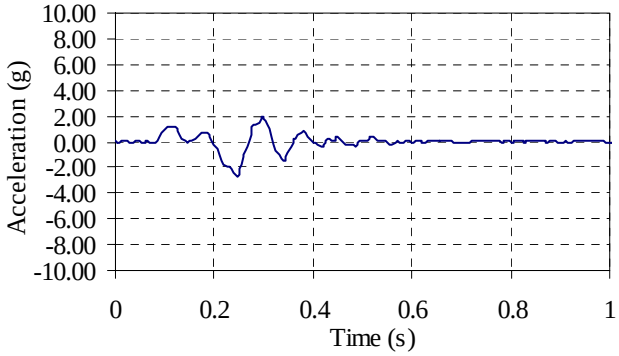

d) horizontal acceleration (*AframTS*)

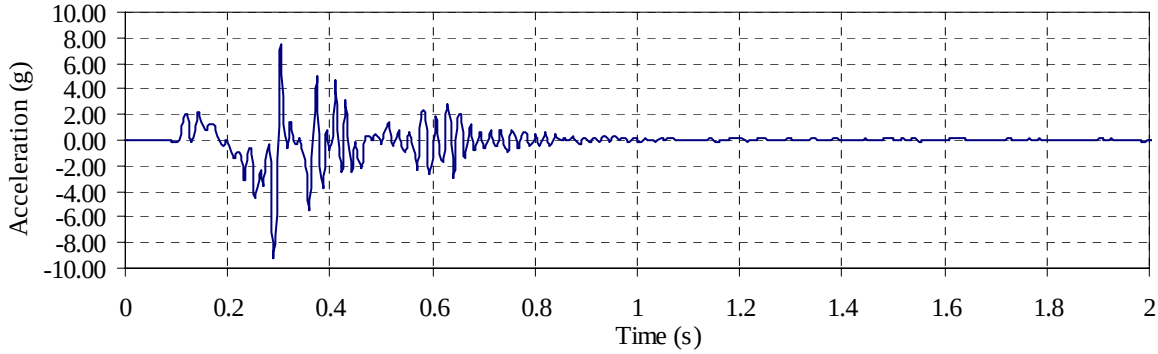

e) horizontal acceleration (*Agrid*)

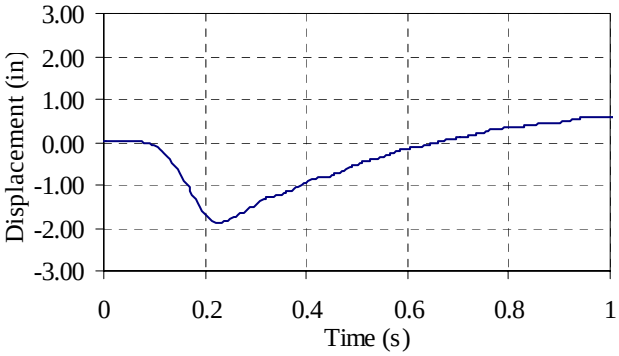

f) horizontal displacement (*Dbase*)

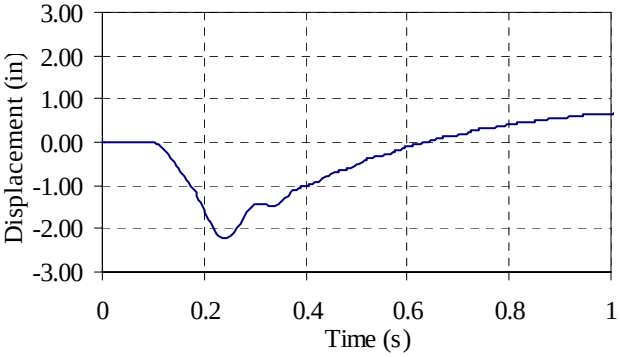

g) horizontal displacement (*Dcntr*)

Figure A–13. Horizontal displacement and acceleration histories for Test 23 on ceiling system CS2.

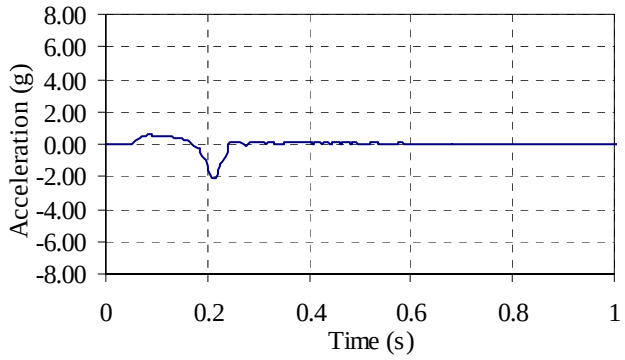

a) vertical acceleration (*Table*)

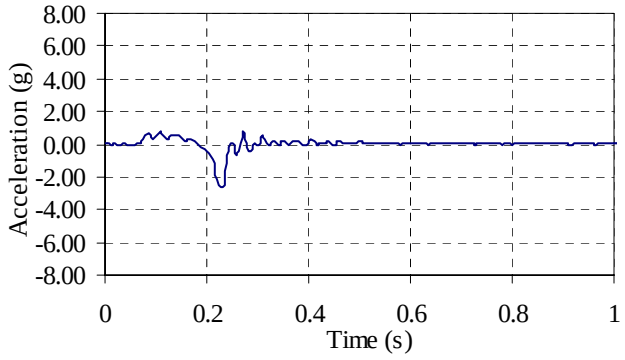

b) vertical acceleration (*Abase*)

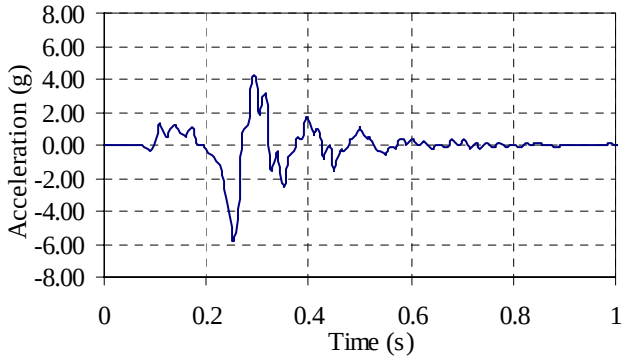

c) vertical acceleration (*Afram*)

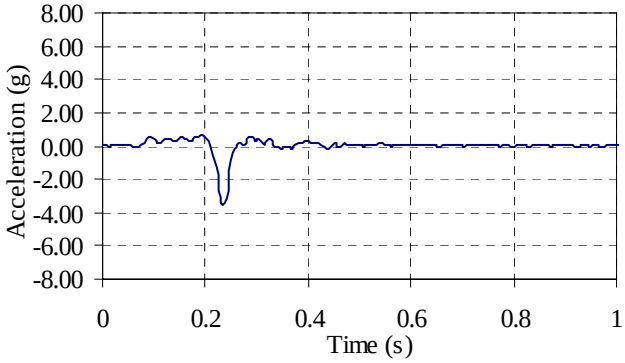

d) vertical acceleration (*AframTS*)

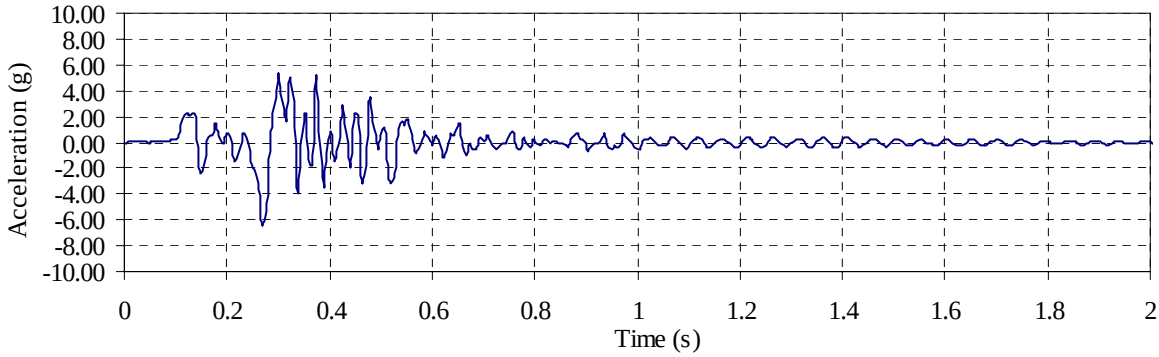

e) vertical acceleration (*Agrid*)

Figure A–14. Vertical acceleration histories for Test 23 on ceiling system CS2.

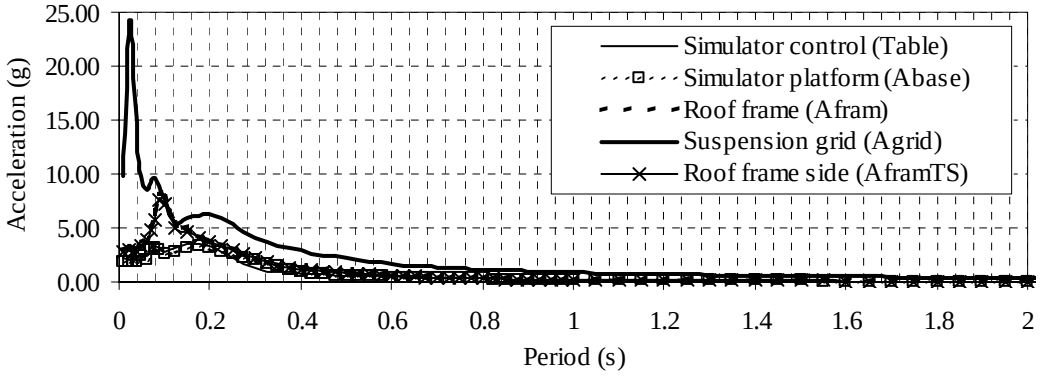

a) horizontal response spectra

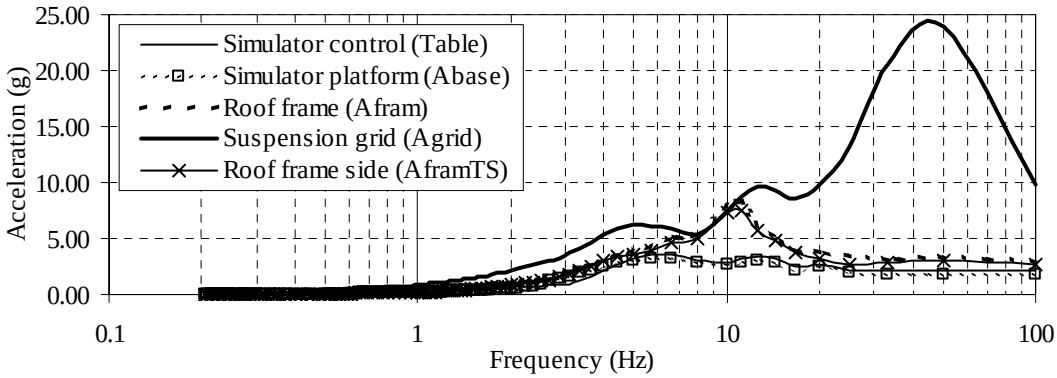

b) horizontal response spectra

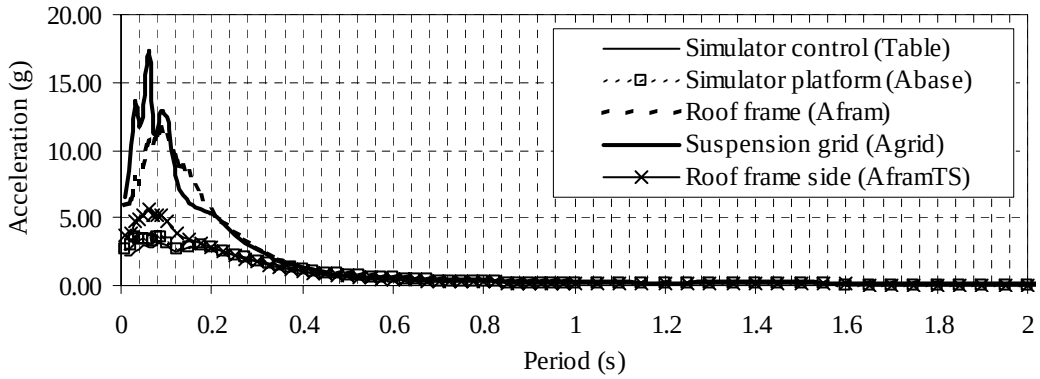

c) vertical response spectra

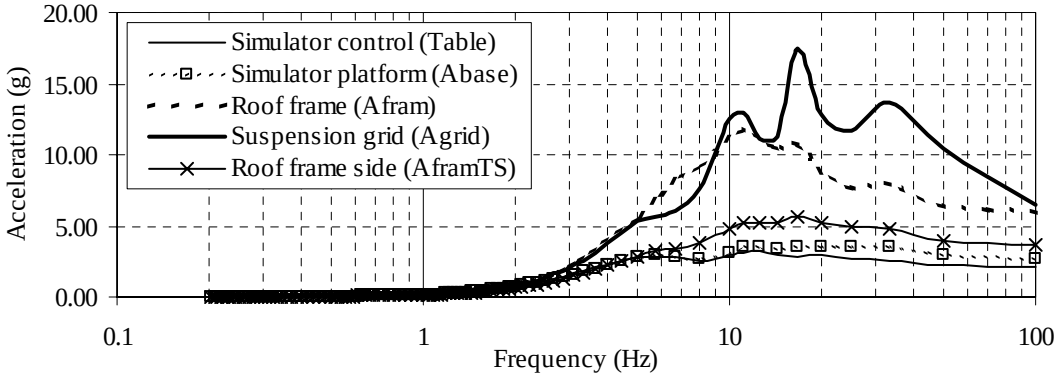

d) vertical response spectra

Figure A–15. Response spectra for Test 23 on ceiling system CS2.

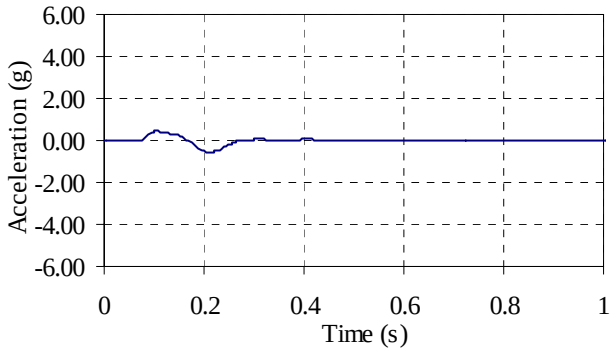

a) horizontal acceleration (*Table*)

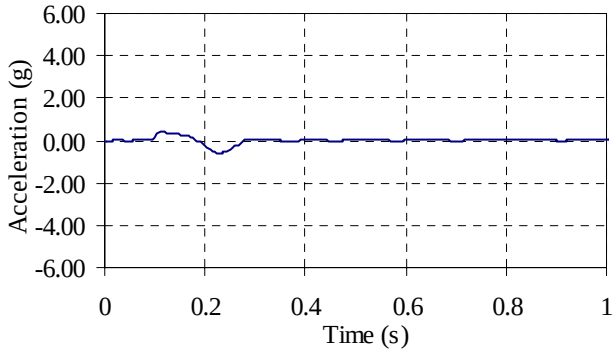

b) horizontal acceleration (*Abase*)

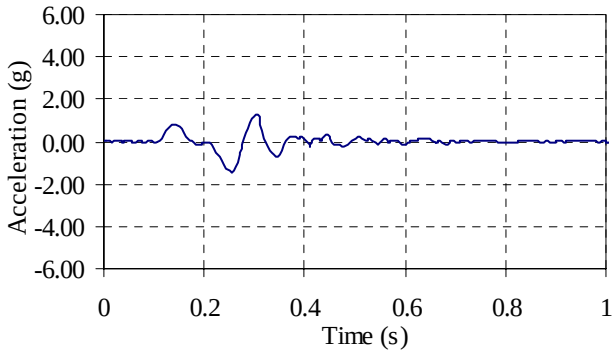

c) horizontal acceleration (*Afram*)

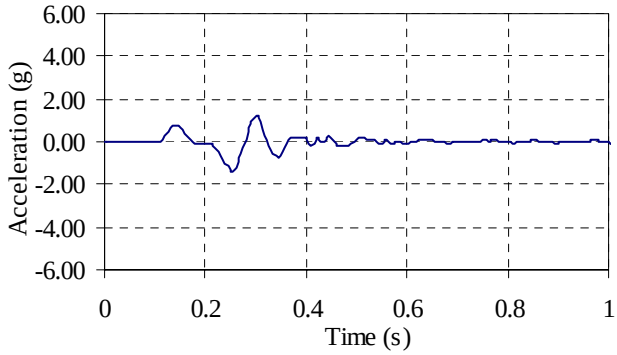

d) horizontal acceleration (*AframTS*)

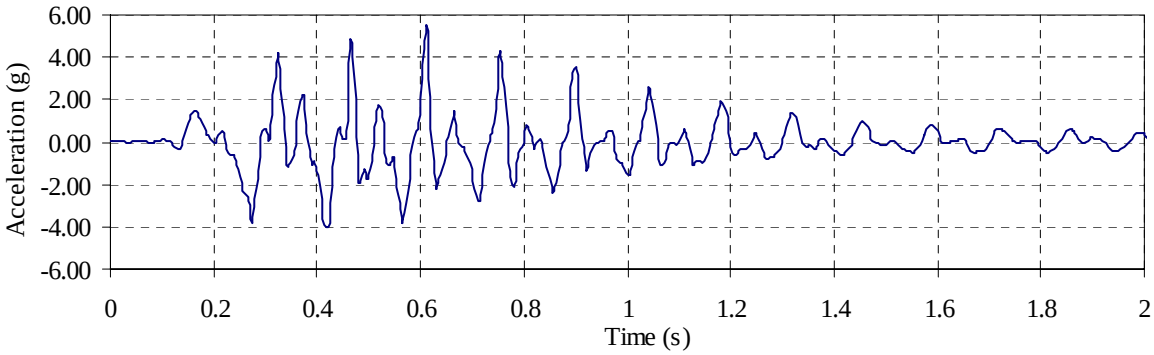

e) horizontal acceleration (*Agrid*)

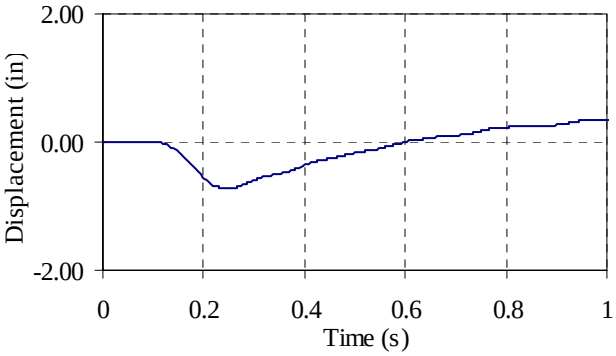

f) horizontal displacement (*Dbase*)

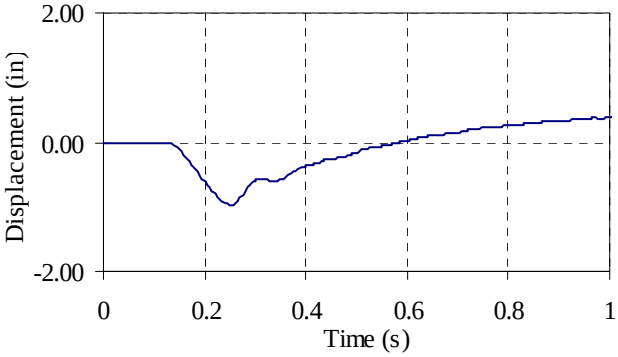

g) horizontal displacement (*Dcntr*)

Figure A–16. Horizontal displacement and acceleration histories for Test 14 on ceiling system CS3.

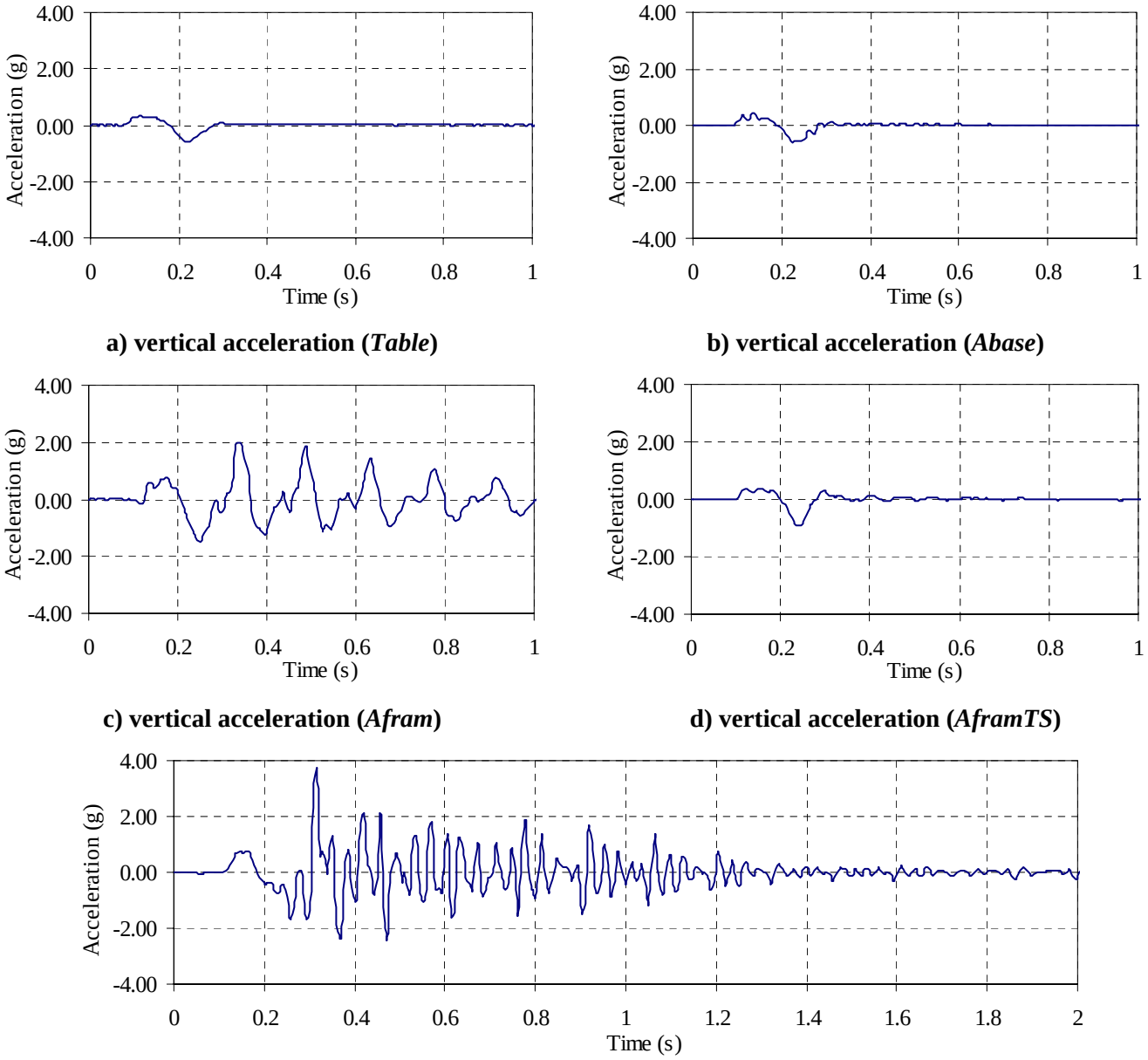

a) vertical acceleration (*Table*)

b) vertical acceleration (*Abase*)

c) vertical acceleration (*Afram*)

d) vertical acceleration (*AframTS*)

e) vertical acceleration (*Agrid*)

Figure A–17. Vertical acceleration histories for Test 14 on ceiling system CS3.

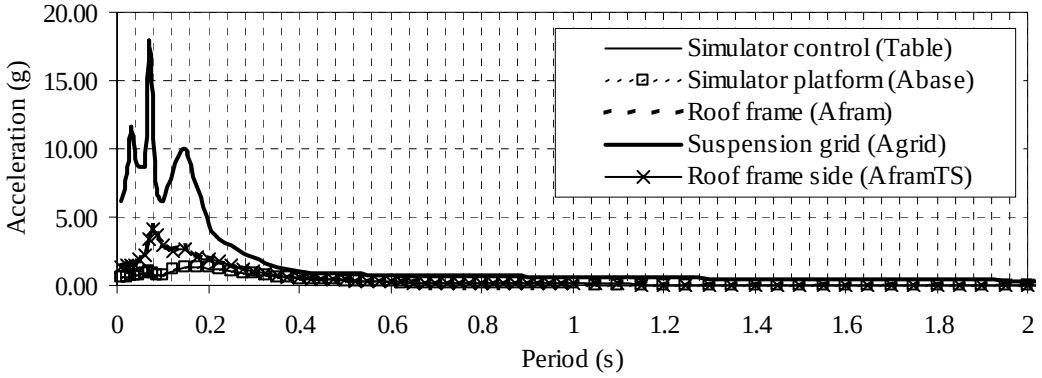

a) horizontal response spectra

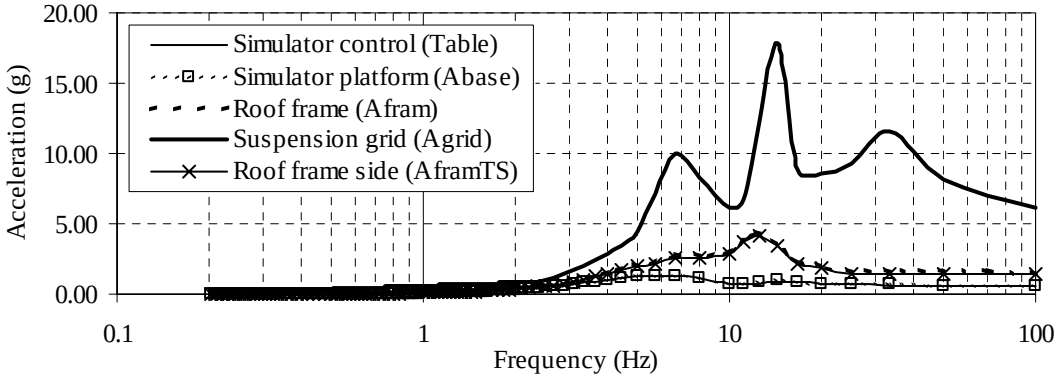

b) horizontal response spectra

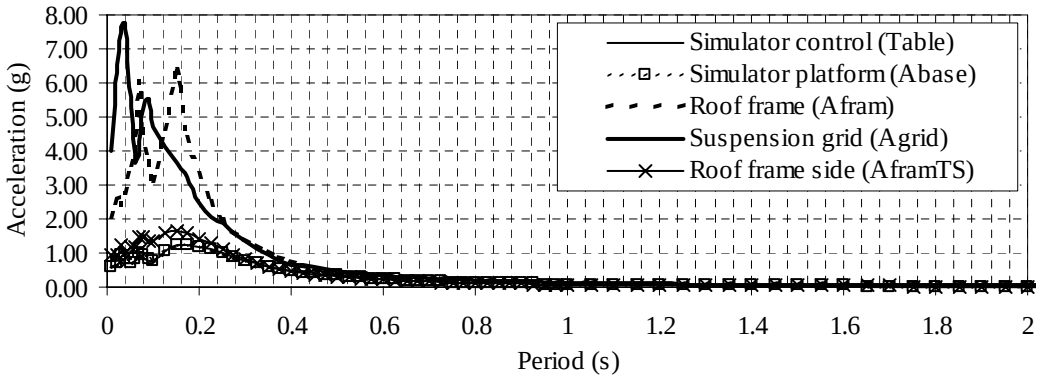

c) vertical response spectra

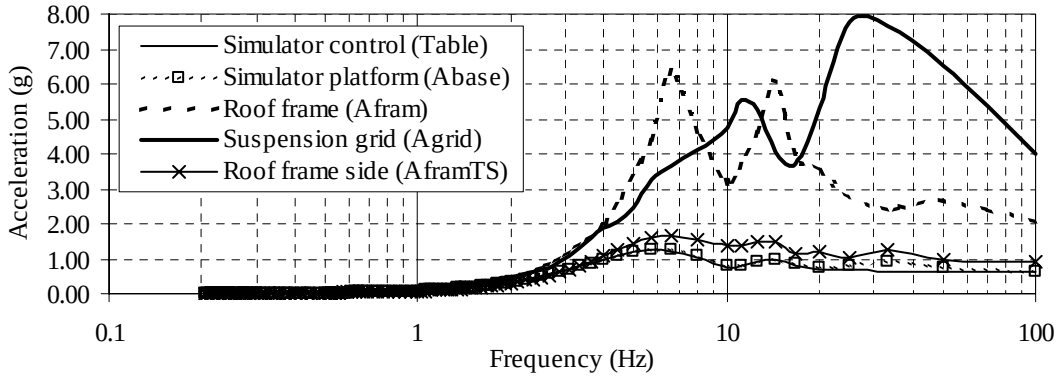

d) vertical response spectra

Figure A–18. Response spectra for Test 14 on ceiling system CS3.

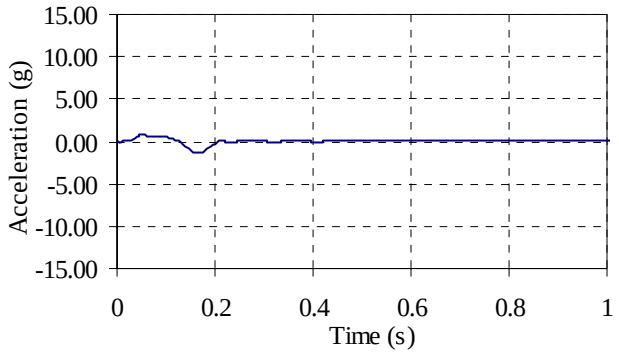

a) horizontal acceleration (*Table*)

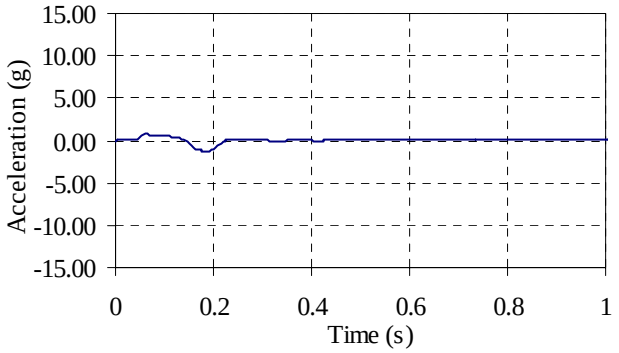

b) horizontal acceleration (*Abase*)

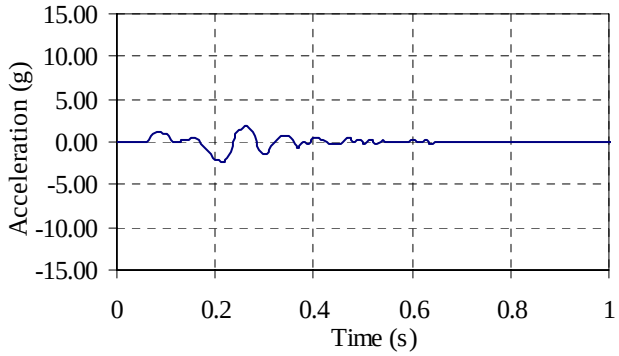

c) horizontal acceleration (*Afram*)

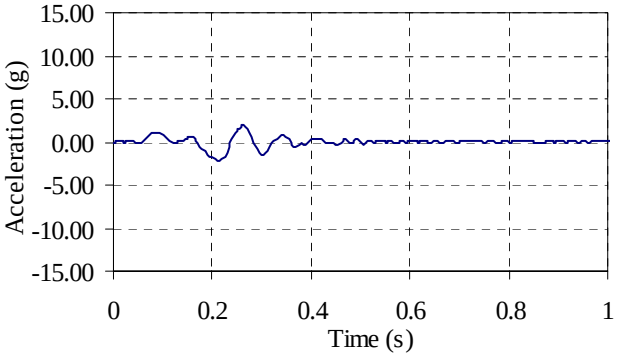

d) horizontal acceleration (*AframTS*)

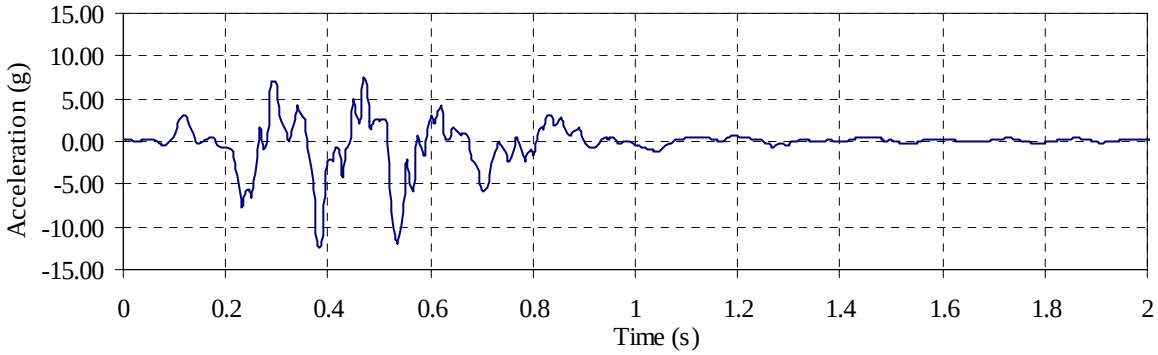

e) horizontal acceleration (*Agrid*)

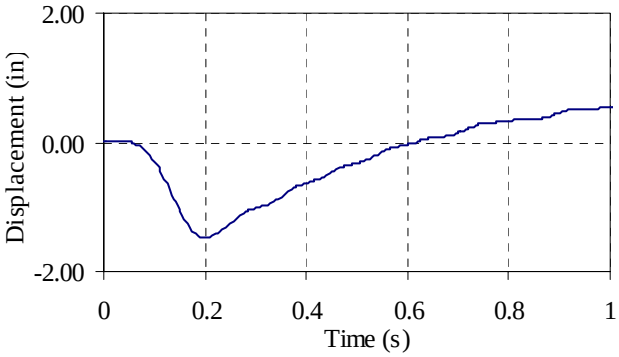

f) horizontal displacement (*Dbase*)

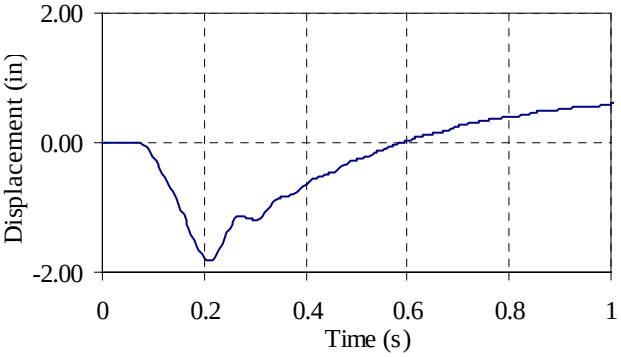

g) horizontal displacement (*Dcntr*)

Figure A–19. Horizontal displacement and acceleration histories for Test 20 on ceiling system CS3.

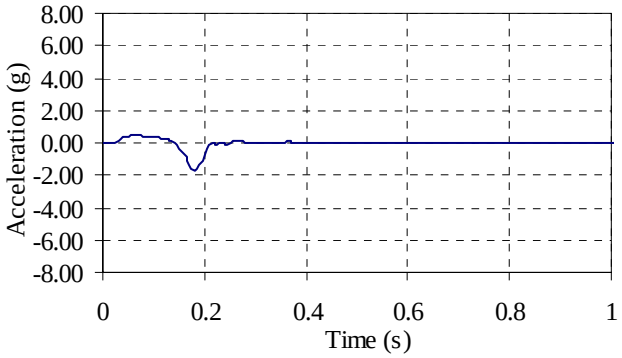

a) vertical acceleration (*Table*)

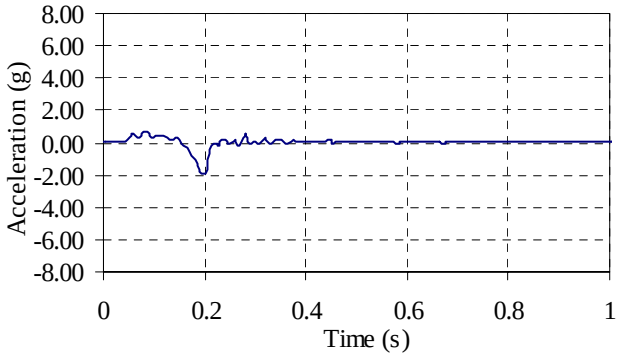

b) vertical acceleration (*Abase*)

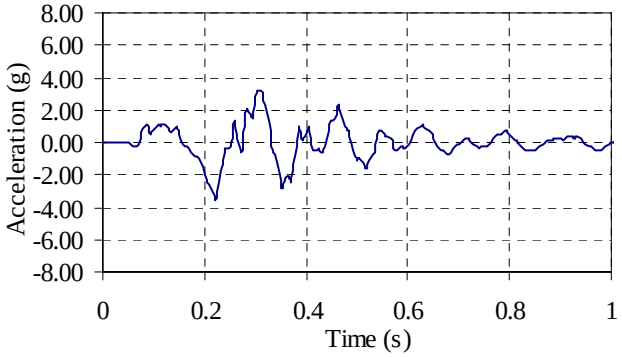

c) vertical acceleration (*Afram*)

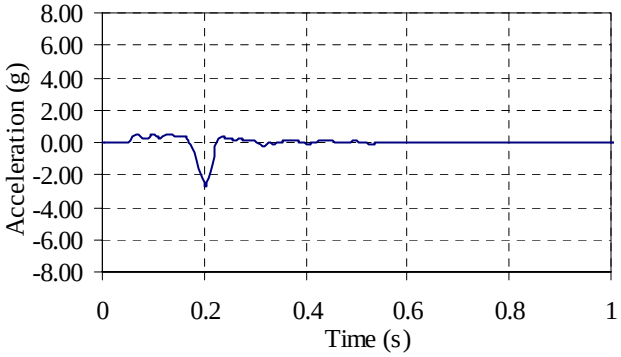

d) vertical acceleration (*AframTS*)

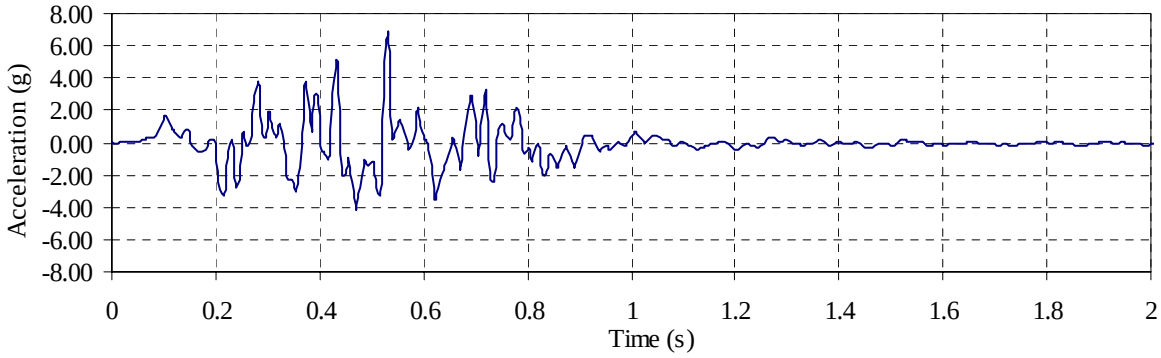

e) vertical acceleration (*Agrid*)

Figure A–20. Vertical acceleration histories for Test 20 on ceiling system CS3.

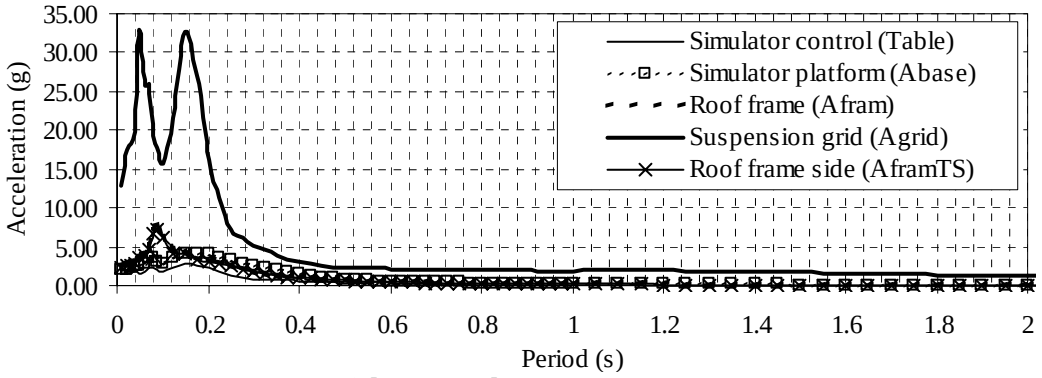

a) horizontal response spectra

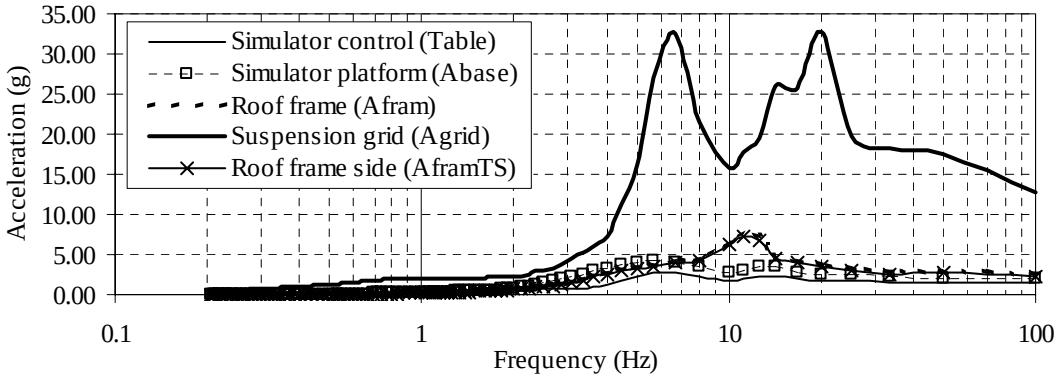

b) horizontal response spectra

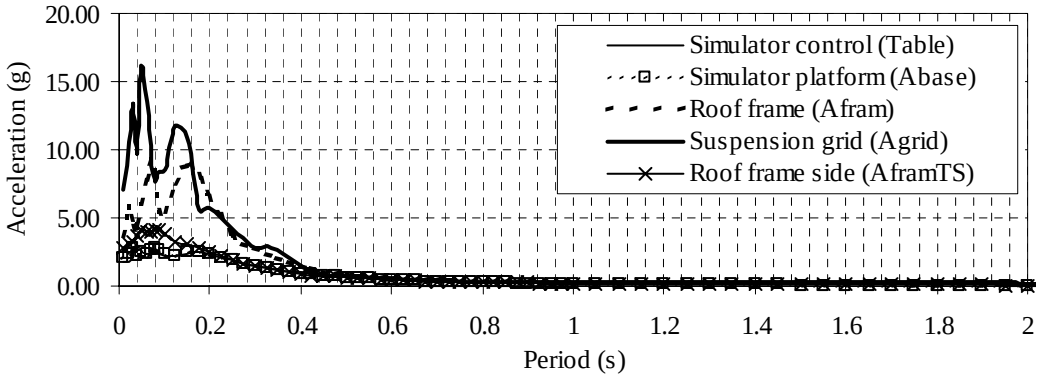

c) vertical response spectra

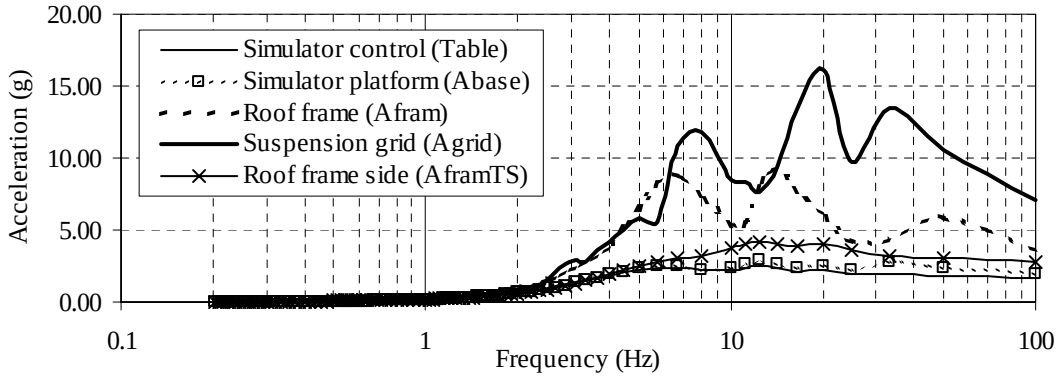

d) vertical response spectra

Figure A–21. Response spectra for Test 20 on ceiling system CS3.

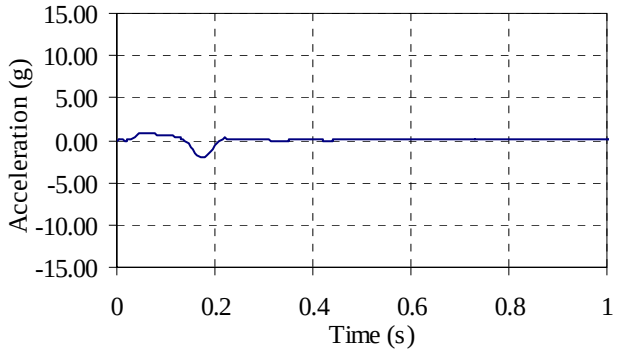

a) horizontal acceleration (*Table*)

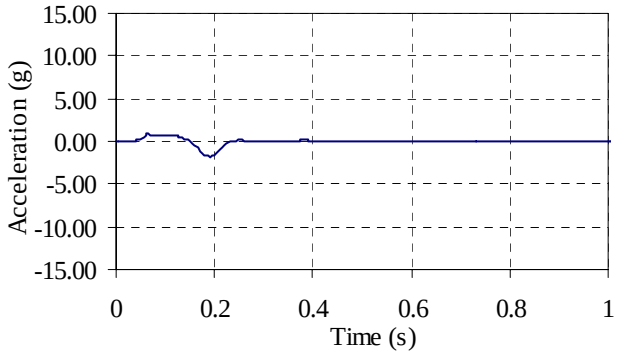

b) horizontal acceleration (*Abase*)

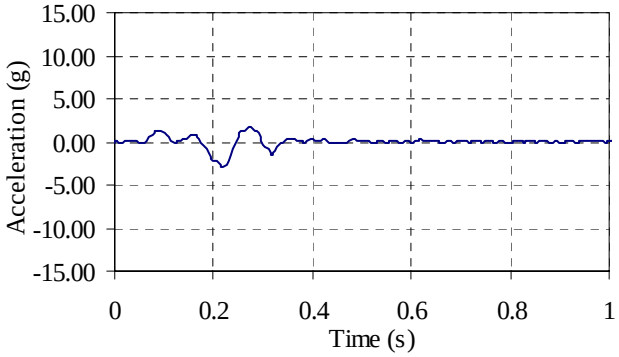

c) horizontal acceleration (*Afram*)

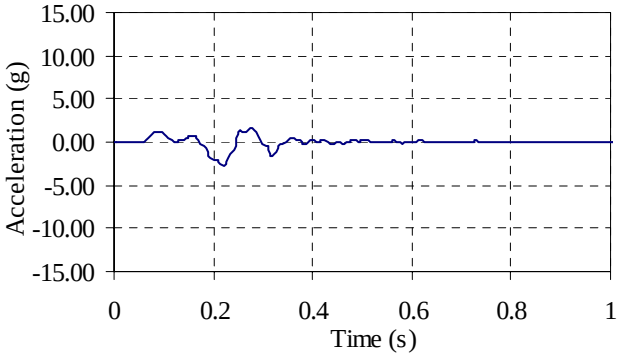

d) horizontal acceleration (*AframTS*)

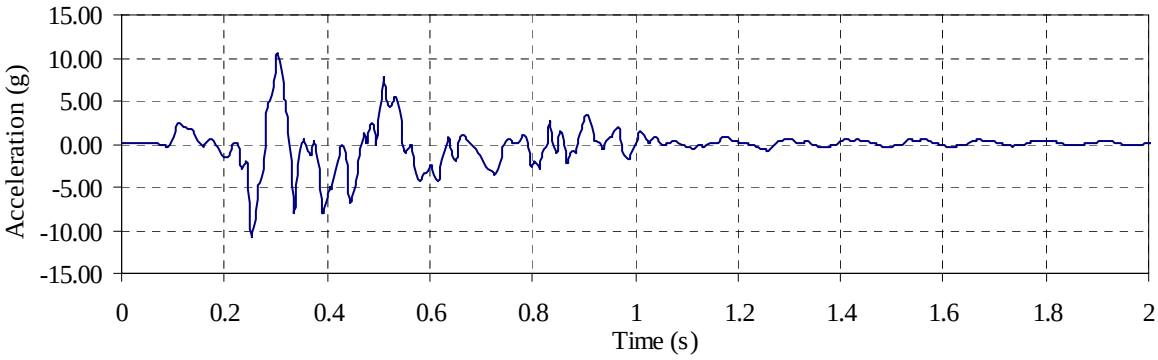

e) horizontal acceleration (*Agrid*)

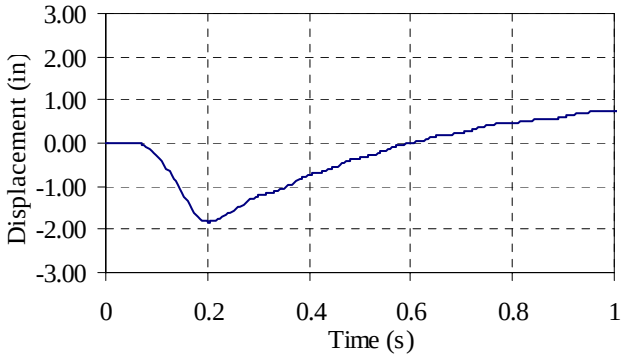

f) horizontal displacement (*Dbase*)

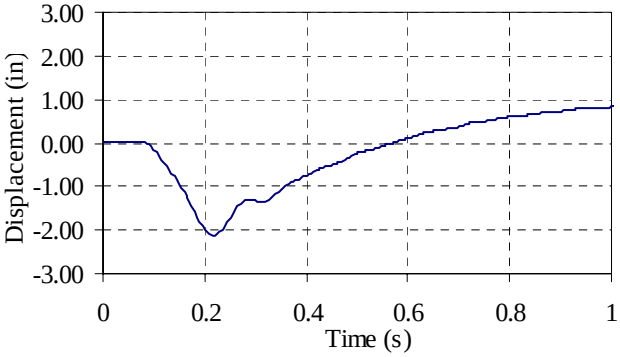

g) horizontal displacement (*Dcntr*)

Figure A–22. Horizontal displacement and acceleration histories for Test 23 on ceiling system CS3.

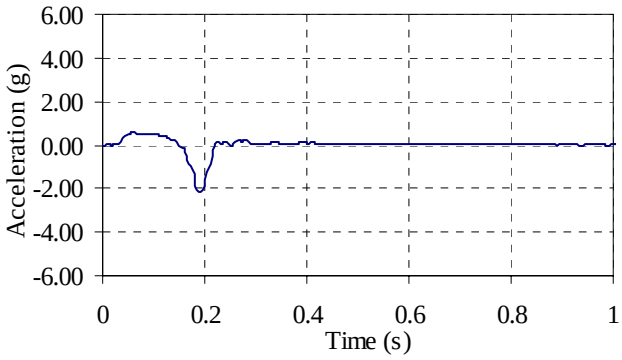

a) vertical acceleration (*Table*)

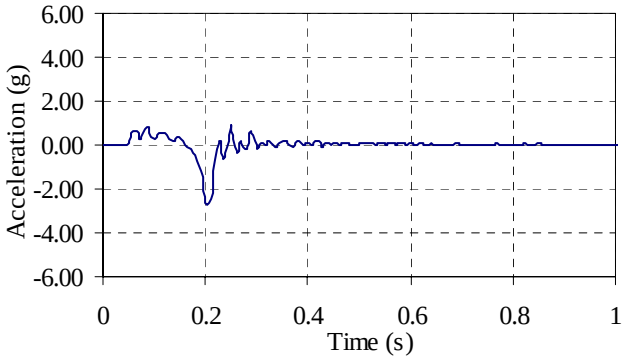

b) vertical acceleration (*Abase*)

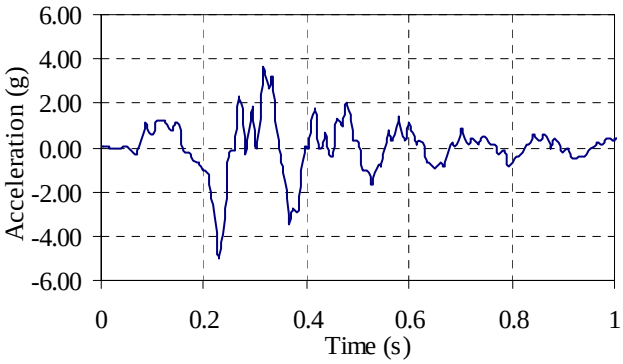

c) vertical acceleration (*Aframe*)

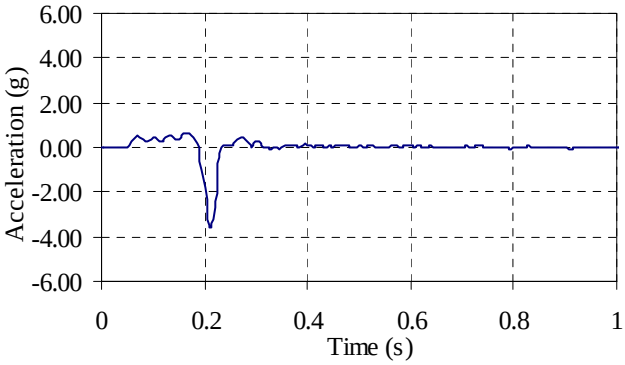

d) vertical acceleration (*AframTS*)

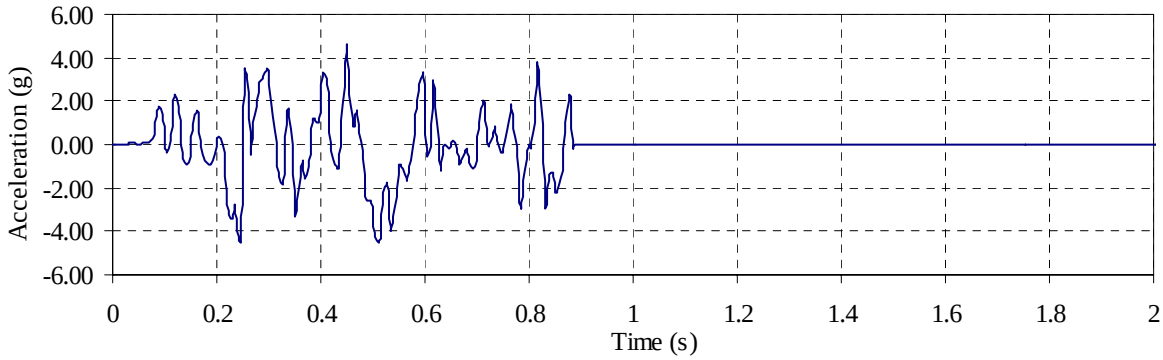

e) vertical acceleration (*Agrid*)

Figure A–23. Vertical acceleration histories for Test 23 on ceiling system CS3.

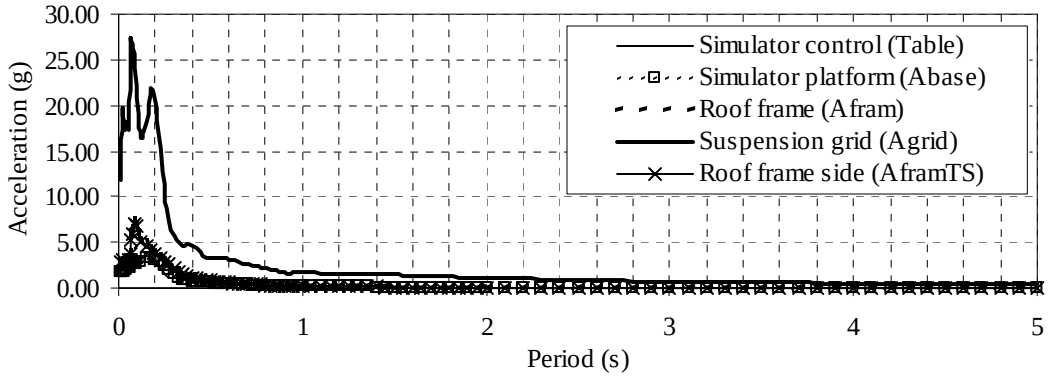

a) horizontal response spectra

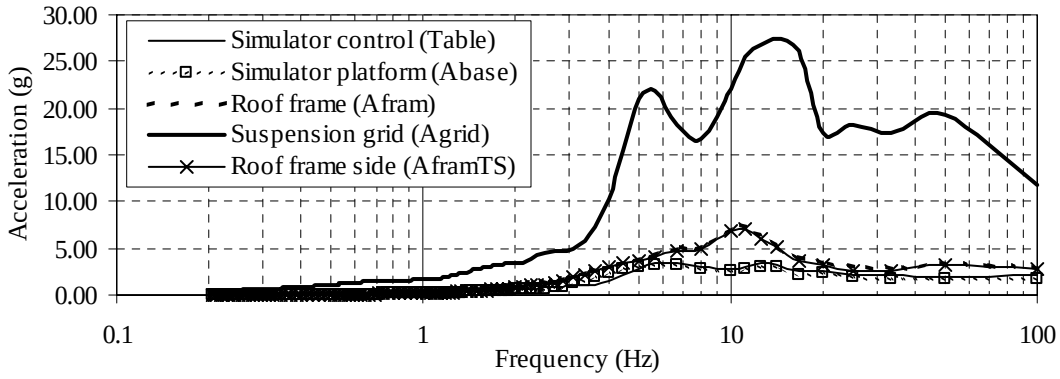

b) horizontal response spectra

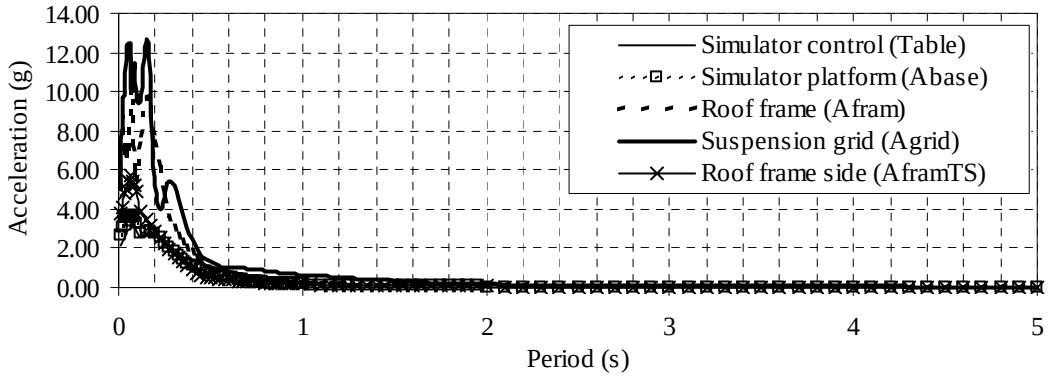

c) vertical response spectra

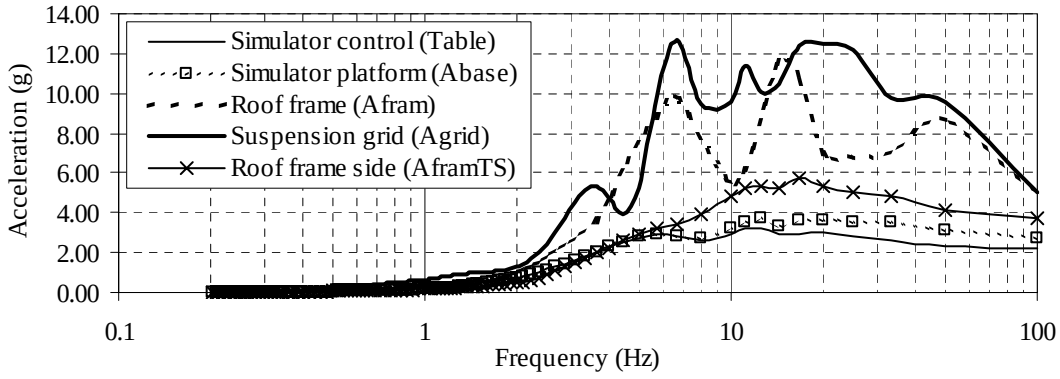

d) vertical response spectra

Figure A–24. Response spectra for Test 23 on ceiling system CS3.

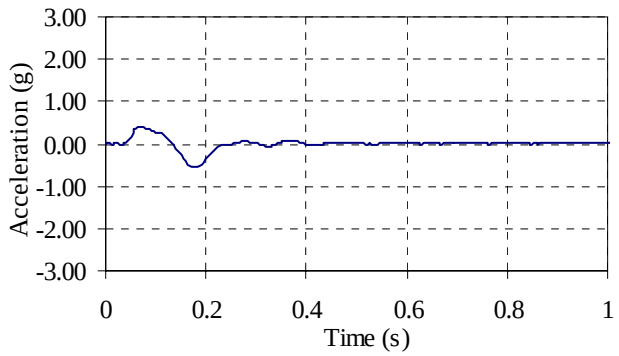

a) horizontal acceleration (*Table*)

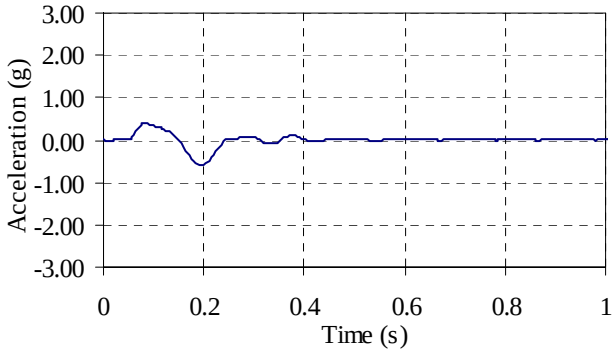

b) horizontal acceleration (*Abase*)

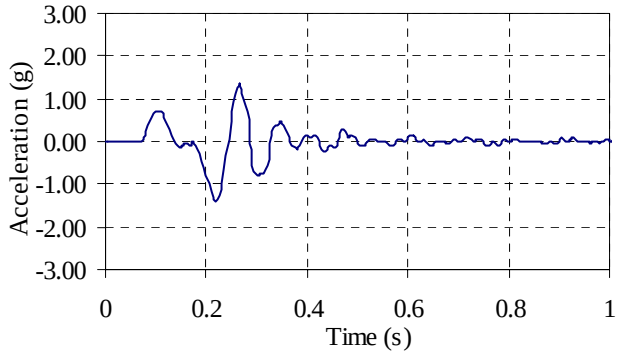

c) horizontal acceleration (*Aframe*)

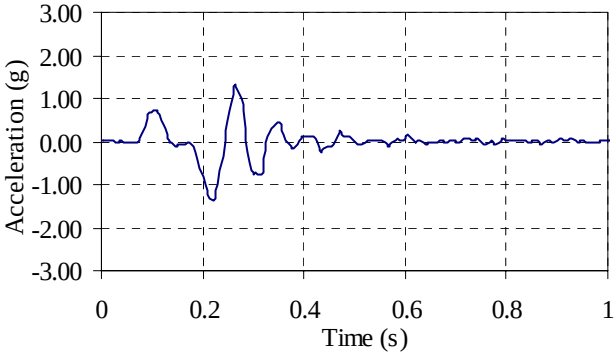

d) horizontal acceleration (*AframTS*)

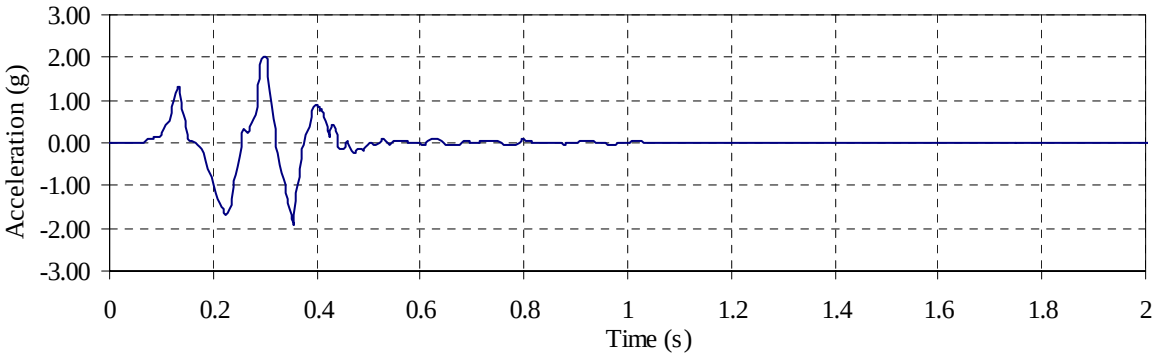

e) horizontal acceleration (*Agrid*)

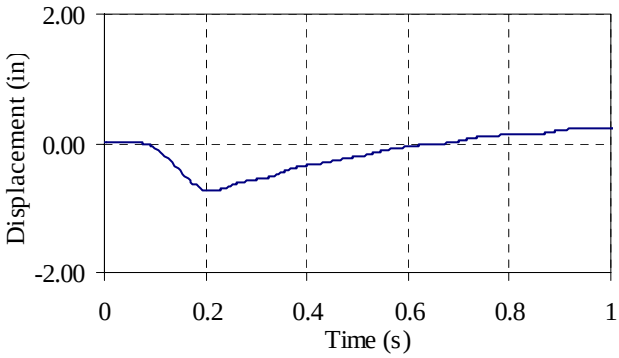

f) horizontal displacement (*Dbase*)

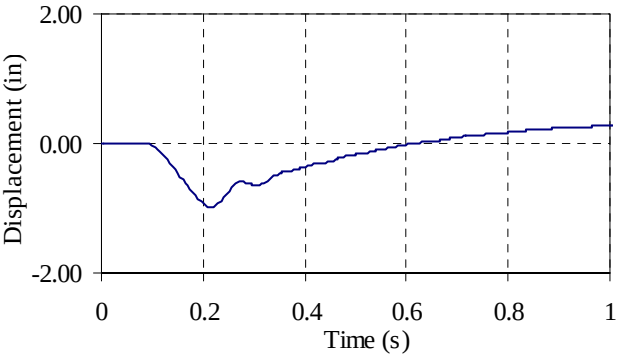

g) horizontal displacement (*Dcntr*)

Figure A–25. Horizontal displacement and acceleration histories for Test 14 on ceiling system CS4.

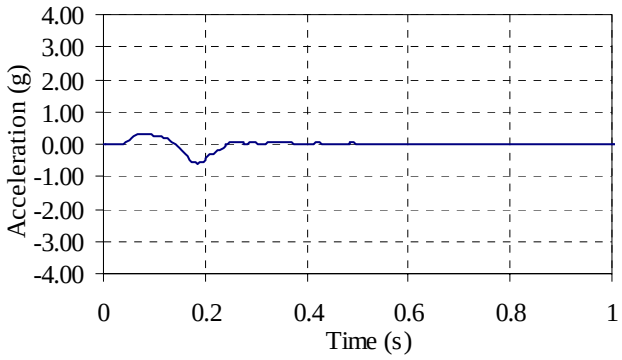

a) vertical acceleration (*Table*)

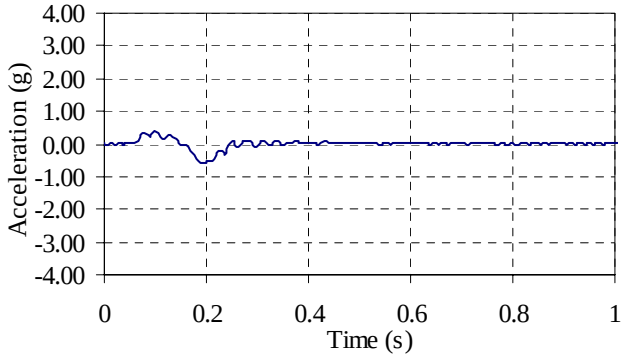

b) vertical acceleration (*Abase*)

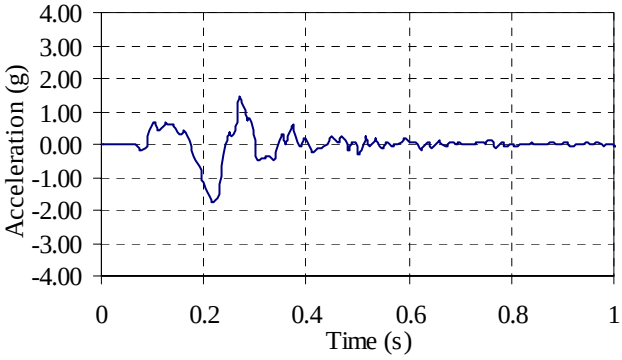

c) vertical acceleration (*Afram*)

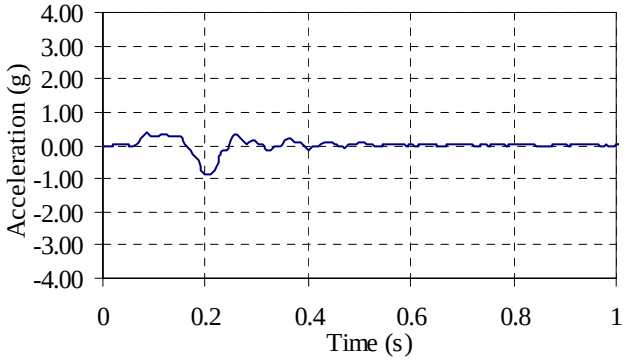

d) vertical acceleration (*AframTS*)

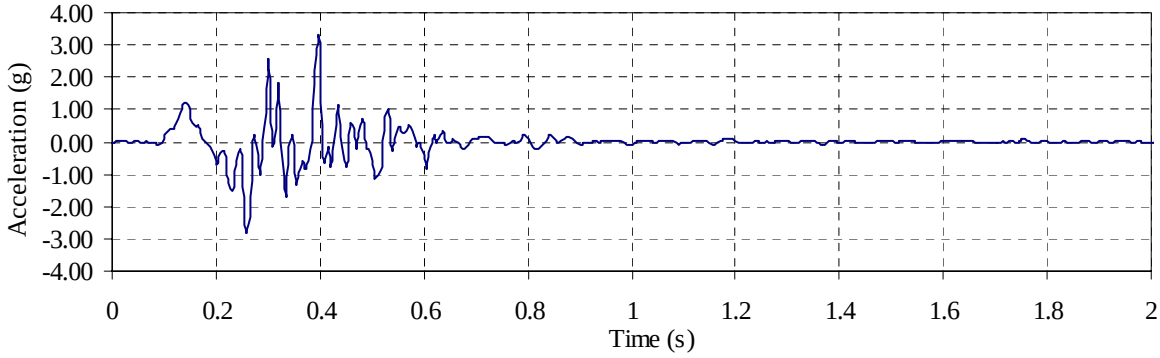

e) vertical acceleration (*Agrid*)

Figure A–26. Vertical acceleration histories for Test 14 on ceiling system CS4.

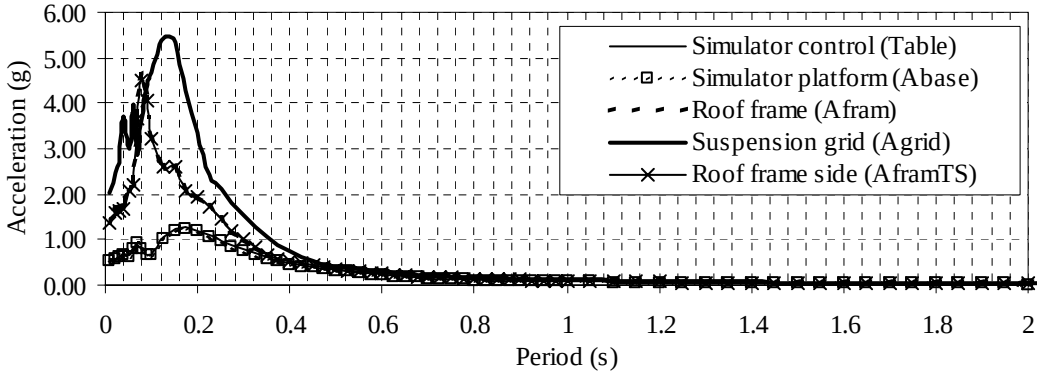

a) horizontal response spectra

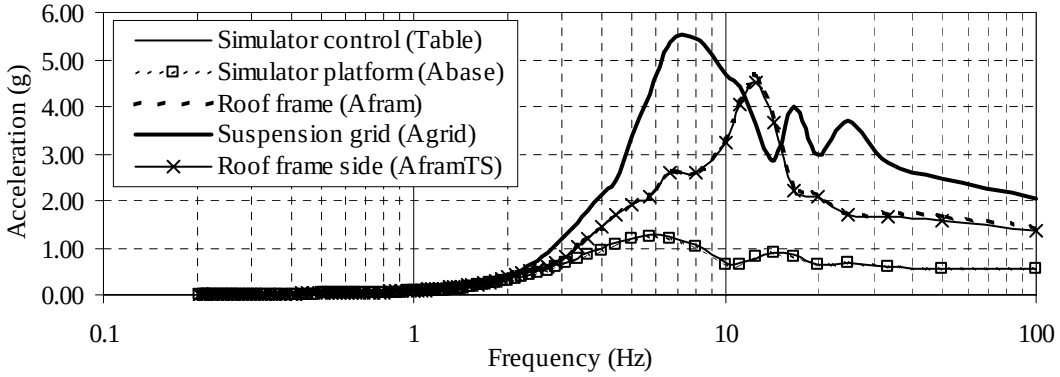

b) horizontal response spectra

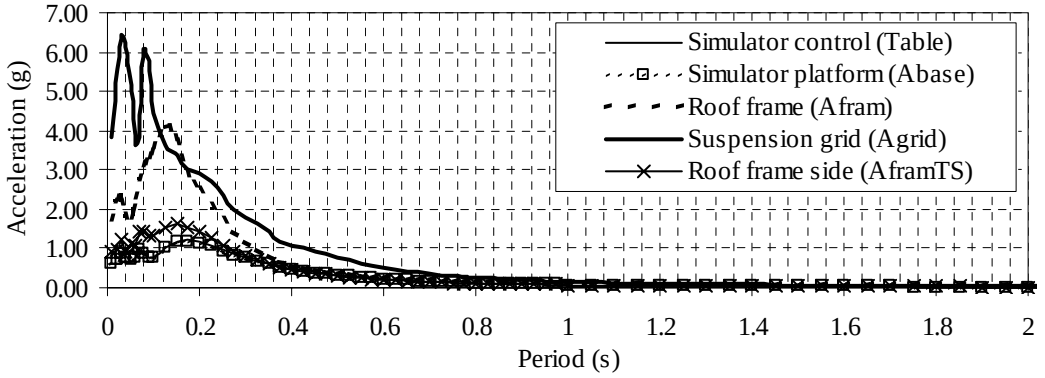

c) vertical response spectra

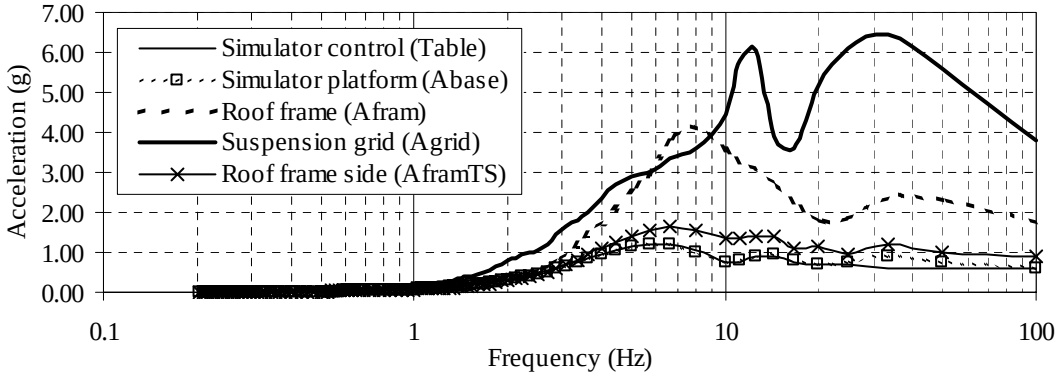

d) vertical response spectra

Figure A–27. Response spectra for Test 14 on ceiling system CS4.

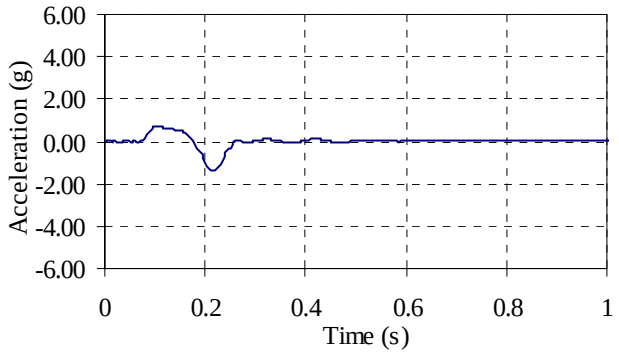

a) horizontal acceleration (*Table*)

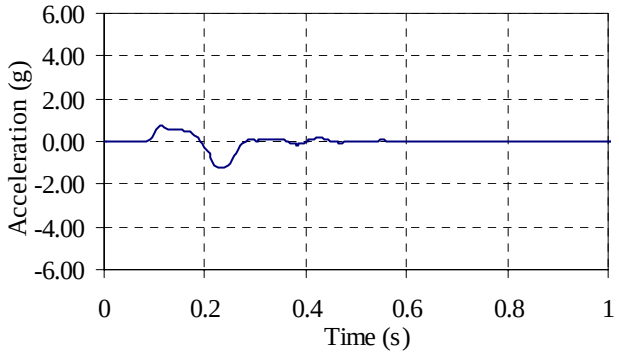

b) horizontal acceleration (*Abase*)

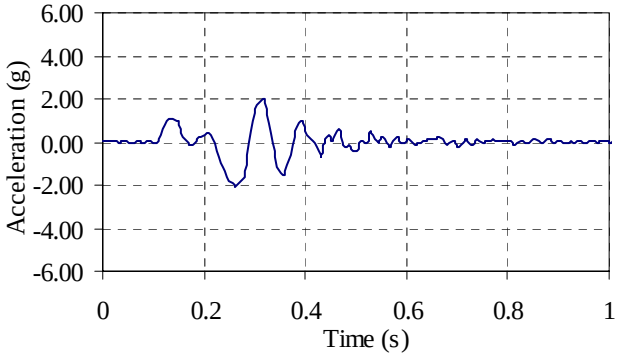

c) horizontal acceleration (*Afram*)

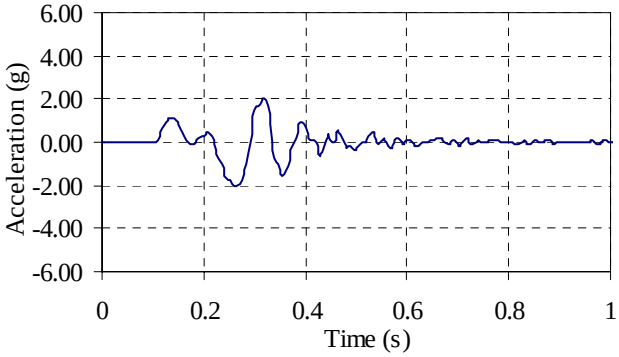

d) horizontal acceleration (*AframTS*)

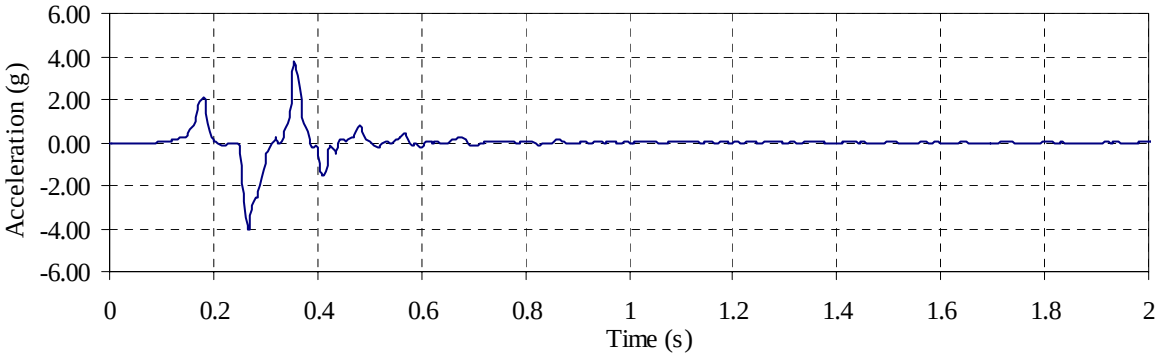

e) horizontal acceleration (*Agrid*)

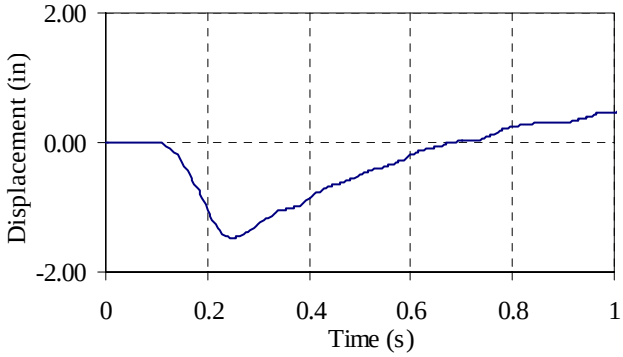

f) horizontal displacement (*Dbase*)

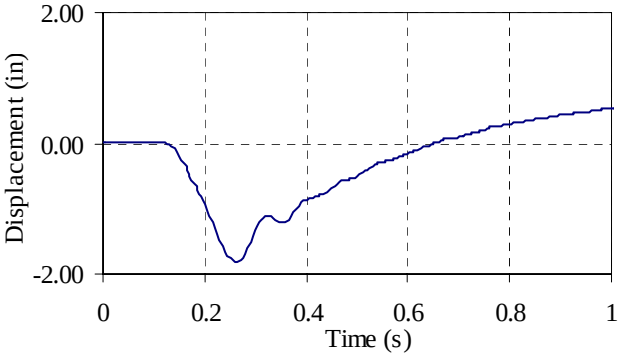

g) horizontal displacement (*Dcntr*)

Figure A–28. Horizontal displacement and acceleration histories for Test 20 on ceiling system CS4.

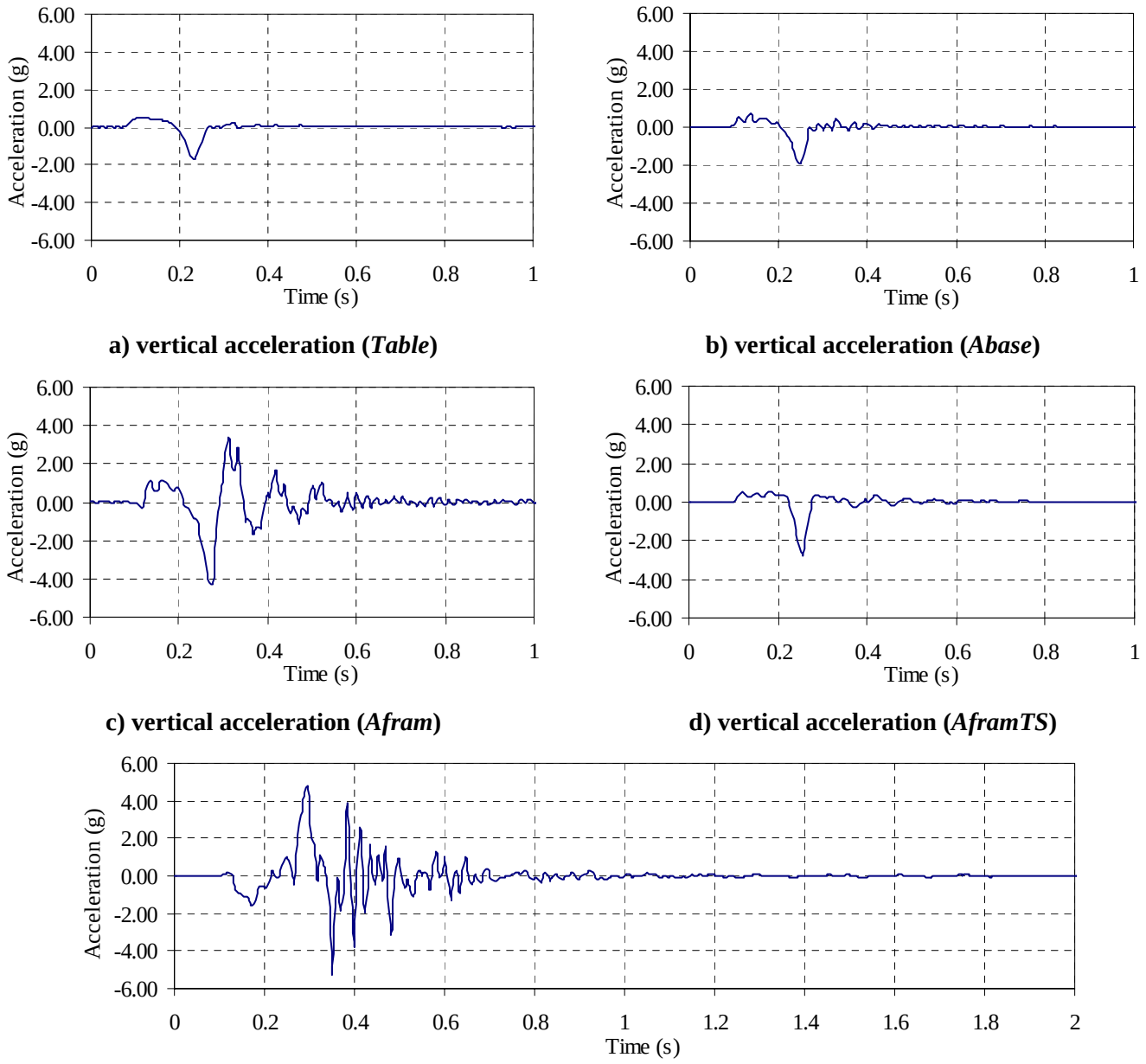

a) vertical acceleration (*Table*)

b) vertical acceleration (*Abase*)

c) vertical acceleration (*Aframe*)

d) vertical acceleration (*AframTS*)

e) vertical acceleration (*Agrid*)

Figure A–29. Vertical acceleration histories for Test 20 on ceiling system CS4.

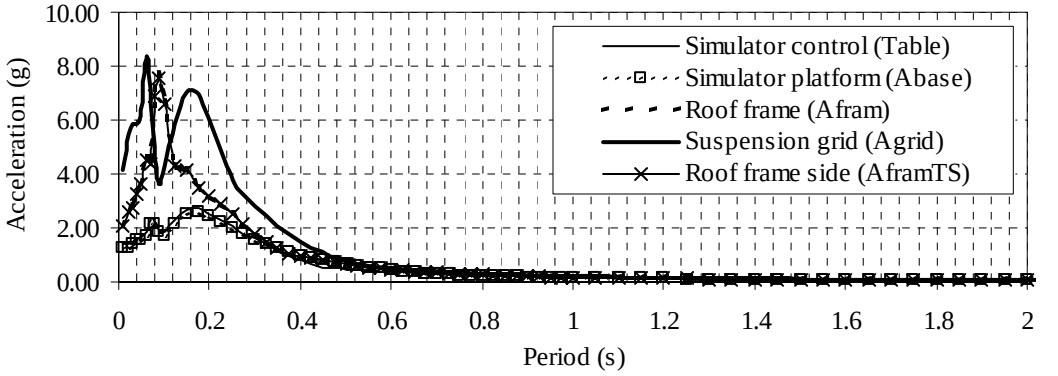

a) horizontal response spectra

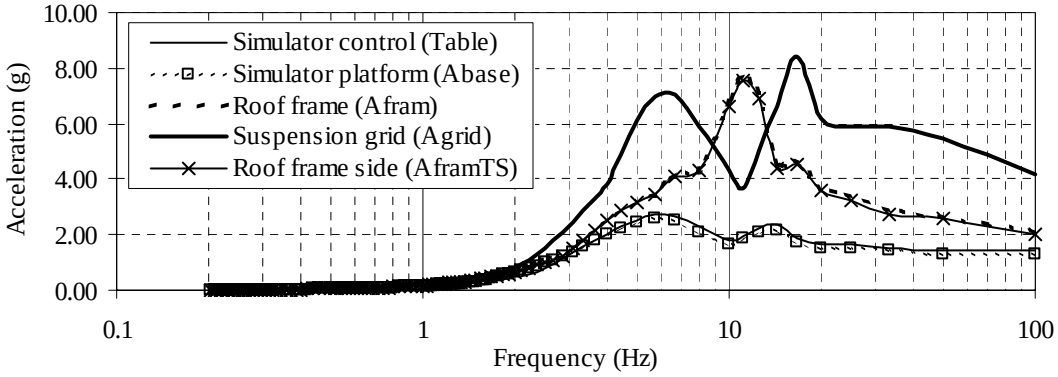

b) horizontal response spectra

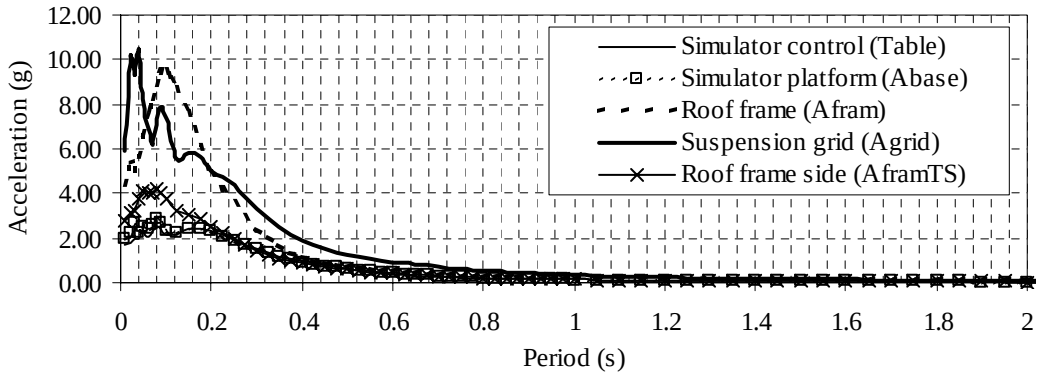

c) vertical response spectra

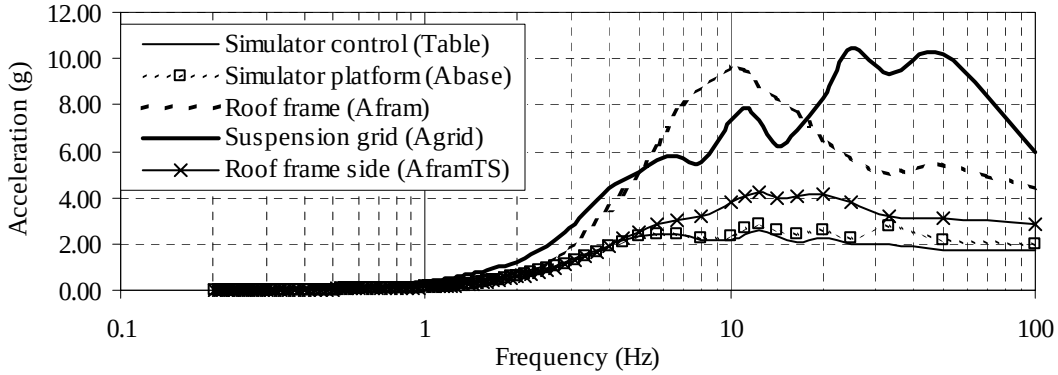

d) vertical response spectra

Figure A–30. Response spectra for Test 20 on ceiling system CS4.

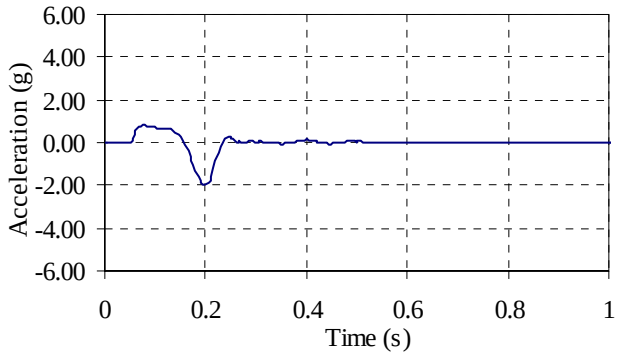

a) horizontal acceleration (*Table*)

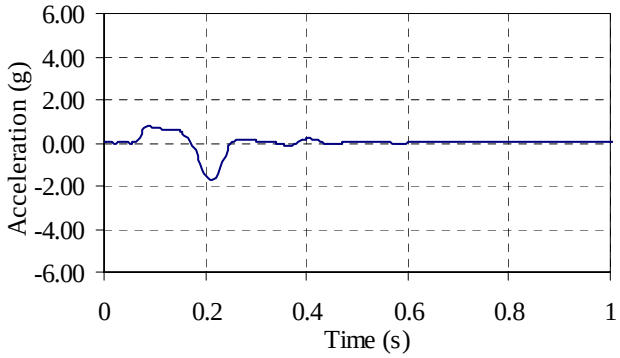

b) horizontal acceleration (*Abase*)

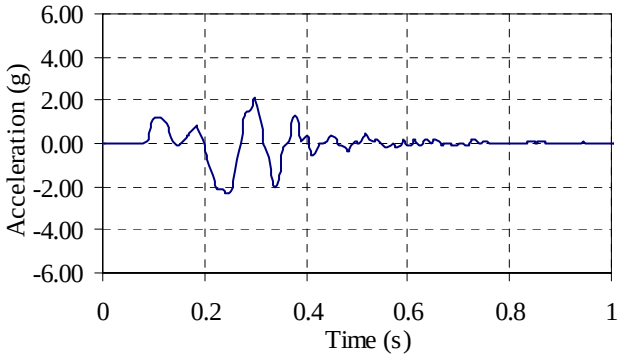

c) horizontal acceleration (*Afram*)

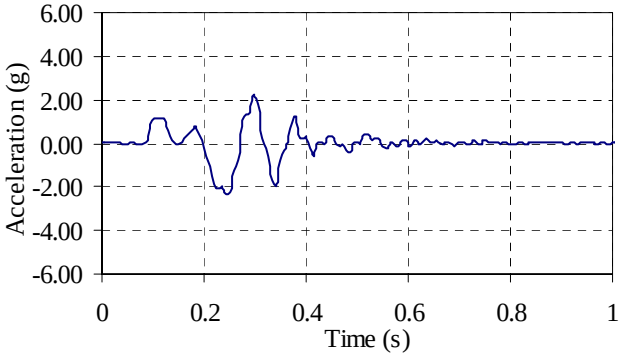

d) horizontal acceleration (*AframTS*)

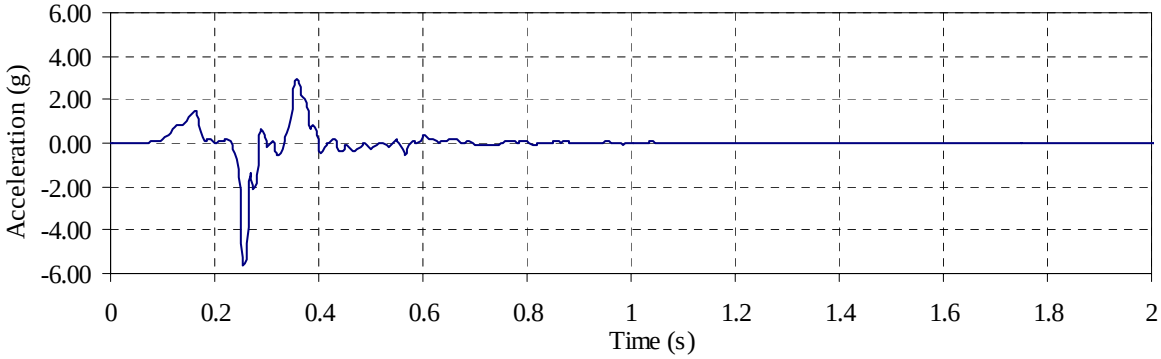

e) horizontal acceleration (*Agrid*)

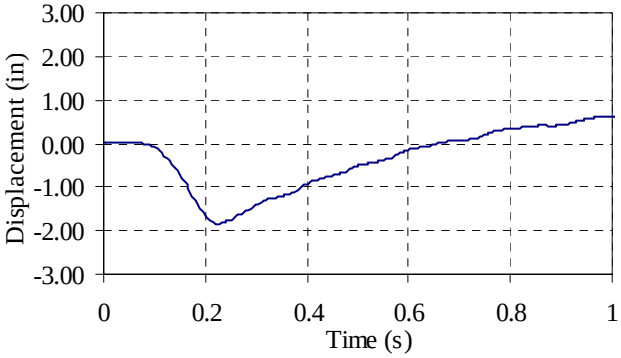

f) horizontal displacement (*Dbase*)

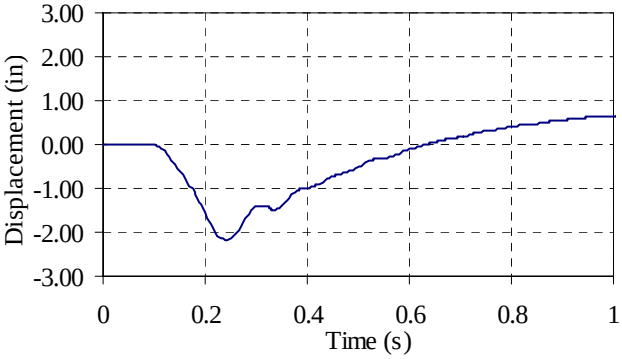

g) horizontal displacement (*Dcntr*)

Figure A–31. Horizontal displacement and acceleration histories for Test 23 on ceiling system CS4.

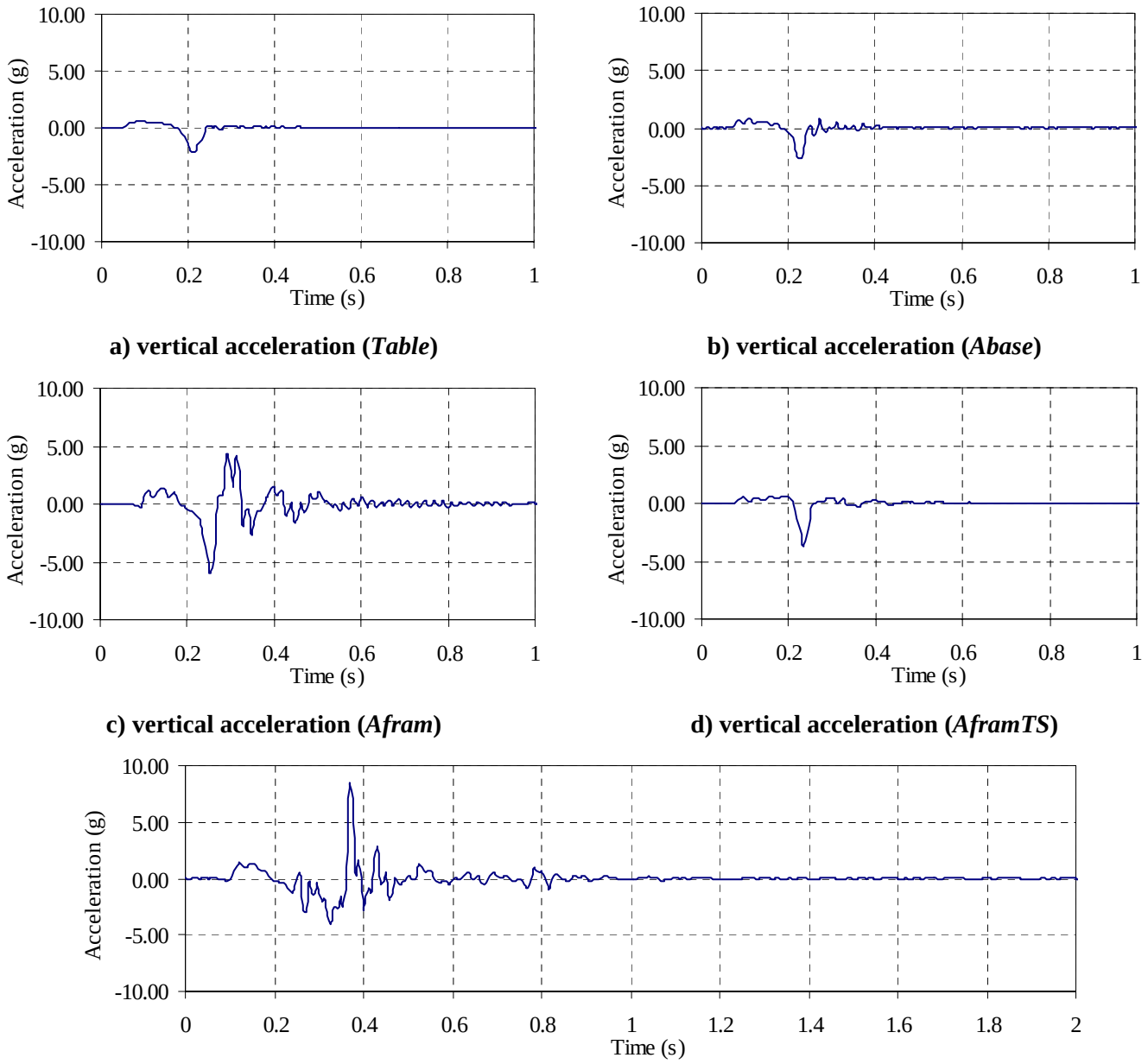

a) vertical acceleration (*Table*)

b) vertical acceleration (*Abase*)

c) vertical acceleration (*Aframe*)

d) vertical acceleration (*AframTS*)

e) vertical acceleration (*Agrid*)

Figure A–32. Vertical acceleration histories for Test 23 on ceiling system CS4.

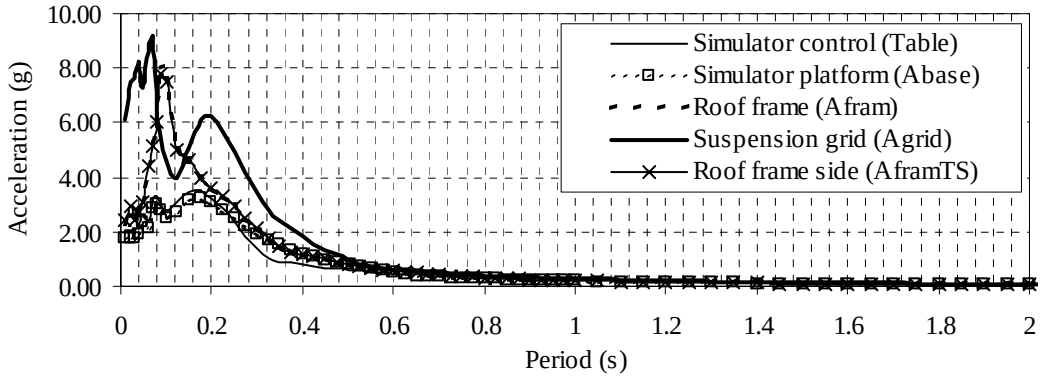

a) horizontal response spectra

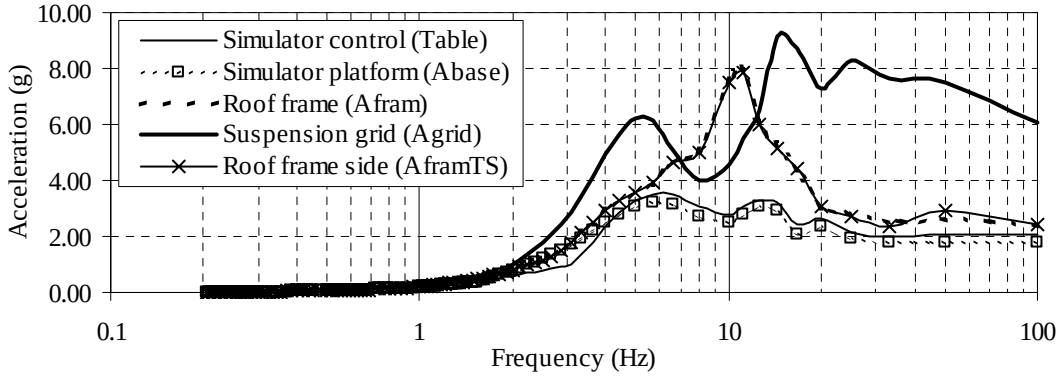

b) horizontal response spectra

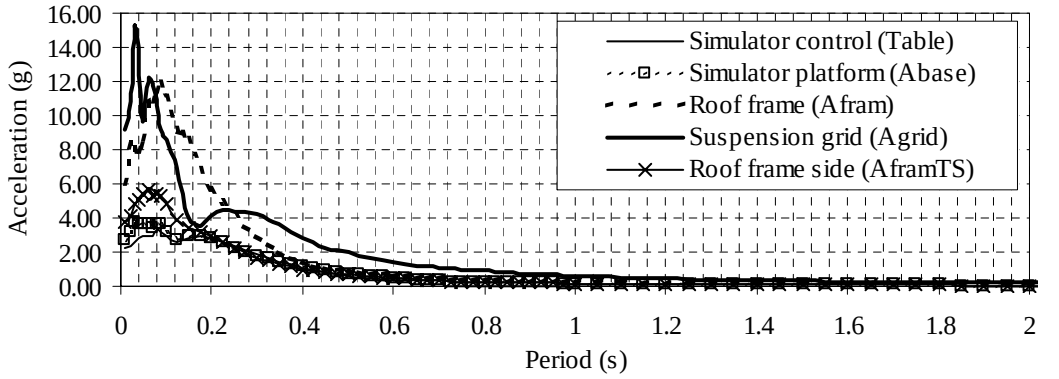

c) vertical response spectra

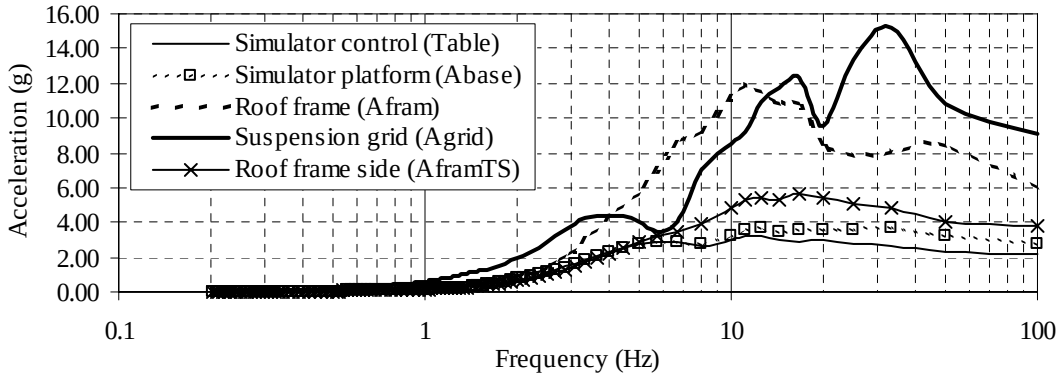

d) vertical response spectra

Figure A–33. Response spectra for Test 23 on ceiling system CS4.